Numerical and Experimental Thermo-Mechanical Analysis of Sheet Forming by Laser Line Heating

A Thesis Submitted in

Partial Fulfillment of the Requirements

for the Degree of

DOCTOR OF PHILOSOPHY

by

BIPLAB DAS

(Roll No. 11610310)

DEPARTMENT OF MECHANICAL ENGINEERING

INDIAN INSTITUTE OF TECHNOLOGY GUWAHATI

GUWAHATI-781039, INDIA

JULY 2024

Dedicated

To

My Family

Declaration

I declare that the present written submission is my thoughts in my own words. I have adequately cited and referenced the original sources, where others' works have been involved. I also declare that I have followed all principles of academic morality and honesty and have neither fabricated nor falsified any idea/data in the present thesis. I realize that any defilement of the above will be cause for disciplinary action by the Institute and can also induce disciplinary action from the sources which have thus not been properly cited.

(Biplab Das)

Dated: 16th July, 2014 Reg. No. 11610310

DEPARTMENT OF MECHANICAL ENGINEERING
INDIAN INSTITUTE OF TECHNOLOGY GUWAHATI
GUWAHATI–781039, ASSAM,INDIA

CERTIFICATE

This is to certify that the thesis entitled **"Numerical and Experimental Thermo-Mechanical Analysis of Sheet Forming by Laser Line Heating"** submitted by **Mr. Biplab Das (Reg. No. 11610310)** to the Department of Mechanical Engineering, Indian Institute of Technology Guwahati, is a record of original research work carried out under my supervision and it has not been submitted elsewhere for the award of any other degree or diploma.

The thesis in my opinion, has reached the standard fulfilling the requirements for the award of degree of Doctor of Philosophy in accordance with the regulations of the institute.

Prof. Pankaj Biswas

Department of Mechanical Engineering,
Indian Institute of Technology Guwahati,
Guwahati – 781039, India

16th July, 2024

ACKNOWLEDGEMENTS

I would like to express my heartfelt gratitude towards all those who have immensely helped me during this long arduous journey and eventually assisted me to emerge as an experienced researcher and a mature individual.

First and foremost, I must express my deepest sense of appreciation and respect for my thesis supervisor Prof. Pankaj Biswas for providing me the opportunity to work under their supervision. His persistent patience and friendliness in the moments of difficulties have always been remembered and also his constant encouragement have played a crucial role in writing the thesis and bringing it to its present form.

I would like to thank my doctoral committee members, Prof. P. S. Robi, Prof. S. Bag, and Prof. S. K. Majumder for carefully reading the reports at various stages of evaluation and providing many useful comments, which have helped in the development of this thesis.

My sincere gratefulness to past and present departmental heads Prof. D. Chakraborty, Prof. P. Mahanta, Prof. A. K. Dass and Prof. S. K. Dwivedy for their kind permission for enrollment, registration and several important supports at IIT Guwahati. I am also grateful to all the faculty members of Mechanical Engineering Department for giving me a comfortable and friendly environment for pursuing my research. I would also like to acknowledge the contribution of office staff, for helping me with various academic as well as non-academic issues.

I would like to express my sense of gratitude to Mr. N K Das, present Assistant Workshop Superintendent and all the staffs of the workshop specially Mr. Dilip Chetri, Mr. Mrinal Sarma , Mr. Chandan Banikya, Mr. Monoj Kr. Baishya, Mr. Gautam Gogoi and Mr. Gakul Das for extending their help in fabrication of the different experimental set-ups for this work.

I also wise to express my gratitude to Mr. Jiten Basumatary of the Advance Manufacturing Lab, Mechanical Engineering, IIT Guwahati for providing technical support for carrying out experiments and allowing me for using Laser instrument facilities with CMM.

The financial support of this research, which was provided by the Department of Mechanical Engineering, Indian Institute of Technology Guwahati, is gratefully acknowledged.

The most important support for this work came from my parents, Sri. Samarendra Nath Das and Smt. Jayashree Das for encouraging me to go still further at every points of life. I would like to thank my extended family for all of their love and support through the years, especially at peak of the economy encouraged me to pursue Ph.D on a modest stipend.

Finally the friends form an important part of this long and enduring journey, and without their constant support and encouragement, the completion of this thesis perhaps would have been an impossible task. I express my sincere thanks to Dr. Anil Deepati, Dr. Arpan Mondal, Dr. Arun Kumar Kadian , Mr. PVSS Sridhar, Mr. Pardeep Pankaj and Mr. Avnish Tiwari, Mr. Pranab Choudhury, Mr. Pranjol Paul, Dr. Purnendu Kr. Mondal, Dr. Jagannath sardar, Mr. Rakesh Bhadra, Dr. Kalpajyoti Bora, Dr. Bhaskor Bora, Dr. Mrinal Kumar Sarma, Mr. Kamaljyoti Nath,, Dr. Polash Pratim Dutta, Mr. Dhiraj Bora, Dr. Karam Mallik, Mr. Prasenjit Mukherjee, Mr. Pankaj Kumar, Mr. Sailen Dutta and many more with whom I have come into contact during my Ph.D study for their help and support.

I would like to extend my deepest gratitude to Prof. Anup Gogoi, Prof. Ashwini Kumar Baruwa, Mr. Ashim Kumar Debroy all the colleagues in the Mechanical Engineering Department and many others at NITS Mirza for their help and support in different ways during my Ph.D study. I shall forever be grateful to all my friends and well-wishers.

I consider myself privileged and fortunate to work in the Indian Institute of Technology Guwahati.

Above all, I am thankful to the Almighty.

16th July, 2024 Biplab Das

Abstract

In this study, a detailed strategy for sheet forming by laser line heating has been presented. The work presented in this thesis is concerned with the evaluation of the effect of process parameters on thermal history, residual deformation, residual stresses, and strains associated with the process of laser line heating. Residual deformation is induced on the metallic sheet due to the heating effect of a laser beam when irradiated over a suitable heating path. The deformation generally takes place due to the combined effect of yielding and temperature distribution across the thickness of the metallic sheet. Both numerical and experimental analyses on laser line heating were carried out to investigate the thermal history and residual deformation.

Numerous experiments were conducted using a CNC-operated CO_2 laser heating machine. The mild steel sheet was used as a substrate material for the process. The effect of each operating parameter was taken into consideration for finding the optimum parameter. The design of the experiment was applied with the help of the Taguchi method and the results were obtained and analysed with the help of Taguchi analysis (signal-to-noise ratio), for the determination of the optimized operating parameters with their effect towards residual deformation in the process. A regression analysis was also performed to obtain a suitable co-relationship between operating parameters and residual deformation.

Initially, a 3-D FE model was developed and was validated with experimentally obtained temperature distribution at various locations of the sheet material. The temperature distributions and residual deformations were evaluated by changing the process parameters of the sheet material. The sheet surface temperature was maintained within the recrystallization temperature of the sheet material. The results obtained from the temperature distribution were further utilized in structural analysis to predict the residual deformation stresses and strain pattern for the line-heated sheets. Here the non-linear elastoplastic transient thermo-mechanical analysis was carried out using temperature-dependent thermal and mechanical properties. The results of residual deformation obtained numerically were again validated with the experimental ones. The 3-D FE model was further utilized for the determination of the magnitude and distribution of the residual stresses and strains by changing the heating parameters.

The second part of the work was concerned with the development of a 3-D compound curved surface by the process of laser line heating. Two different compound curved surfaces i.e. a pillow and a saddle shape were considered. A large deformation elastic FEM technique was applied for the generation of blank. The principal stresses, strains, and bending strains distribution over the top and bottom surface for the individual curved shape were evaluated. Based on the results obtained from FE analysis, the position of the heating path was determined. The heating parameters for the individual heating path were decided based on the magnitude of the strain associated with the heating path for the individual curved surface. The laser operating parameters for the individual heating path were obtained from the results of the thermal strain from the heated zone obtained from different operating parameters from the 3-D FE model. Since, finite

element calculations are enormously time-consuming, in this work Artificial Neural Network (ANN) is used for the estimation of the heating parameters for the unknown strain values. Based on the stresses and strains field distribution pattern the experimental process parameters were decided and experiments were conducted to develop the compound curved surfaces by using the laser line heating processes. The experimentally obtained doubly curved shape matched fairly well with that of the actual shape.

Table of content

List of Figures

List of Tables

Nomenclature

Symbol	Description	Units
α_b	Bend angle	Degree (°)
α_{th}	Coefficient of thermal expansion of the work piece	$°C^{-1}$
P	Laser power	W
A	Absorption coefficient	m^{-1}
ρ	Density of the material	kg/m^3
c	Specific heat of the material	J/kgK
V	Traverse speed	mm/s
s	Sheet thickness	mm
l	Half-length of the heated zone	mm
E	Young's modulus of the material	N/m^2
Y	Yield strength	N/m^2
σ_s	Flow stress	N/m^2
r_b	Laser beam radius	mm
r	Distance from the center of the laser beam	mm
t	Heating time	sec
K	Thermal conductivity	W/mK
q	Heat flux	W/m^2
T	Temperature	°C
h_f	Convective heat transfer coefficient	W/m^2K
φ	Thermal diffusivity	m^2/s
q_c	Heat flux due to convection	W/m^2
q_r	Heat flux due to radiation	W/m^2

Chapter 1

Introduction

1.1 Preamble

Line heating with a suitable heat source is a process of shaping metallic plates (Ishiyama et al.1999). It is generally used for the fabrication of complicated shapes having double curvature. Its primary application can be in the automobile and shipbuilding industries; however, the same technique can also be gainfully utilized in any other metal forming applications (Dearden et al. 2003). A sheet with a single curved shape can be simply being produced by rolling, but for forming of double-curved sheet required skilled maker and use of heavy machinery. The double-curved sheets can be fabricated by applying force using press (with or without a die) or forming with the help of narrow rollers. Although these are proven techniques, there are some problems associated with them. In the case of press forming it is a very challenging task to predict the amount of over bent the sheet should be given for obtaining the correct shape after 'Spring back', and further the narrow roller forming makes the sheet thin in the worked areas.

Despite its advantageousness, the process is still not very well developed to enable an online application leading to an automated sheet bending facility, because the controlling of the process is very much difficult task. For that reason, it is generally regarded as the art performed only by the most skilled maker. Research interest on the mechanism of the line heating process aims to predict the final shape of the metal sheet subjected to heating conditions. A judicious method for the estimation of the pattern of heating lines and the heating amount would be very much beneficial.

In line heating process basically, a suitable heat source is traversed over a sheet surface, which induces thermal stresses. When the magnitude of thermal stress value exceeds the yield stress it leads to the formation of a permanent set of deformation on the sheet and the desired shape is obtained. The production of compound curved sheets is a tedious job. It solely depends on the pattern of heating lines that induce curvature by thermo-plastic effects (Chalfrant et al. 1998).

The process is controlled by the intensity of moving heat source, its rate of movement over the sheet and the position of scanning lines where the heat is to be applied to produce the desired shape of the curved patch.

Normally this process was initiated with the usage of oxy-acetylene flame as a heat source. It was extensively used for developing heavy engineering components, which are to be used in various sectors such as automobiles and shipbuilding industries. The heat source to be used for the line heating process must maintain the thermal gradient across the thickness of the sheet. Achieving a steep thermal gradient in an oxy-acetylene flame is a very difficult task and it solely depends on the operator's skill. The difficulty in getting the temperature gradient across the thickness direction of the sheet can greatly be resolved by using a laser as a heat source. The kinematics of the line heating process is shown in Fig.1.1.

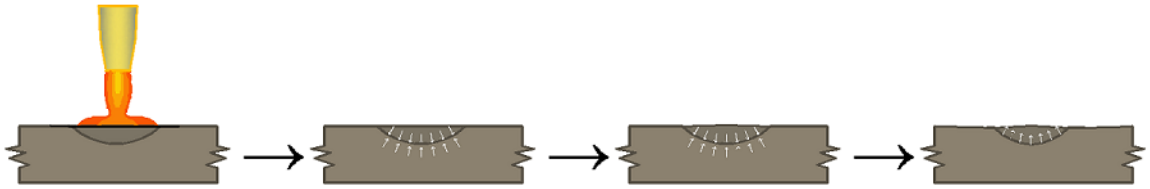

Fig. 1.1 Line heating kinematics

The line heating kinematics can be explained as below. In the process of line heating, the metallic sheet surface is heated under the action of a suitable heat source. With the rise in temperature the metallic sheet exhibits a reduction in yield strength followed by thermal expansion. Reduction in yield strength leads to the softening of the sheet material. The softening of the material is confined to the material, which is exposed directly to the heat source leaving the adjacent material with its original material property. This makes the sheet slightly thicker during heating. Now during the time of cooling, the material regains its original strength and the upper region which experiences more thermal expansion contracts during the time of cooling as shown in Fig.1.1. The rate of contraction is more for the material which is experiencing more thermal expansion, as a result, the sheet bends towards the beam.

1.2 Types of heat sources

The process of line heating has been categorized based on the type of heat source used:

- **Oxy fuel gas flame**: It is one of the cheapest and simplest heat sources based on availability and maintenance. For controlling the deformation precisely, the heat flux should be easy to control. It is found that the heat flux obtained from the Oxy-fuel (considering Oxy-propane) mixture is difficult to control because of the heat generation characteristics resulting from the reaction of gases. As in some cases, there is the requirement of high precision control of the deformed shapes, the use of oxy-fuel gas flame may be confined to certain specific applications. Here the gas amount is difficult to control and maintaining a constant distance between the gas torch and the sheet is very much strenuous.

- **Induction heating**: It allows precise control of the diffusion of heat and is dependent on the induced electrical field frequency. For knowing the feasibility of induction heating for line heating process various experimental studies and numerical calculations were carried out. This shows that the temperature obtained from the induction heating reaches the temperature required for steel sheet bending. It has been also found that the transverse shrinkage achieved in induction heating is the same as that of flame heating and the deformation profiles are found to be similar. Apart from that due to rectangular shape of the inductor, the residual plastic stress distribution in the center of the heating area is found to be even, in comparison to the flame heating where the heat source is Gaussian in nature and the residual plastic stress distribution is found to be uneven in the center of the heating area.

- **Laser beam heating**: It is one of the most precise controlled heating processes. It has become the most feasible process for shaping a metallic component. The process is similar to that of the flame bending process but accuracy in the development of the final product can be achieved by the process. The process uses a defocused laser beam for inducing thermal stresses in the work piece to produce controlled distortion. This technique does not require any mechanical contact between the tool and the work piece. In this study, the laser heat source is used for line heating purpose. The detailed about the laser heat source is given in section 1.3.

1.3 Laser generation

Laser is a consistent intense beam of light or electromagnetic radiation. The phenomenon of light amplification is achieved by stimulated emission due to the incident photons of high energy. It consists of three principal components, they are: laser medium, means of exciting the laser medium into its amplifying state and optical delivery system (Majumdar and Manna 2003). In case of the CO_2 laser, CO_2 gas is used as a laser medium. Here the energy is supplied by current flow. The energy causes the laser medium to fluoresce and generate intense monochromatic, unidirectional and consistent rays. The schematic set up of CO_2 laser is shown in Fig.1.2.

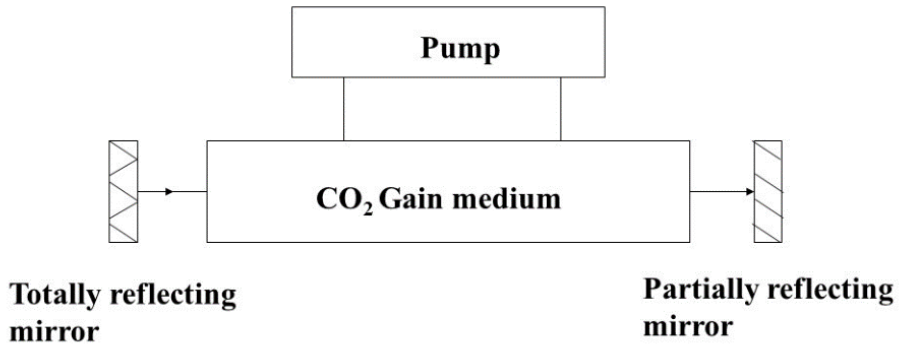

Fig.1.2 Schematic set up of CO_2 laser

A CO_2 laser device consists of three main elements: a laser medium, a cavity with two mirrors and an energizing source that supplies energy to the laser medium as shown in Fig.1.2. According to the principle of quantum mechanics, when energy is supplied to an atom, it attains an excited state as shown in Fig.1.3.

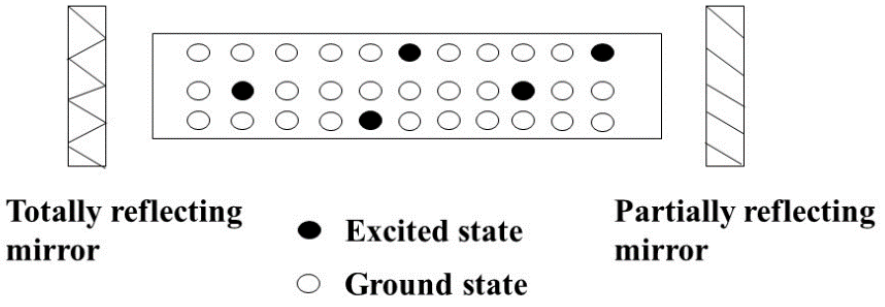

Fig.1.3 Excitation of atoms

The excited atom doesn't stay in higher energy state for a long period and spontaneously returns to the ground state from the higher energy state by emitting of energy difference as a photon of frequency (ν):

$$\nu = (E_2 - E_1)/h \tag{1.1}$$

where E_2 represents energy at higher energy state, E_1 is the energy at lower energy state and h is the Planck's constant. This phenomenon is known as spontaneous emission as shown in Fig.1.3. A spontaneously emitted photon again excites another atom and stimulates it to emit a photon by de-exciting it to a lower energy level. The process is called stimulated emission of radiation as shown in Fig.1.4.

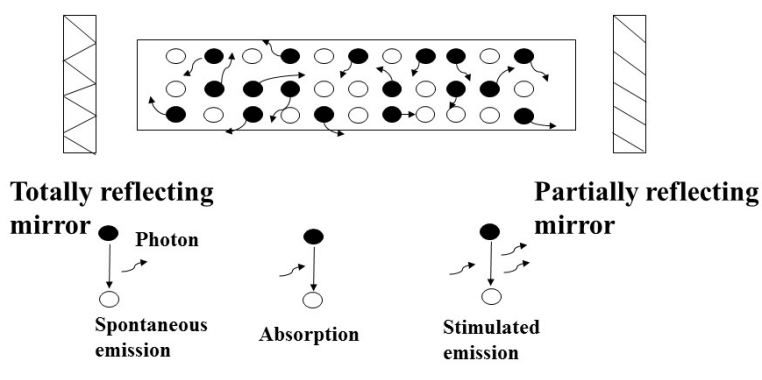

Fig.1.4 Spontaneous emission of radiation

The emitted photons have a matching wavelength, phase, and polarization. A photon interacting with an unexcited atom may get absorbed by it and excite it to a higher energy state. This condition is called "population inversion" and is created by energizing source. The photons moving along the optic axis interact with a large number of excited atoms, it stimulates them and as a result of this process, the photons get amplified as shown in Fig.1.5.

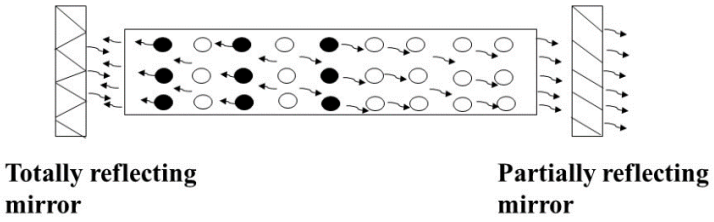

Fig.1.5 Stimulated emission of radiation

The photons are reflected back and forth by the totally reflecting and partially reflecting mirrors and at last pass through the excited medium creating more photons. These photons exit through the partially transmitting mirror as an intense laser beam as shown in Fig.1.5. Finally, the laser beam is allowed to fall on the work piece.

1.4 Laser-matter interaction in material processing

The laser material processing involves the combination of laser radiation to the electrons within the metal surface. The laser-matter interaction within the surface region achieves extreme heating and cooling rates. The process starts with the absorption of photons from the incident laser beam promoting electrons within the metal to states of higher energy. The energy of the CO_2 laser photon is 0.12 eV. The electron in the higher energy state loses energy to return to its equilibrium state after photon excitation. The overall effect comes in the form of heat. That heat is necessary for material processing applications.

1.5 Laser forming mechanism

In the case of the laser line heating process, the laser source induces a constant heat flux through the surface which makes a high thermal gradient across the thickness of the sheet. With that, for maintaining a high thermal gradient the surface temperature of the sheet must be maintained below the melting temperature of the sheet material. The deformation in the sheet material during laser-material interaction depends on both laser process parameters and the material properties of the metallic sheet. The strain induced in the material depends based on the selection of laser operating parameters for the process. If the strain-induced is uniform throughout the thickness of the material, then the material behaves to shrink and shorten in length. If the strain-induced is non-uniform throughout the thickness, the material tends to bend resulting in in-plane or out of plane bending. There are different distinct mechanisms of laser forming process. The laser process parameters play a very significant role in the selection of a laser forming mechanism, which is to be used for the process. The laser line heating process uses the laser forming mechanism, which has been classified into three different categories and are outlined below.

- **Temperature gradient mechanism (TGM):** It is the most widely used mechanism for bending the metallic sheet out of the plane towards the laser (Edwardson 2000). The process parameters selected for maintaining TGM are such that it led to the development of a steep temperature gradient across the through-thickness of the metallic sheet as shown in Fig.1.6.

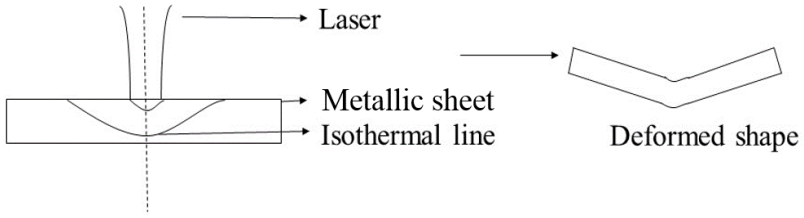

Fig.1.6 Temperature gradient mechanism

Here the selected laser diameter is of the same order or a bit larger than that of the thickness of the metallic sheet. The traverse speed along the heating path should be selected large enough so that a steep temperature gradient is to be maintained along the through-thickness direction. The temperature gradient needs to be varied based on the material to be used. The laser scanning path on the sheet surface is selected as a straight line across the whole sheet. Initially, the bending of the sheet occurs in the direction away from the laser. The bending occurs because of the development of the bending moment obtained due to the amount of plastic tensile strain at the heated surface. With the development of heat, the mechanical properties associated with the material get reduced. Once the thermal stress attains the temperature-dependent yield stress, any additional thermal expansion is converted to plastic compressive strain because free expansion is inhibited by surrounding material. During cooling, material contracts again in the upper layer and because it has been compressed, there is a local shortening of the upper layer of the sheet and a bend angle develops that bend the specimen towards the laser beam as shown in Fig.1.6.

- **Buckling mechanism (BM):** In this mechanism the diameter of the laser beam is considered to be ten times that of the thickness of the sheet material. Here, the temperature gradient is found to be negligible across the thickness of the sheet as shown in Fig.1.7.

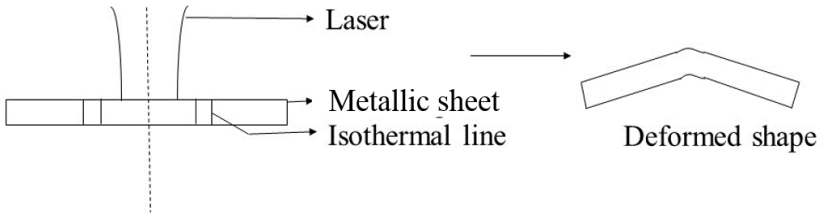

Fig.1.7 Buckling mechanism

During heating, thermal compressive stresses are developed in the sheet material which results in the generation of a large amount of thermal strain. With the development of high temperature and generation of thermal strain, results in thermo-plastic buckling of the material as shown in Fig.1.7. The phenomenon of buckling of the sheet material is induced along the entire line heating path of traversing heat source. One of the most important features associated with the buckling mechanism is related to the direction of bending. The bending of the sheet may take place towards (positive bending) or away (negative bending) from the laser beam. The bending behavior can be effectively controlled by various important factors which include: initial pre-bending of the sheet, pre-existing of residual stress and counter bending due to temperature gradient. The forming of the pre-bend sheets may be positive or negative depends on the pre-bend angle and it increases with subsequent laser forming. The presence of pre-existing stresses also influences the angle of bend. If the surface of the sheet has pre-existing compressive stresses, then the subsequent laser forming facilitates the positive bending of the sheet. The bending direction can also be influenced by counter bending during heating operation. Even though the buckling mechanism is not associated with temperature gradient developed in the material, a minimum amount of temperature gradient is always present in the material during heating. This negligible amount of counter bending facilitates the development of a negative bend of the sheet material.

- **Shortening mechanism:** In this mechanism, the diameter of the laser beam is considered to be much smaller as compared to that of sheet thickness as shown in Fig.1.8.

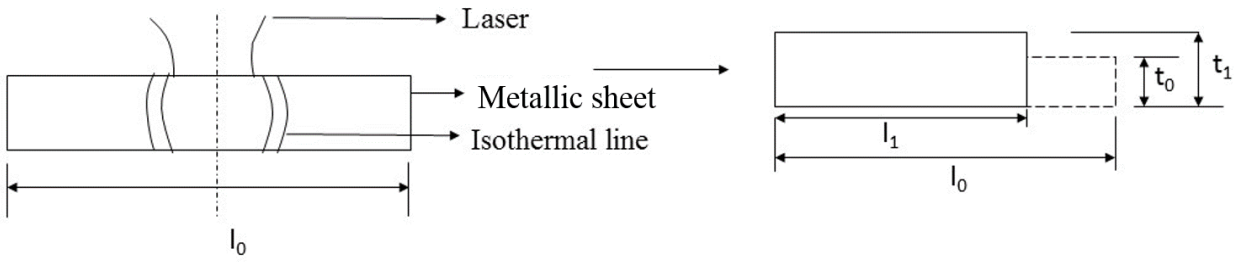

Fig.1.8 Shortening mechanism

This results in homogeneous heating of the sheet surface. Due to restriction in thermal expansion from surrounding material, the sheet is compressed with an almost constant strain along the thickness causing shortening of the sheet with an increase in sheet thickness as shown in Fig.1.8. It is seen that the length of the specimen l_0(initial length of the specimen) is reduced to l_1 (final length) with corresponding increase in thickness from t_0 to t_1 of the material. Subsequent heating of the sheet along the line across the sheet width leads to an increase in overall thickness with a shortening of the sheet.

Out of which temperature gradient mechanism (TGM) is most widely used for bending of sheet and plates. In the present work, the temperature gradient mechanism (TGM) has been used for the entire process.

1.6 Present investigation

In laser line heating process, more control of the final product can be achieved as compared with flame bending process. The process uses a defocused laser beam, which induces thermal stresses without melting the surface of a work piece to produce control distortion as shown in Fig.1.9. This internal stress induces plastic strains, bending or shortening the material, which results in local elastic-plastic bending of the work piece depending on the mechanism used.

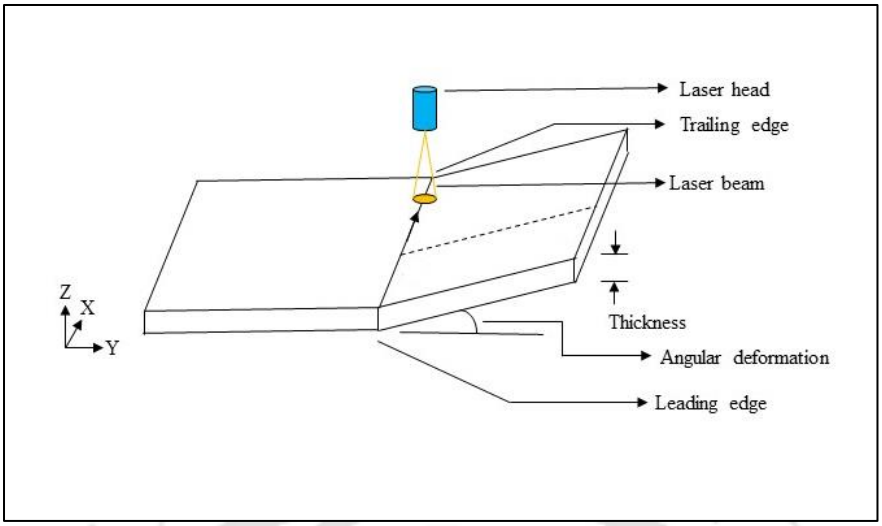

Fig.1.9 Schematic diagram of straight laser line heating

The process imparts a significant value to the industries that previously relied on expensive stamping dies and presses for prototype evaluations. In this work mainly TGM was employed to develop the compound curved surfaces by laser line heating process.

1.7 Advantages

The advantages of laser line heating process are as below:

- Forming without the need for specialized dies i.e. the mechanical contact between the work piece and the forming tool (the laser beam) is not required.
- In this process, the amount of heat obtained from the heat source can be greatly controlled. There is a decrease in energy consumption because in this process heating is confined to the line to which bending is to be done.
- The set up time for the process is very much low.
- The overall advantages can be summarized as increasing process flexibility (Rykalin 1960).

1.8 Limitations

- The process is comparatively slow. Due to the repeated movement of the heat source on a particular path there occurs deformation, which results in increment in tensile strength with a decrement in ductility and fracture toughness of the material.

- Laser bending is not acceptable from energy and economic point of view for making simple shapes.

1.9 Applications

In the present-day scenario, lasers are being used in numerous applications. Laser forming process is considered to be the most cost-effective in the designing and manufacturing processes (Fay 1967), these include:

- Rapid prototyping of irregular shapes for turbine blade applications.
- Non-contact forming for installation and adjustment of non-accessible parts.
- Automotive shapes for prototype and validation testing.
- Aerospace shapes for the precision shaping of tanks and pressure vessels.
- Unbending techniques for repairs and alignment applications.
- Tube and pipe precision forming.
- Profile making of ship hull structure for the improvement of production quality.

1.10 Research objectives

The main focus of this thesis is on sheet forming along with the development of the compound curved surface by laser line heating. Based on the gaps found in the published literature the following objectives of the present study have been decided:

- Thermo-mechanical analysis of the sheet forming by laser line heating.
- The theoretical determination of the heating parameters and heating pattern for achieving a given 3D curved surface.

➢ The following steps are to be followed for achieving these objectives:

- Modeling of the moving heat source and evaluation of transient thermal history.
- Transient elasto-plastic thermo-mechanical analysis of the laser line heating process.
- Effect of operating parameters on thermal history, residual deformation and stresses/strains.
- Estimation of strain field distribution for a given curved surface.

- Blank generation from the given patch.
- Determination of the heating path and suitable heating parameters, which are required for producing the patch.
- Experimental validation of the proposed scheme for the generation of the compound curved surface.

1.11 Target application

The process can be gainfully utilized for the development of the compound curved surface by the laser forming process. This proposed process and mechanism have a high potential towards the shipbuilding and automobile industries for the development of accurate net shape manufacturing of sheet metal components along with a secondary distortion correction process.

1.12 Thesis structure

The overall aim of the current work is to explore and analyze the mechanics of the laser line heating process and to establish an overall procedure for the estimation of the amount of heat required for obtaining certain curved shapes.

The content of the thesis is divided into following chapters:

- Chapter 1: gives background, types of heat source, laser-material interaction as well as laser forming mechanism associated with the laser line heating process. It also presents the objective of the thesis work.
- Chapter 2: provides the detailed literature review of the various study conducted on the laser line heating process through numerical and experimental approach.
- Chapter 3: it contributes to the information regarding the methodology applied to the current numerical and experimental study.
- Chapter 4: it presents the results of the effect of operating parameters on sheet forming by laser line heating.
- Chapter 5: it covers the transient thermal analysis and thermo-mechanical analysis of sheet forming by laser line heating
- Chapter 6: it dedicates to the development of the compound curved surface by laser line heating.

- Chapter 7: it summarizes the entire work of the thesis, the conclusions drawn from the study and the future scope associated with the present investigation.
- The thesis ends with bibliography and research outcome.

Chapter 2

Literature Review

2.1 Introduction

The research activity in the process of line heating started decades ago. Till date, less number of researchers have taken up the scope of line heating process for better control. Different methods have been taken into consideration for understanding the mechanics of the process. The process is basically based on localized heating without exceeding the recrystallization temperature of the substrate material and then followed by normal cooling.

The process of line heating has been found to be most efficient and popular for various surface development activities, for that reason many attempts has been taken by various shipyards across the world for implementing the line heating technique for sheet bending operations. Some of them are Todd Pacific shipyard (Chirillo1982), astillerosEsplanos (Spain) (Clausen 2000), Fincantieri (Italy), Daewoo (South Korea), Mitsubishi,IHI (Ishiyamaetal.1999) and NKK(Kitamura et al.1996) in Japan, Atlantic Marine Shipyards, NASSCO and Norfolk Naval Ship Yard in the USA.

This section has been sub divided into important sub groups and a brief review has been described, topic wise under the above subgroups.

2.2 Categories of line heating process

2.2.1 Based on types of heat sources

- **Oxy fuel gas flame**: It is one of the cheap and readily available heat source. For obtaining precise control over deformation, there should have ease control on the amount of heat flux. Poor control of heat flux has been obtained from mixed gases (for oxy fuel gas) as it is difficult to control the heat generation features resulting from the reaction of gases (Bae et al. 2009). It is also difficult to control as regards repeatability

in gas amount and as regards keeping a constant distance between the gas torch and the sheet (Clausen 2000).

- **Induction heating**: It allows for much precise control of the penetration of heat and depends on the frequency of induced electrical field (Biswas 2008). For knowing the feasibility of induction heating for line heating process various experimental studies and numerical calculations were carried out which reveals that sheet bending in case of steel as a material can be achieved by induction heating (Zhang et al.2011).
- **Laser beam heating**: It is one of the most precise controlled heating processes. It is one of the most applicable techniques for forming of metallic sheet component (Dearden & Edwardson 2003). The process is similar to that of flame bending process but high precision can be obtained on the final end product, formed by this process. The process can be best suited for automation and combination with protective gas which reduces the risk of oxidation of the surface (Dearden & Edwardson 2003).

2.2.2 Based on the mode of operation

On the basis of operating mode, the process of line heating can be classified into-Manual mode, Semi-automatic mode and Automatic mode.

- **Manual line heating process**: Reports on the procedure for the implementation of manual line heating are being obtained through the National Ship Building Research Program (NSRP) of the United States (Biswas 2008). Among these the first report was published from the Todd Pacific Shipyard (Chirillo 1982) is a manual on the guidelines for performing the line heating for forming of sheet and stiffeners. This work was supplemented by Scully (Scully 1987) with an investigation of the possibility of using laser as a heat source. The philosophy of manual line heating process was transferred to the Spanish Shipyard AstillerosEspanoles in the early 1990s and a manual was published (Clausen 2000) on that occasion. Compound curved surface forming technique can be avoided, if the parts of a ship are designed by means of developable spline surfaces as described by Chalfrant and Maekawa (1998), however, presence of certain critical constraints lacks the feasibility of the process in most of the ship types.

- **Semi-automatic line heating process**: Iwamoto et al. (2010) published one article on line heating technique which describes about the operations, where there is interactively working of worker with the help of a monocular video see- through head mounted display. This interactive work support technology must be extended for further research, so that workers can perform the task with ease without much expertise in skills. The process of different forming technology needs experienced and skillful individual for the required process. This technology can be applicable to various applications, especially for the line heating process.
- **Automatic line heating process**: In case of traditional method for sheet bending, the process basically comprises of two steps: firstly, the plane sheet is rolled for obtaining transverse bending deformation in short edge direction by using the three-roller bending machine. Then the curved sheet is then relocated to the line heating workshop for longitudinal deformation by line heating. Thus, the plane sheet is formed to a 3 D surface patch as per the requirement or designed. The main drawback lies in the spring back effect in the rolling process, which is very much difficult to control the appropriate over bending magnitude in the rolling process. Based on the above difficulties investigation on the process design method of forming plane sheet to 3 D surface sheet by pure line heating technology without the mechanical rolling process has been proposed by Wang et al. (2006a), where the present process of line heat forming can be done by using curvature analysis. Apart from that based on expert system of steel sheet forming a robotic controller has been used for bending of the steel sheet by the process of line heating of a large complex curved surface. The research work has been designed and proposed by Wang (2002).

2.3 Temperature field analysis

Temperature gradient is the main driving force for bending thick sheets, various analytical methods are proposed for the determination of temperature field which is required for the simulation of the line heating technique.

2.3.1 Heat input estimation

Wang et al. (2006b) has developed a heat flux model of gas flame by utilizing Gauss distribution heat input model and the method of experiment combining with numerical simulation. The parameters of the heating and heating radius in the heat input model are adjusted to a possible range to make the temperature distribution of numerical simulation approach to the data measured in experiment and then the heat flux model is determined. The reliability of the heat input model in the simulation is well verified.

Osawa et al. (2007) has proposed a new hypothesis regarding heat transmission during line heating. It states that the distribution of the temperature of the gas adjacent to the sheet and the overall heat transfer coefficient is dependent on the gap between the tip of the torch and the substrate material. The technique has been developed and the experiment has been carried out and it has validated well. The values of sheet temperature obtained from direct heat conduction analysis were well validated for both spot heating and line heating process. Here the temperature of the gas adjacent to the sheet and overall heat transfer coefficient were used as a thermal boundary conditions for the analysis. This indicates that heat transmission can be estimated for any desired sheet shape, dimension and torch movement history.

Zhang et al. (2006) presented the effect of line heating factors including: heat input, heating line position from sheet edge and sheet size on angular deformation was explored with the numerical simulation. The main motto was to develop a co-relationship between the angular deformation and the heating parameters, which are required for fabrication of ship hull by the process of line heating.

2.3.2 Analytical models

Rosenthal (1946) and Rykalin (1960) proposed the analytical method for the determination of the temperature distribution. Fay (1967) has described the total heat flux from a gas torch, where he has used a calorimeter for measuring the power from a range of different burners and fuels. In reference to the line heating process, the heat flux distribution is assumed to follow Gaussian distribution nature. Rykalin (1960) has proposed the idea, which has been adopted by Moshaiov and Lattore (1985), Ueda et al. (1994c) and Shin et al. (1996).

Yu et al. (1999) has presented an idea for modeling a laser beam. They have just modified the Gaussian distribution of heat flux by increasing the core radius. Moshaiv and Lattore (1985) has used point heat source for obtaining analytical solution. Jang et al. (1997) has proposed a model which uses a point source resulting in predicting the temperature field but considerable errors is present in the solution. Tomita et al. (2001) has obtained the heat flux of measuring the velocity profile of the torch flame. Ogawa et al. (1994) has simulated the process of heating by high frequency induction.

Himmati and Shin (2007) made a practical implementation of the analytical solution to investigate the phenomena of heat transfer during forming of sheets by the process of flame bending. An analytical solution was developed by Manca et al. (1995) which was then used for solving 3-D quasi stationary problem by Hemmati and Shin (2007) for finite width and depth problem. Here the circulating Gaussian moving heat source has been used.

Cheng et al. (2000a) has developed a model for obtaining the temperature field distribution in relation to the process of laser forming. The analytical modeling requires less computing time than that of finite element method (FEM) and finite difference method (FDM). It reveals that the temperature decreases with the increase in thickness and remains same till the critical thickness is reached. Kalyon and Yilbas (2001) have proposed that the variation in temperature field leads to the creation of thermal strain in the region irradiated by laser beam, which leads to the development of stress field.

Xiufeng et al. (2003) has verified the simulation result with the experimental ones. Here the lower surface temperatures of the sheet metal were well verified with the temperature obtained from simulation under the laser scanning line. The simulation results act as a basis for the selection of suitable laser parameters. Ash-by and Easterling (1984) has adopted an analytical approximation of temperature field in material.

Zhihui et al. (2011) has investigated on the basis of DOE (Design of Experiment) based on numerical investigation of the factors affecting temperature field during line heating. Three main influencing factors were sourced out, they are: sheet thickness, flow of acetylene and velocity of heat source. The analytical result indicates that there exist interaction effects among the three main influencing factors. The investigation demonstrates that DOE is an efficient method for the study of temperature field during line heating.

Tangyunyong (2003) proposed the thermal distribution of the interconnect geometries where spreading has been dominantly making a difference by interconnect geometries than by variation in the size of the laser spot. Mild temperature increase has been observed during laser heating of the interconnected structure, composed of copper and dielectric material (low thermal conductivity value) than those of conventional aluminum, tungsten and silicon dioxide. The heat conduction is mainly affected due to the material densities. The temperature rise varies slowly. In laser heating process the temperature can be expressed as a function of density of the material. Yilbas and Al-Aqeeli (2003) have proposed a mathematical formulation for predicting the stress and temperature distribution under the laser pulse heating process. The selection of parameter for laser pulse heating process is such that, the surface temperature of the substrate material is maintained below the melting temperature of the material (substrate). Marya and Edwards (2002) proposed a suitable mathematical model on laser forming of Ti-6Al-2Sn-4Zr-2Mo and the model is developed on the basis of laser power, traverse speed and sheet thickness to radius of the beam ratio. It has been perceived that significant bending angle is obtained when the surface temperature is near to 0.48 times of the melting temperature and optimum is obtained at 0.65 times of the melting temperature.

2.3.3 Numerical models

Holzer et al. (1994) modeled the buckling mechanism (BM) by using commercial FE-software. For modeling the amount of heat as an input obtained from non-uniform heat flux FORTRAN functions has been used for the purpose. Ji and Wu (1998) has proposed a numerical model for methodically determination of the temperature distribution over a metallic sheet under the process of laser forming along with the effect of process parameters.

Chen et al. (2002a) has also developed a computational model for the determination of the temperature field with an idea of non-Fourier heat transfer equation and the changes were taken into consideration. Shen et al. (2007a) proposed a model for heat transfer for the laser forming process. The outcome shows that the heat exchange by radiation along the boundaries has an insignificant effect. Choi et al. (2012) proposed the distribution of temperature by the process of line heating over a metallic sheet. The variation of temperature was observed under the influence of heating parameters in the process of automatic line heating process. The variation of temperature was seen with change in variables, which includes: moving velocity

of heat source, heating strength and heating ways. The numerical result shows that increasing moving velocity of heat source leads to decrease in peak temperature. It also reveals that peak temperature varies linearly with the quantity of heat from the heat source.

2.4 Thermo-mechanical analyses

Sheet forming by line heating using laser is a non-linear thermo mechanical process. Various numerical and analytical analyses have been carried out for the prediction of parameters (mainly deformation) in response to the line heating process. Iwamura and Rybicki (1973) have presented a solution to a 2-D problem consisting of beam perpendicular to the heating direction by using FDM. Moshaiov and Shin (1991) has presented a theory where the heated sheet is represented by a spring. This concept has been implemented successfully to the case of elastic phenomena, but it is difficult to determine the spring constant, when plasticity is considered. More work out to be done in finding the load and angular deformation for the process of line heating.

2.4.1 Estimation of bend angles

2.4.1.1 Analytical models

- **Based on temperature gradient mechanism (TGM)**

  Vollertsen (1994) has developed an expression for obtaining the bend angle. The expression obtained is on the basis of two-layer model for TGM. The expression for the bend angle, considering the process parameters and material properties is as follows:

$$\alpha_b = \frac{3PA\alpha_{th}}{\rho V S^2 C_p} \tag{2.1}$$

  where α_b,α_{th}, P, A, ρ,c_p, V and s are bending angle, coefficient of thermal expansion of the work piece, laser power, absorption coefficient, density, specific heat capacity, velocity and the sheet thickness.Yau et al. (1997) also proposed a similar model where a two-layer model approach, which has been extended for including the counter bending effect, for taking into account of some of the pure elastic strains, which resulted into two equations, one for obtaining the counter bending angle and

another for obtaining the bending angle after cooling. The expression for the bending angle which is obtained by this method is

$$\alpha_b = \frac{2lPA\alpha_{th}}{2\rho V s^2 C_p} - \frac{36lY}{sE} \tag{2.2}$$

where l is the half length of the heated zone, E is the Young's modulus, Y is the yield stress, s is the sheet thickness, C_p is the specific heat, V is the velocity, ρ is the density, α_{th} is the coefficient of thermal expansion, A is the absorption coefficient and P is the laser power.Mucha et al. (1997) has derived an expression for obtaining the angular deformation, the expression obtained is based on TGM. The output obtained reveals that the heat capacity and the coefficient of thermal expansion have a significant effect as material parameters with reference to that of laser forming process. Kyrsanidi et al. (2000) has developed a parametric mathematical model where plastic bending is considered at the time of heating. It is also found that the developed model took very less computing time in comparison to the existing model. Similar model has been given by Cheng and Lin (2001). Yu et al. (2001a) has developed a thermo-mechanical model for predicting the deformations of metal sheets under the line heating process. The model utilizes the effect of heat loss and the semi-analytically determined temperature distribution and distributed moving heat source has been deployed for obtaining the dimensions of the critical heat affected zone (HAZ).Mucha et al. (2003) has developed a formulation for the determination of the surface temperature for evaluating the effective bending. Cheng et al. (2005) proposed an analytical model for predicting the size effect on the basis of numerical and experimental results. Here the effect of sheet width is taken into account by modeling the moving strip heat source over a finite strip width. The model compares well with the existing analytical model. Shen et al. (2006a) has derived a formula for obtaining the bending angle by the process of laser forming. The model has been developed on the basis of conventional equilibrium and compatibility conditions. Mucha (2007) has developed a model for the process of sheet bending on the basis of TGM. The model provides solution for longitudinal and transversal angular

deformation. Shi et al. (2007) presents the study of temperature gradient mechanism (TGM) for the forming process. Under processing condition of TGM, the sheet bends in the direction of both *x* and *y* axis. The model has been developed for estimating the bending angle about y-axis; it is being build based on theories of heat transfer and mechanics of elasto- plasticity. Bending along y-axis has been studied and described for the deformation of sheet. Sistaninia et al. (2009) introduced a new technique for laser forming by using dithering and rotating beams. Both analytical and numerical solutions were developed for solving transient conduction equation. In this case a plane slab is heated with the help of a rotating or dithering beam on the surface. The temperature distribution act as a input load for 3-D nonlinear structural analysis for determination of bending angle and distortion. Nguyen et al. (2009a) proposed a simplified elasto plastic model for determination of deformation by triangle line heating by analytical means. For determination of the plastic region in the case of induction heating, the induction heating process has been modeled with numerical heat flux and heat flow analysis. Chen et al. (2010) presented a model for the prediction of the temperature distribution; it has been developed on the basis of the similarity of temperature obtained at different thickness for predicting the angular deformation. In this process the deformation field is dependent on the temperature field. The analytical results validate well with the experimental ones. Das and Biswas (2017) proposed a procedure for obtaining the optimized values of the operating parameters, which include scanning speed, laser power and number of scans on the angular deformation with the change in thickness of the substrate material based on TGM. The results are analyzed under Taguchi analysis and analysis of variance (ANOVA). A regression analysis has also been performed for obtaining a suitable co-relationship between bending angle and other operating parameters.

- **Based on buckling mechanism (BM)**

This mechanism uses beam diameter, larger compared to that of sheet thickness. This lead to the development of large quantity of elastic plastic strain develops which results in elastic-plastic buckling. According to the Vollertsen model (Vollertsen et al.

1995), the strain near the center of the laser is considered to be elastic in nature. The expression, gives the final bending angle obtained using mechanical bending theory is

$$\alpha_b = \left(\frac{36\alpha_{th}\sigma_s PA}{E\rho C_p V S^2}\right)^{\frac{1}{3}} \quad (2.3)$$

where α_b,α_{th},σ_s,P,A,E,ρ,C_p,V and S are bending angle, coefficient of thermal expansion of the work piece, flow stress, laser power, absorption coefficient, young's modulus, density, specific heat capacity, velocity and the sheet thickness. Shen et al. (2006d) proposed a model. Here the plastic deformation has been calculated by considering both heating and cooling and history dependent stress-strain relationship. Shi et al. (2008) proposed a decision-making criterion of working conditions for BM ($F_{buckling\ value}$) for the determination of bending directions for different process parameters. The results suggested that the bending direction is solely dependent on the $F_{bukling}$ value.

- **Based on upsetting mechanism (UM)**

  Krauss (1997) proposed a model for obtaining a box section by the process of laser bending. Under upsetting mechanism, the box section can be obtained by selecting suitable sequence of laser irradiations. Similar model has been developed by Vollertsen where strain relationship is correlated with process parameters. The final expression for the bend angle was found to be:

$$\alpha_b = \frac{1}{b}\left(\frac{2\alpha_{th}PAb}{\rho C_p V(2dS - S^2)} - \frac{\sigma d\rho_s}{E}\right) \quad (2.4)$$

  where b is the breadth of the bending edge, and d is the laser beam diameter.

2.4.1.2 Numerical models

Hu et al. (2001) has developed a 3-D FEM simulation which contain non-linear transient indirect coupled thermal-structural analysis for the temperature dependent thermal and

mechanical properties of the materials. Here the thermal flux densities act as a thermal load in the process of simulation as shown in Fig.2.1 as follows:

$$I = \frac{2AP}{\pi r^2}\exp(-\frac{2r^2}{r_b^2}) \tag{2.5}$$

where I, A, P, r_b and r, are thermal flux density of the laser beam, the absorptivity of the sheet metal surface, the laser power, laser beam radius and distance from the center of the laser beam. The mean thermal flux density within the region of laser scanning over the sheet metal surface is given by:

$$I_m = \frac{1}{\pi r_b^2}\int_0^{r_b} I(2\pi r)dr = \frac{2\pi}{\pi r_b^2}\int_0^{r_b}\frac{2AP}{\pi r_b^2}\exp\left(-\frac{2r^2}{r_b^2}\right)rdr = \frac{0.865AP}{\pi r_b^2} \tag{2.6}$$

The heating time "t" directly depends on the laser beam radius r_b, inversely depends on the relative motion "V" between work piece, laser beam and the as follows:

$$t = 2r_b/V$$

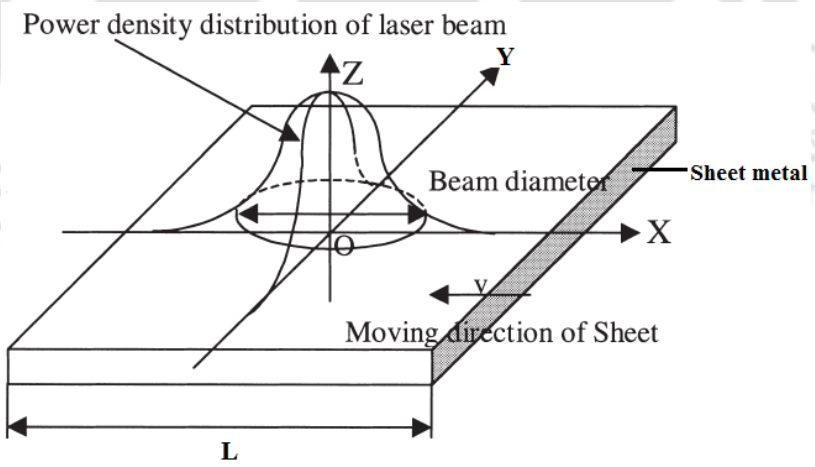

Fig.2.1 Model of laser beam scanning on the sheet metal (Hu et al. 2001)

The bending angle, stress-strain distribution, temperature and residual stress are obtained from computer simulation. The angular deformation is affected by both thermal and mechanical properties of the substrate material.

Zhang et al. (2004) has proposed a model based on finite element method for the process of laser forming. Steel is used as a substrate material. The numerical results under different discretization conditions were considered and this validates well with the experimental ones. Zhang and Michaleris (2004) proposed a comparative study between a 3-D Eulerian and Lagrangian FEM models. Both the Lagrangian and Eulerian approach compares well within the experimental result. Eulerian results give result faster than that of the Lagrangian approach especially for large parts.

Hsieh and Lin (2004) presented a study on transient deformation of thin sheets of stainless steel under pulse mode of laser heating. The study reveals a good agreement of bending angle obtained numerically and experimental method. The magnitude of bending angle increases with the increase in laser power, beam radius and vice versa. It decreases with increase in thickness, keeping peak temperature constant. Okuda et al. (2004) proposed the deformation mechanism of magnesium alloy sheets along with the plastic bending properties obtained under the laser forming process. The work is based on experiments and FEM simulation analysis. The temperature distribution in the work piece is evaluated by using FEM thermal conduction analysis. The bend angle obtained is proportional to that of the substrate surface temperature. Venkadeshwaran et al. (2010) presented a 3-D numerical simulation model for a circular sheet under laser bending process. Here continuous heating has been replaced with discrete section heating in certain regions. Chakraborty et al. (2016) proposed that with constant spot diameter and laser power, the sheet blanks bent more for higher irradiation time. The trend of experimental results obtained has been well explained with the finite element simulations.

2.4.2 Line heating induced stresses, strains and residual deformations

2.4.2.1 Analytical models

Line heating stresses, strains and deformation are closely related phenomena. Rao (1998) has proposed that line heating plastic deformations a metal originate from thermal stresses and

strains. Thermal stresses disappear with equalization of temperature. During the process of heating and cooling there is a development of thermal strains in the line heated zone and its adjacent area. The strain induced at the time of heating is associated with the plastic deformation which enables it for undergoing residual deformation. Watanabe and Satoh (1961) have calculated the line heating deformations using analytical approaches. Analytical methods are being used for estimating the deformations, which has undergone due to line heating process. Thermo-mechanical analysis of rate of line heating is not dependent on the material model with temperature dependent material properties. Michaleris and DeBiccari (1997) have assumed kinematic work hardening for mild steel. This is the common material model available for the process of line heating analysis together with Von Mises yield criterion and associated flow rules (Clausen 2000; Zienkiewicz (2001)).

Moshaiov and Vorus (1987) determine a combination of the differential equation of a Kirchoff plate and a membrane theory coupled by constitutive relations (plasticity). However, boundary element solution to the plastic Kirchoff plate was found and solved. Adak and Mandal (2004) has proposed a technique in which initial non-linear problem with varying modulus along with the variation of temperature has been converted to a pseudo linear equivalent system with constant rigidity and the problem is effectively dealt by linear analysis. Kalyon and Yilbas (2001) proposed about the analysis on generation of thermal stress by laser pulse heating technique. Analytical results for the determination of temperature and stress fields were acquired by Laplace transformation. In case of stress free surface condition, the stress wave propagates towards the substrate material.

Jang et al. (1997) has developed a model for the determination of the deformation of sheet on the basis of thermo-elasto-plastic analysis. It has been again adopted by Jang et al. (2005) for the determination of deformation of steel sheet under the process of triangle line heating. For the induction of the strain, a circular disk spring model has been put forwarded for undergoing 2-D thermal elasto-plastic analysis. Son et al. (2007) developed a model for analytically determination of deformations of metallic sheet by the process of line heating. The heat source used here is the gas tungsten arc (GTA). The results of the vertical displacement validate well with that of the experimental. Following cases were observed, while experiment and analysis: (i) Deformation near the region closed to the heating lines (local). (ii)Entire

displacement in vertical direction near the heating lines. Both the case validates well with the experimental ones. According to Son et al. (2007) proposed a formulation for estimating the deformation of sheets by the process of line heating. The parameters were also developed using Eigen strain concept. The calculated results from the model validates well with the experimental ones.

2.4.2.2 Numerical models

Zienkiewicz (2001) and Jang et al. (2005) has performed FE analysis using commercially available software and reference books (Reddy 2003) for basic formulation of thermo mechanical analysis. Biswas et al. (2007) proposed a model on determination of the pattern of deformation with reference to the heat input for a single pass line heating process. A 3-D transient thermo-mechanical analysis for the process of line heating has been studied using oxy-acetylene gas flame used as a heat source. During the analysis temperature dependent material properties, Newton's convection and Gaussian distribution of heat source is taken into consideration.

Biswas et al. (2010) proposed a dimensional analysis for obtaining a co relation between input parameters with the residual deformations for the process of line heating. The distribution of temperature and residual deformations for different thickness of substrate material (steel sheets) were predicted and it validates well with the experimental results. Vega et al. (2010) has performed a 3-D thermo-elasto-plastic FEA for obtaining the deformation induced by the process of line heating for thick steel sheet. Using FEA the edge effect on inherent deformation is clarified. Based on the outcome of the study, a suitable methodology was developed for predicting the yield effect. Using this technique, the edge effect on inherent deformation for broad range of sheet thickness can be estimated, along with the heating conditions for the same can also be easily predicted.

Zhou and Shen (2011) introduced the prediction of the deformation by the process of laser forming based on the theory of inherent strain by FEM. The methodology is convenient to use and only elastic analysis is necessary. The comparative studies match well with the experimental results. Biswas et al. (2011) has presented the transient distribution of temperature over the sheet for the process of line heating. Here the heat input is proportional to that of the rise in temperature over the surface of the sheet. Comparing the deformations

obtained in case of double pass line heating, it has been found that about 1.92 to 2.13 times increase with respect to that of single pass line heating process. Liang et al. (2006) has proposed the distribution of strain produced in the thick sheet by heating using FEM. In this the 3-D FEM using the iterative substructure method (ISM) was employed. Using the deformation computed by ISM, inherent deformation induced in sheet by the process of line heating has been estimated through inverse analysis.

Ogawa et al. (1994), Yu et al. (1999), Clausen (1999), Lee (1999) and Ishiyama et al. (1999) has proposed a 3-D FEM model. Where the input heat and output deflection has been described. Morinobu and Yoshihiko (1999) have confirmed that inherent strain distribution in a sheet can be acquired by flattening the objective curvature and is stated on the basis of the elastic FEM simulation.

Yu et al. (2001b) has presented about the development of a FEM model for thermo-mechanical analysis for the process of laser line heating. Here the technique of rezoning has been implemented for obtaining the result with desired accuracy with the reduction of simulation time. The numerical results obtained from the model validates well with that of the experimental ones. Khan and Yilbas (2004) have proposed a model analytically for the process of laser forming and determination of thermal stress field was done by using FEM. It was based on the influence of scanning speed on temperature and stress field. It has been found that higher the scanning speed, there occurs lower in temperature. Laser beam was considered to be the line heat source traversing in a constant speed, in reference to the analysis point of view.

Vollertsen et al. (1993) has developed a FDM for a 2D analysis for the process of laser forming. The model obtained provides in obtaining the effect of various process parameters with in a quick period of time, however the approach has been limited with the use of simple boundary conditions, which led for modeling with the FEM (Geiger et al. 1994). Alberti et al. (1994) has used finite element model for TGM for evaluating the temperature field. The results obtained were put into the mechanical analysis. A constant decay law is assumed for relationship between rise in temperature and in lowering of yield stress. A numerical model was also developed by Alberti et al. (1997) for determining the combined thermal and mechanical bending process. Hsiao et al. (1997) have used ABAQUS for modeling of the

process. However, they have used the model for emphasizing the significance of specimen size. The outcome shows that short specimen has less angular distortion in comparison to long specimen. Yilbas et al. (2014) also used finite element code in line with the experimental conditions for the prediction of temperature and stress fields in the heated region. The results of temperature and residual stresses are in good agreement with the experimental data and XRD results. Hu et al. (2002) has made a 3D FEM simulation which includes non-linear, transient, indirect coupled, thermal-structural analysis for geometric and material non-linearity. The after effect such as deformation due to buckling, bend angle and the distribution of stress-strain with residual stress with temperature were obtained.

2.5 Heating line generation

The most challenging task of every line heating process is the determination of the locations of the heating lines. Regarding generation of heating lines different methods are described in the literatures.

2.5.1 Elastic analysis and "similarity" measure

Lee (1996) has developed an algorithm for fitting the heating lines through points of similar curvature on the surface. These were subjected to bending moments which follow the heating and the shape obtained was compared to the required or target shape obtained. It was compared to the required or target shape by a square root norm of the differences between the points on the two surfaces. Then an optimization procedure was followed by varying the bending moments for achieving a better fit.

2.5.2 Points of maximum curvature

A method was developed by Jang and Moon (1998), which compares with the target surface with the current (initially flat) surface. The objective was to make the difference surface (target minus current) as flat as possible. This can be achieved by finding the points of maximum curvature on the difference surface and then grouping them into simulated heating lines. By iteration the difference surface gradually becomes flat.

2.5.3 Concentration of heating line

According to Letcher (1993) for producing positive Gaussian curvature, heating lines are concentrated towards the periphery of the sheet and for producing negative Gaussian curvature, heating line are concentrated towards the center of the sheet.

2.5.4 Normal strain direction

Shin and Kim (1997) has used the method of differential geometry for mapping between initial flat sheet and the curved sheet. Thus the bending in plane principal strain was evaluated. The most crucial part was the selection of the mapping method which resembles the line heating process as much as possible.

Hinds et al. (1991) has refined the method which has been developed by Manning (1980) by replacing the involutes with traces of geodesic curvature. The geodesic curvature thus developed can be traced on to the plane where any line can be traced given a curvature and an arc length, which was developed by Nutbourne et al. (1972).

2.5.5 Principal strain and principal curvature directions

Ueda et al. (1994a) has developed a procedure in which the strain obtained due to deformation from initial to final transformation has been computed using elastic FE analysis. The computed strain was decomposed the computed strain into in plane and bending components and distribution of their principal values were displayed on graphics display. From the distribution of in plane strain, the region where the magnitude of compressive principal strain was large was chosen to be the heating zone, and the heating direction were assumed to be normal to the direction of plane strain having the maximum absolute value.

Xuebiao et al. (2005) presented a numerical method for the determination of the heating lines for producing the required bend angle. The principal curvature distribution provides information on the deformation distribution and the heating lines. Liu et al. (2004) has proposed the position of the heating path, heating path is perpendicular to the principal strain direction. Strain developed along the principal curvature direction is perpendicular to each other with no shear strain developed in the process. The heating path is perpendicular to the principal curvature direction in every point present on the path. Jang et al. (2005) proposed a study related to triangular heating. An attempt was successfully made for simulating the

process of steel sheet forming by the process of triangular line heating. Here the simplified elastic analysis has been carried out using a circular disk-spring model for the problem related to complicated thermal elasto-plastic problem of triangle heating. The results obtained from the simulation were found to be in good agreement with the experimental ones. The study also results in improved computation efficiency and for that reason this process can be applied to real time control of triangle heating process. Zhu and Yang (2012) has proposed a method for heating path generation and simulation for ship sheet steel based on sound transmission loss (STL) mode this laid to the foundation of automation for line heat forming process.

Kim et al. (2009) has discussed about the triangle heating and an algorithm has been proposed for the determination of location of heating paths. The heating shape can be obtained by in-plane strain distribution which can be evaluated from non-linear kinematic analysis between the designed and initial shapes. Cheng et al. (2006) has developed a strategy based on strain for the process of laser forming of thin sheets with different sheet thickness. This has been used for the determination of the scanning paths along with the condition of heating. In case of variation in thickness of the sheets, both the plane strain and the bending are to be taken into consideration for the design process.

2.5.6 Influence of heating lines on mechanical properties

Shi et al. (2012) developed a numerical model for the process of simulation including coupled transient thermal and structural analysis. The numerical model validates well with the experimental results. Deformation of sheet was studied along with the heating position and direction of deformation. Shi et al. (2013) presented a work on carbon dioxide laser. The work is basically about the heating path effect on strain distribution of sheet. For parallel scanning path (heating lines): The heating paths do interfere with each other when the path spacing is less than the spot diameter and continuous strain field can be achieved by choosing appropriate path spacing and process parameters. When the scanning path (heating lines) is vertically and diagonally crossed the compressive plastic strains heavily increases compared to single laser scanning. Aihui et al. (2012) presented a study on the torsional mechanical properties of sheet metal for different heating lines for laser forming process. The mechanical properties of the material, such as: modulus of elasticity, yield strength, ultimate strength, TEI (Total Elongation Index) and EIU (Elongation Index of Uniform) with different spacing of

heating lines were proposed. The stress strain curve was complied with modified swift law, where the hardening exponent and strain hardening exponent of material are controlled by strain. Don and Zhang (2011) has presented a study on the mechanical properties of the sheet metal with that of the heating lines after laser scanning based on the thermal-micro structural-mechanical model. The phase transformation due to the laser scanning of sheet metal has been evaluated by coupling the thermal history from FEA with a phase transformation kinetic model. Walczyk and Vittal (2000) has proposed various regression equations on bend angle, area of HAZ (Heat affected zone), area of molten zone, depth of HAZ, depth of molten zone, width of HAZ and width of melt.

2.5.7 Effect of single and multi-heating lines

Shen et al. (2006b) underwent a study on the process of laser forming of sheets under simultaneous laser scanning in parallel directions. The outcome reveal that the deformations obtained from simultaneous laser scanning is higher than that of the single scan along the same line, when the distance between the two scanning lines is not too large. Shen et al. (2006c, 2007b) also observed the effect of time interval and overlapping on the bending angle in multi scanning laser forming process using finite element method.

Cheng and Yao (2001) have investigated numerically the effect of cooling for multi-scan forming. The forming accuracy in terms of offset of the nozzle, air pressure and multi scan were also studied. The result reveals that high cooling rate reduces the forming time in case of multi scan laser forming process. Vega et al. (2008) presented the influence of multi heating lines on line heating inherent deformation. It has been experimentally observed that the inherent deformation produced by multi heating lines is not a simple addition of inherent deformation by single heating lines. For accurate prediction of the inherent deformation, the objective has been proposed. For the analysis, the influence of the proximity to sheet size edge on inherent deformation is taken into consideration. The effect of residual stress produced by previous heating lines influence the inherent deformation of multi heating lines. Influence of proximity to sheet side edge due to multi heating lines can be neglected.

2.6 Edge effect

The edge effect phenomena were first observed by Magee et al. (1997) for laser forming process. Bao and Yao (2001) studied the effect numerically for both BM and TGM mechanisms. Edge effects are being characterized by the concave for BM, convex pattern with variation in the scanning path under TGM mechanism.

Shen et al. (2007c) presents 3-D nonlinear model for simulating the laser forming process of sheets. It has been used for finding the edge effect for the process. From the numerical study it is revealed that, with variation in scan speed the edge effect reduces significantly. Shen and Yao (2008) also proposed that the combined effect of both the acceleration and deceleration of scanning schemes minimizes the edge effect. Shen et al. (2005) proposed a model on 3-D non-linear coupled thermo-mechanical model accounting for dependency of temperature of the thermal and mechanical properties of the material. Based on this formulation, by varying scanning speed the edge effect in laser bending was investigated. Shen et al. (2010) investigated the edge effects in the straight-line laser bending process under TGM. The edge effects are assigned to the distribution of the peak temperature along the scan line and the geometry constraint of the sheet as it varies with distance from the scan path. The study of the effects of scan velocity and scan line position on the edge effects reveals that the edge effect is smallest at scan velocity of 30mm/s and it increases as the scan line approaches to free edge of the sheet. The results also show that combination of acceleration and deceleration scan schemes can minimize edge effect. Hu et al. (2013) established a temperature model by taking scanning process into account. The reason of edge effects has been unveiled from the analysis of the maximum temperature distribution and constraint conditions. The proposed strategy helps in reducing the edge effect in laser forming process.

2.7 Generation of compound surfaces

Engineering surfaces are broadly classified (Patrikalkis and Maekawa 2002; Rogers and Adams 2003) as:

- **Developable surface**: A surface has zero Gaussian curvature. This is applicable to the process of sheet metal forming and can be easily flattened. The residual stress strain remains in the surface after forming is very less.
- **Non-developable surface**: - Surface having non-zero Gaussian curvature in some parts of the surface. Here shearing and tearing of surface occurs during the conversion of surface to flat plate or sheet.

It has been found that for the past few decades, the ship hull sheets having very small Gaussian curvature, the surface development procedures are based on the geodesic development.

Line heating techniques have lots of benefits (Chirillo 1982) over sheet forming by mechanical means. Line heating process is faster, safer and accurate shape can be expected by this process. The existing methods are basically based on manual operation, skills and trial and error methods (Chirillo 1982). Manning (1980) proposed a process for the development of surface based on the isometric tree. Here the disadvantage lies as it does not provide the strain field.

Hinds et al. (1991) has proposed a process for obtaining a doubly curved surface where it is done by first approximating it as a quadrilateral facet and then by flattening allowing some gaps in the developed pattern. The disadvantage lies that the developed shape depends on starting edge chosen in metal forming. The work of Hinds et al. (1991) has been extended by Azariadis and Asprogathos (1997) for reducing the gaps by reducing the Euclidean distances of pair of corresponding points between two successive strips. Letcher (1993) has developed a procedure for flattening and fabrication of doubly curved sheets. The mapping technique from curved surface to planar development was modeled by adding in plane strains to the curved surface. The strain field was acquired by solving the Poisson's equation.

Cho et al. (1998) developed an algorithm for developing a doubly curved surface by reducing the mapping error between given and developed surface net. This technique has been relevant in getting auxiliary planar domain of triangulation for tessellating trimmed parametric surface patches. Ha and Jang (2007) were studied a problem related to sheet deformation by line heating, they approached the problem in two ways:

(i) Thermal elasto-plastic analysis with usage of FEM code through direct heat input.

(ii) Equivalent load method based on the inherent strain.

Li and Yao (2001) have developed a scanning scheme, where laser scanning starts from middle location of the work piece instead of edges. Here the convex forming is experienced under BM conditions, different from that of the scanning staring from the edges. Convex forming is realized with high certainty under the BM conditions, unlike the scanning from the edge. Shi et al. (2008) has also studied similar effect on the location of heating and the startup point on bending direction make adequate further insight into the process of convex forming, which is benefited for parameter selection for future planning. Concave laser forming and convex forming are essentially required for obtaining complicated shape during the process of sheet forming. Both this type of forming can be achieved by utilizing two separate forming mechanisms (i.e. TGM and BM). Concave laser forming can be achieved by TGM while the convex forming can be obtained by buckling mechanism. Wang et al. (2006a) concentrated on the process of forming a pillow shape. It can be obtained by the process of line heating by analyzing the basic parameters; the extent of local contraction can be generated by line heating. The combination of computational result of local deformation helps in determination of curved shape optimally.

Various mapping techniques are being implemented successfully for attaining the actual forming (Lamb 1995) technique, so that cut sheet fits each other perfectly at the stage of erection. The results obtained are unsatisfactory as the mapping is based on differential geometry in reference to line heating and other forming methods. Hennige (2000) has reported the basic investigation on the difference in forming behavior of parts obtained from sheet metal by linear and curved irradiations. Edwardson et al. (2001) has set up for positioning as well as sequencing of the lines of irradiation for controlling the 3 D laser forming process for obtaining symmetrical saddle shape from a rectangular blank. Combination of TGM and upsetting mechanism are being used for developing the surface. Similarly, Safari and Farzin (2015) proposed and investigated the experimental development of saddle shape using spiral irradiating scheme. The technique is found to be a very good method for producing a saddle shape part with considerable amount of curvatures. Here the curvatures and symmetry of similarly formed edges are studied with variation of pitch in the

spiral path and the mode of scanning of the laser (i.e. out to in and in-to-out) of the spiral path.

Liu et al. (2004) has presented an optimal approach for laser forming for obtaining a doubly curved shape using strain field calculation on the basis of formulation based on the principal curvature and minimum strain optimization. The scanning path and heating condition (laser power and scanning velocity) were obtained by considering both analytical and practical constraints. Similar model has been developed by Liu and Yao (2005) for thin sheet thermal forming. The model has been developed based on numerical approach. The amount of heat flux needed is based on the path of scanning and has been related with bspline curve by Zhang et al. (2007). Chakraborty et al. (2012) has developed a cup like shape. Here the radial and circular scan lines (heating) are being used to get the desired shape. The procedure for the measurement of the bend angle of sheet has been obtained strategically. Safari and Mostaan (2016) proposed a new method for the development of cylindrical surfaces with arbitrary radius of curvature. The method includes simple linear irradiating lines and the process parameters are determined analytically. In addition, it has been endowed that the key parameters that directly affects the radius of curvature of the laser formed cylindrical surface is the number of irradiating lines and the distance between them. It has been interpreted that by maintaining distance equals to 4 times the radius of laser beam, the individual irradiating lines does not get affected with the transfer of heat during laser irradiation of neighbor heating line. The outcome of the proposed method is very much successful for the production of cylindrical surfaces.

Shin et al. (1995) has proposed a conceptual configuration of sheet forming for the production of ship. It is necessary to integrate the line heating process for the usage of minimal requirement of thermal energy. The mechanics of line heating process was studied and the modeling of heating torch, water cooling and sheet forming by this process were done under the aegis of finite element analysis. Tetsuya and Hironori (2011) proposed the effect of heating direction due to laser forming which is used for forming curved surface from a thin sheet. Researchers have already proposed new development method with curvature lines as a solution to the problem. Curvature lines can be obtained for combining primary curvature directions. In-plane strain is being evaluated from the change of distance of these lines.

Heating direction is chosen parallel to curvature line because in plane strain is put as transverse shrinkage caused by heating. Cheng and Yao (2004b) proposed an approach for designing of the process for obtaining doubly curved shapes for thin plates. The important part of this method is obtaining strain field required for calculation in obtaining the desired formed shape. The scanning lines were evaluated on the basis of in-plane strain, principal minimum strain, bend strain and temperature gradient mechanism (TGM) for the laser forming process. The condition of heating has been determined by lumped method. This method is numerically and experimentally validating well. Shahabad et al. (2017) developed a dome shaped product made from the laser forming process of circular aluminum 6061 sheet using spider scan strategy. The effect of process parameters including laser power, beam diameter, scanning velocity and number of pass on dome height is also studied. It has been found that with increase in laser power and number of scans, the dome height increases whereas it has a reverse effect with the increase of scan velocity and beam diameter. A statistical fit equation is also developed using analysis of variance (ANOVA) in predicting the dome height as a function of the variables.

2.8 Soft computing approaches for line heating

Artificial Neural Network (ANN) (Fausett (1994), Haykin (1994), Rajasekaran&Pai (2003); Biswas et al. (2006)) has been applied in all fields of engineering (Rafiq et al. 2001) and has given promiscuous results. ANN has the ability in generalization of the relationships in a set of data by providing a quick and satisfactory estimations, which enables particular non-traditional optimization technique attractive for different applications. ANN has the ability in learning and generalization of the relationships in data set for providing quick and satisfactory estimations, which enables in making the particular non-traditional optimization technique attractive for many different applications.

Line heating processes are non-linear and highly multivariable systems. Use of soft computing approaches like Artificial Neural Network (ANN) (Patterson 1995; Tsoukalas& Robert 1996; Shin et al. 1999) has become popular in this regard for predicting line heating process parameters based on experimental observations and numerical analysis. It should be considered that the large structures such as ship are not built in large series and at the same time each piece of curved shell of ship's hull is not identical. This means that every single

piece of curved sheet is fabricated using different combination of forming parameters. Thus, it is necessary to generate new parameters from the calculated results for the convenience of the line heating process. In such a situation ANN helps in obtaining new line heating parameters.

In general, numerical thermal analysis is highly time consuming. For analyzing the test sample of size 300mm × 300mm, 25.4 mm thick in a SGI work station rated at 200MHz running under OSIRI × 6.2, the CPU time required is about 12695 seconds (Yu et al. (2001a)). Numerical analysis in real life situation in generally for panel size is about 3.0 m to 4.0 m is quite impossible. ANN provides sufficient data to train the network. Jeng et al. (2000) used back propagation neural networks and learning vector quantization networks for predicting laser welding parameters. Lee and Um (2000) compared the back-head prediction for gas metal arc welding process by the help of multiple regression analysis along with the ANN. Shin et al. (1999) used ANN in line heating process for saddle type shells forming for prediction of shell forming process parameters. Cheng and Lin (2000b) have supervised three neural networks for evaluating the bending angle formed by laser bending process. The process parameters act as an input to these neural networks. The effectiveness of the model has been tallied experimentally and it validates well.

Casalino and Ludovico (2002) has proposed a feed forward neural network with back propagation technique for evaluating bend angle and for selecting the TGM and BM laser forming parameters. The result reveals that neural network provide fast and precise outcome in compare to finite element analysis and is easier in using them than the multivariate regression analysis. Chen et al. (2002b) has also developed an adaptive fuzzy neural network for the evaluation of the deformation. The process combines the learning power of neural network along with the fuzzy interface systems. Shen et al. 2006e has proposed a model for the determination of bend angle by the process of laser forming using adaptive fuzzy logic called adaptive network fuzzy inference system (ANFIS). Cheng and Yao (2004a) presented a methodology for obtaining shapes using genetic algorithm (GA).

Nguyen and Yang (2009) proposed an ANN model for obtaining the position of heating line for the process of induction heating. Here the vertical displacement acts as an input parameter for the development of the model. The training pattern of neural network was obtained by using analytical solution for predicting sheet deformation. The developed model is well

feasible for determination of heating position in a flat sheet by the process of line heating for obtaining desired shape. Nguyen et al.(2009b) obtained the training pattern of neural network by using analytical solution and it is obtained from the plate theory for predicting plate deformations by the process of induction heating. The analytical solution for obtaining the angular deformation of the sheet is obtained by using thermal analysis, with heat input calculation obtained from electromagnetic analysis of the process of induction heating.

Biswas et al. (2009) presented a work on GA based on optimization of strain field distribution approach for the minimum blank generation and strain energy, optimum material requirement and blank generation for the process. For obtaining curved surface the strain extent is needed to know along with the direction of application. The deformation formed is perpendicular to that of the heating path. The curved sheet can be obtained by the process of forming by using various starting template using various amount of strain. Liu et al. (2006) presents a mathematical model for optimization of line heating parameters. Here sheet processing time and goodness of fit of shrinkage ratio curvature taken as two objective functions for the development of the model. The two objective optimization problems are translated into one by changing power coefficient. Based on the HGA (Hierarchy Genetic Algorithm) the interpolation function with cubic spline, error analysis etc. is used to change the objective function into individual fitness function of colony. Lambiase et al. (2015) developed a procedure based on ANN for the development of optimal processing conditions, to produce a given bend angle which contributes to the reduction of the processing time. The procedure can further be extended for the prediction of temperature under given processing conditions as well and the bending angle and its variation with number of scans.

2.9 Summary

The key points and some concluding remarks can be made in reference to the investigation on line heating process are as below.

- There are three types of heat source generally used for line heating process. The selection of heat source is based on its precession control of heat flux and ease of operation.

- The key factor associated with the line heating process includes: energy parameters, material properties and sheet geometry. Energy parameters include the amount of heat flux supplied, velocity, beam diameter, sheet thickness and number of scans.
- Numerous efforts have been made for the development of numerical and analytical model in relation to bend angle and temperature field.
- The edge effect phenomena associated with the process is described with a suitable numerical model. The phenomena are described with different types of laser forming mechanism.
- Development in relation to the generation of compound curved surface with the process of optimization is also discussed for obtaining suitable pattern of surface. Suitable theories have been proposed for heating line generation and effect of heating lines on the mechanical properties of the material.
- Efforts have been made for the prediction of line heating process parameters with usage of soft computing approach.

2.10 Gaps found in literature review

- From the past literatures it was observed that the work related to 3-D FE thermo-mechanical analysis of laser line heating is rarely found in the published literature.
- The literature review does not give any idea in relating to the sequences of line heating. It needs to be further studied to establish the appropriate line heating sequence, which will enable efficient production of compound curved sheets.
- FE stress and strain field analysis of compound curved surfaces are rarely found in past literature.
- Research work related to laser line heating soft computing approaches are rarely found in the published work and less work have been carried out in the development of some analytical model along with simulation results in the process using laser as a heat source.
- Work related to optimum blank size is rarely found in literatures. In determination of suitable blank size for developing compound curved surface by the process of laser line heating is a very trivial task in contrast to material optimization.

- Research work related to proper planning of automation of line heating process is lacking in published literature.

2.11 The scope of the thesis

- Numerical and experimental investigation of the planning of heating lines.
- Development of an effective simplified thermal and mechanical model for deforming of shapes and application of the model for the development of blank, which is required for the generation of compound curved surface.
- Accurate estimation of the heating parameters such as: heat absorption rate, laser power, traverse speed which are some of the important parameters to be taken into consideration for the effective simulation of laser line heating process.
- Investigations are required for each formed part and the variables affecting the process effectiveness. Effective simulations can enable in reducing the problem-solving time associated with the process.
- Effect on sequencing of heating needs to be studied and appropriate line heating sequence is to be established, which will enable efficient production of compound curved surface.

Chapter 3

Model Methodology

3.1 Introduction

A methodology with a suitable description of theories selected in this investigation for fulfilling the objectives is presented in this chapter. The theories and assumptions that have been made for the formulation of the numerical models are detailed below. The first section of this chapter deals with the thermo-mechanical analysis of sheet forming by laser line heating. At first, the thermal FE- analysis which can be used for accurate prediction of thermal history for the laser line heating process is given. Then the structural analysis is used for the prediction of residual deformation, thermal stresses and strains for the metallic sheet by the process of laser line heating is presented. The second section holds the details of the generation of the compound curved surface by the process of laser line heating. It includes the generation of blank, strain field distribution and generation of the heating path for the curved shape. The methodology of predicting the heating parameters by artificial neural network (ANN) is also discussed in this section. The above section is followed by numerous theories and models used for performing an experimental analysis of the process for the determination of optimum operating parameters for the process.

3.2 Outline for thermo-mechanical analysis

A FE-model is developed for transient thermal and mechanical analysis of the process. The models are built using ANSYS APDL (Ansys Parametric Design Language). In this process, the thermal analysis is performed first then the result obtained from the thermal analysis is used as an input for carrying out structural analysis. The methodology followed is shown in Fig.3.1.

3.2.1 Thermal analysis

3.2.1.1 Three dimensional (3-D) Finite element thermal model

A 3-D FE-model (Alberg 2005; Fanous et al. 2003 and AnsysInc 2002) is presented for analyzing the temperature distribution in the laser line heating process. The temperature-

dependent material properties are considered for the analysis. The temperature-dependent material properties of mild steel are shown in Tables 5.1-5.3.

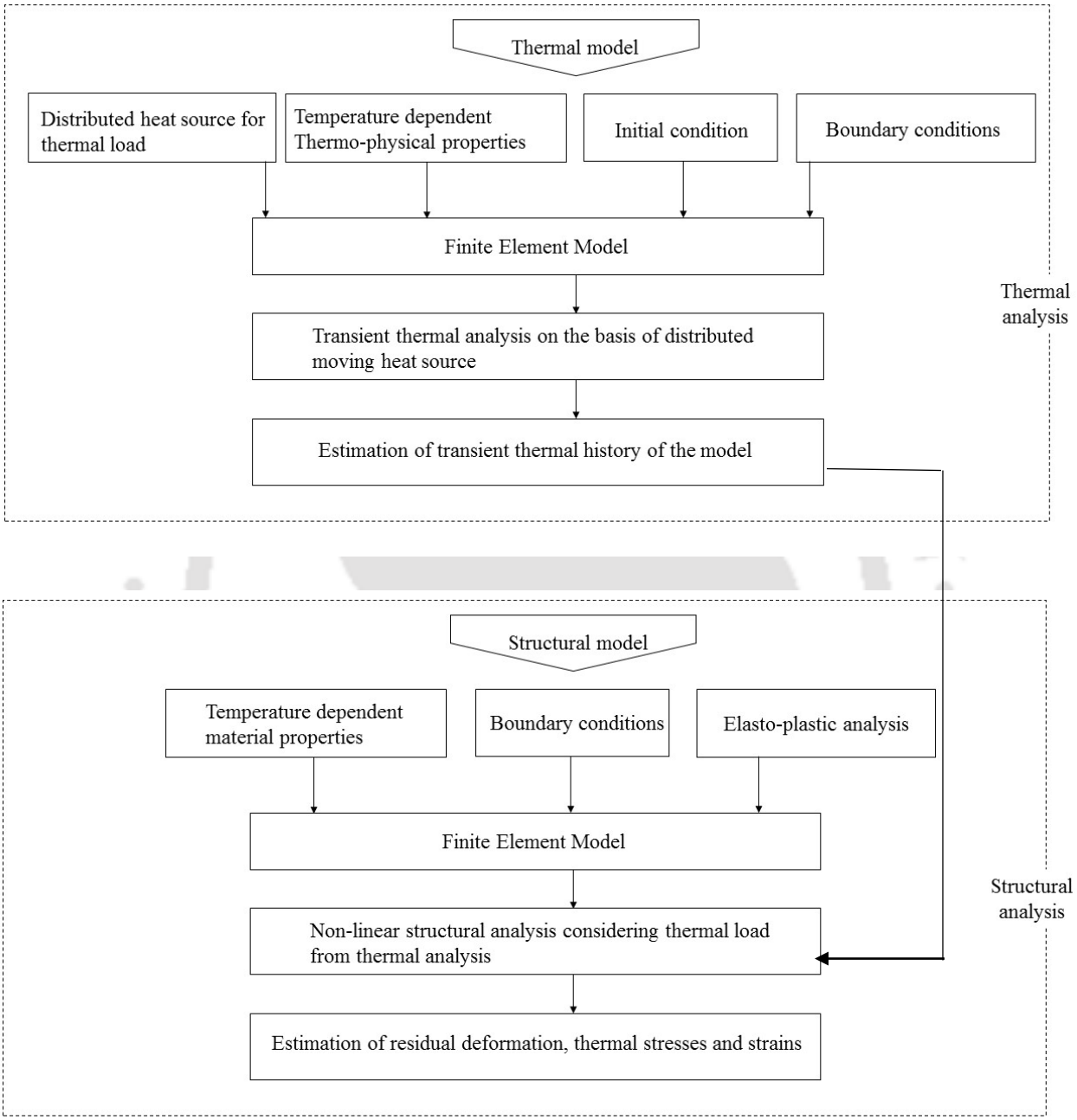

Fig. 3.1 Flow chart of numerical modeling of laser line heating process

The conduction mode of heat transfer is much higher than the convection mode of heat transfer. The assumptions that are made in developing the present thermal model of line heating process are as follows:

i) The thermal and mechanical properties of the materials are considered to be a function of temperature.

ii) Linear Newtonian convection cooling is considered on all the surfaces.

iii) The heat is considered as a thermal load for the process.

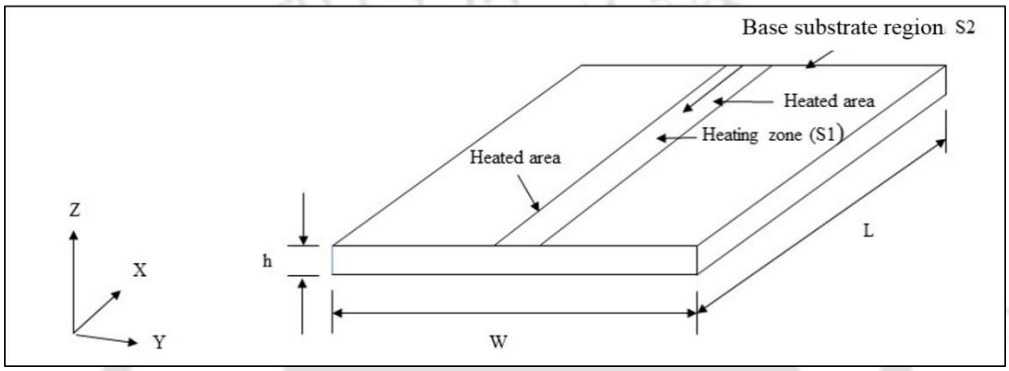

Fig. 3.2 Various regions of a sheet subjected to line heating process

The governing differential equation of heat conduction for a homogeneous, isotropic solid without heat generation in the rectangular coordinate system $(x, y, z)$is expressed as:

$$\frac{\partial}{\partial x}\left[K\frac{\partial T}{\partial x}\right]+\frac{\partial}{\partial y}\left[K\frac{\partial T}{\partial y}\right]+\frac{\partial}{\partial z}\left[K\frac{\partial T}{\partial z}\right]=\rho c\frac{\partial T}{\partial t} \tag{3.1}$$

where $K =$ thermal conductivity, $T =$ temperature, $\rho =$ density of the material, $c =$ specific heat and $t =$ time.

The above equation can be rewritten as:

$$\rho c\frac{\partial T}{\partial t}=-\{L\}^T\{q\} \tag{3.2}$$

where $\{L\}=\begin{Bmatrix}\partial/\partial x\\ \partial/\partial y\\ \partial/\partial z\end{Bmatrix}$ = vector operator,

$\{q\}$ =heat flux vector,

$\{L\}^T\{q\} = \nabla.\{q\}$, and

$$\{L\}T = \nabla T$$

where ∇ represents grad operator.

The Fourier's law is used to relate the heat flux vector to the thermal gradient

$$\{q\} = -[D]\{L\}T \tag{3.3}$$

where

$$[D] = \begin{bmatrix} K & 0 & 0 \\ 0 & K & 0 \\ 0 & 0 & K \end{bmatrix} = \text{Conductivity matrix}$$

Eq. (3.2) can be written as:

$$\rho c \frac{\partial T}{\partial t} = \{L\}^T([D]\{L\}T) \tag{3.4}$$

For solving Eq. (3.4), the following boundary conditions are needed to be set.

(i) Initial condition

A specified initial temperature for the line heating process that covers all the elements of the specimen is shown in Eq. (3.5).

$$T = T_\infty \text{ for } t = 0 \tag{3.5}$$

where T_∞ is the climate temperature for developing other boundary conditions, we need to consider the energy balance at the work surface as:

Heat supply = Heat loss.

(ii) First boundary condition

A specific heat flow acting over surface1 as shown in Fig.3.2 is as follows:

$$q_n = -q_{sup} \tag{3.6}$$

The quantity q_n represents the conduction heat flux vector component normal to the work surface. The quantity q_{sup} represents the heat flux supplied to the work surface, from an external heat source.

$$q_n = \{q\}^T\{n\} \text{ on the surface S1 for } t > 0 \tag{3.7}$$

where $\{n\} =$ outward normal vector.

(iii) Second boundary condition

Considering heat loss (q_{conv}) due to convection over remaining surface S2 (Newton's law of cooling):

$$q_n = q_{conv} \tag{3.8}$$

$$\text{or } \{q\}^T\{n\} = h_f(T - T_\infty) \text{ on the surface S2 for } t > 0 \tag{3.9}$$

Pre-multiplying Eq. (3.4) by a virtual change in temperature, integrating over the volume of the element, combining with Eq. (3.7) and (3.9) and with some algebraic manipulation we get:

$$\int_{vol}\left(\rho c\delta T\left(\frac{\partial T}{\partial t}\right) + \{L\}^T(\delta T)([D]\{L\}T)\right)d(vol) = \int_{s_1}\delta T q_{\sup}\, d(S_1) + \int_{S_2}\delta T h_f(T_\infty - T)d(S_2) \tag{3.10}$$

where $vol =$ volume of the element and $\delta T =$ an allowable virtual change in temperature ($= \delta T(x, y, z, t)$).

3.2.1.2 Derivation of heat flow matrices

As stated earlier, the variable T is allowed to vary in both space and time. This is expressed as:

$$T = \{N\}^T\{T_e\} \tag{3.11}$$

where

$T = T(x, y, z, t) =$ temperature,

$\{N\} = \{N(x, y, z)\} =$ element shape function,

$\{T_e\} = \{T_e(t)\} =$ nodal temperature vector,

The time derivative of Eq. (3.11) may be written as:

$$\dot{T} = \frac{\partial T}{\partial t} = \{N\}^T \{T_e\} \tag{3.12}$$

δT has the same form as T as shown in Eq. (3.13).

$$\delta T = \{\delta T_e\}^T \{N\} \tag{3.13}$$

The combination of $\{L\}T$ is written as:

$$\{L\}T = [B]\{T_e\} \tag{3.14}$$

where $[B] = \{L\}\{N\}^T$

The Eq. (3.10) can be combined with Eq. 3.11 to 3.14 to yield:

$$\int_{vol} \rho c \{\delta T_e\}^T \{N\}\{N\}^T \{\dot{T}_e\} d(vol) + \int_{vol} \{\delta T_e\}^T [B]^T [D][B]\{T_e\} d(vol) = \int_{S_1} \{\delta T_e\}^T \{N\} q_{\sup} d(S_1) + \int_{s_2} \{\delta T_e\}^T \{N\} h_f \left(T_\infty - \{N\}^T \{T_e\}\right) d(S_2) \tag{3.15}$$

The density ρ is assumed to remain constant and specific heat c may vary over the element. Finally,$\{T_e\}$, $\{\dot{T}_e\}$ and $\{\delta T_e\}$ are the nodal quantities and they do not vary over the element. So they can be taken out of the integrals. Since all the quantities are pre-multiplied by $\{\delta T_e\}$, this term may also be dropped from the resulting equation. Thus Eq. (3.15) may be reduced to:

$$\rho \int_{vol} c\{N\}\{N\}^T d(vol)\{\dot{T}_e\} + \int_{vol} [B]^T [D][B] d(vol)\{T_e\} = \int_{s_1} \{N\} q_{\sup} d(S_1) + \int_{s_2} T_\infty \{N\} h_f d(S_2) - \int_{S_2} h_f \{N\}\{N\}^T \{T_e\} d(S_2) \tag{3.16}$$

Eq. (3.16) can be rewritten as:

$$[C_e^t]\{\dot{T}_e\} + ([K_e^{th}] + [K_e^{tc}])\{T_e\} = \{Q_e^f\} + \{Q_e^c\} \tag{3.17}$$

where $\left[C_e^t\right] = \rho\int_{vol} c\{N\}\{N\}^T d(vol)$ = element specific heat matrix,

$\left[K_e^{tb}\right] = \int_{vol}[B]^T[D][B]d(vol)$ = element diffusion conductivity matrix,

$\left[K_e^{tc}\right] = \int_{S_2} h_f[N][N]^T d(S_2)$ = element convection surface conductivity matrix,

$\left\{Q_e^f\right\} = \int_{S_1}\{N\}q_{\sup} d(S_1)$ = element heat flow vector for surface S_1,

$\left\{Q_e^c\right\} = \int_{S_2} T_\infty h_f\{N\}d(S_2)$ = element convection for surface S_2heat flow vector.

The solution is obtained by using ANSYS Finite Element (FE) package.

3.2.1.3 Heat source model

The heat flux q is applied on the top surface of the metallic sheet which is moving with a constant velocity of V along the metallic sheet. The distribution of heat flux over the sheet surface is considered as in Gaussian mode (Mulay et al.), which is expressed by Eq. (3.18).

$$q(x,y,t) = \frac{2AP}{\pi {r_b}^2}\left(\frac{-2r^2}{{r_b}^2}\right) \tag{3.18}$$

where q is the heat flux in W/mm^2, $A$is laser absorption coefficient which is considered as 0.65 in the model. P is the laser power in W.$r_b$is the laser beam radius in mm and r is the distance from the center of laser beam in x and y direction in mm.

3.2.2 Structural analysis

3.2.2.1 Three dimensional (3-D) Finite element stress-strain relationship

The structural analysis of line heating process requires thermal stress and material non-linearity. The formulations of the stress-strain (Ansys Inc 2002) which are used in the present study are presented below. The stress is associated with strain within the elastic limit, is shown in Eq. (3.19).

$$\{\sigma\} = [D]\{\varepsilon^e\} \tag{3.19}$$

where $[D]$ = stress-strain co-relation matrix,

$\{\varepsilon^e\} = \{\varepsilon\} - \{\varepsilon^t\}$ = elastic strain vector,

$\{\varepsilon^t\}$ = thermal strain vector,

$\{\sigma\}$ = stress vector = $[\sigma_x \quad \sigma_y \quad \sigma_z \quad \sigma_{xy} \quad \sigma_{yz} \quad \sigma_{zx} \quad]^T$

and

$\{\varepsilon\}$ = total strain vector = $[\varepsilon_x \quad \varepsilon_y \quad \varepsilon_z \quad \varepsilon_{xy} \quad \varepsilon_{yz} \quad \varepsilon_{zx} \quad]^T$.

Eq. (3.19) may be written as,

$$\{\varepsilon\} = \{\varepsilon^t\} + [D]^{-1}\{\sigma\} \tag{3.20}$$

For 3-D cases the thermal strain vector can be exhibited as:

$$\{\varepsilon^t\} = \Delta T[\alpha_x \quad \alpha_y \quad \alpha_z \; 0 \quad 0 \quad 0] \tag{3.21}$$

where α_x, α_y and α_z= coefficient of thermal expansion in x, y and z direction.

The temperature difference is given by, $\Delta T = T - T_\infty$.

The compliance matrix is:

$$[D]^{-1} = \begin{bmatrix} \frac{1}{E_x} & \frac{-\vartheta_{xy}}{E_x} & \frac{-\vartheta_{xz}}{E_x} & 0 & 0 & 0 \\ \frac{-\vartheta_{yx}}{E_y} & \frac{1}{E_y} & \frac{-\vartheta_{yz}}{E_y} & 0 & 0 & 0 \\ \frac{-\vartheta_{zx}}{E_z} & \frac{-\vartheta_{zy}}{E_z} & \frac{1}{E_z} & 0 & 0 & 0 \\ 0 & 0 & 0 & \frac{1}{G_{xy}} & 0 & 0 \\ 0 & 0 & 0 & 0 & \frac{1}{G_{yz}} & 0 \\ 0 & 0 & 0 & 0 & 0 & \frac{1}{G_{xz}} \end{bmatrix} \tag{3.22}$$

where ϑ_{xy}= Major Poisson's ratio,

ϑ_{yx} = Minor Poisson's ratio,

E_x= Young's modulus in x direction,

G_{xy} = Shear modulus in x-y plane.

Since D^{-1}matrix is presumed to be symmetric

$$\frac{\vartheta_{yx}}{E_y} = \frac{\vartheta_{xy}}{E_x} \tag{3.23}$$

$$\frac{\vartheta_{zx}}{E_z} = \frac{\vartheta_{xz}}{E_x} \tag{3.24}$$

and

$$\frac{\vartheta_{zy}}{E_z} = \frac{\vartheta_{yz}}{E_y} \tag{3.25}$$

for isotropic material $E_x = E_y = E_z$ and $\vartheta_{xy} = \vartheta_{yz}$=$\vartheta_{xz}$. From the above equation's it is seen that:

$$\varepsilon_x = \alpha_x \Delta T + \frac{\sigma_x}{E_x} - \frac{\vartheta_{xy}\sigma_y}{E_x} - \frac{\vartheta_{xz}\sigma_z}{E_x} \tag{3.26}$$

$$\varepsilon_y = \alpha_y \Delta T + \frac{\sigma_y}{E_y} - \frac{\vartheta_{xy}\sigma_x}{E_x} - \frac{\vartheta_{yz}\sigma_z}{E_y} \tag{3.27}$$

$$\varepsilon_z = \alpha_z \Delta T + \frac{\sigma_z}{E_z} - \frac{\vartheta_{yz}\sigma_y}{E_y} - \frac{\vartheta_{xz}\sigma_x}{E_x} \tag{3.28}$$

$$\varepsilon_{xy} = \frac{\sigma_{xy}}{G_{xy}} \tag{3.29}$$

$$\varepsilon_{yz} = \frac{\sigma_{yz}}{G_{yz}} \tag{3.30}$$

$$\varepsilon_{xz} = \frac{\sigma_{xz}}{G_{xz}} \tag{3.31}$$

where typical terms are:

ε_x= direct strain in the x- direction,

σ_x = direct stress in x-direction,

ε_{xy} = shear strain in the x-y planeand

σ_{xy} = shear stress on the x-y plane.

$$\sigma_x = \frac{E_x}{h}\left(1 - (\vartheta_{yz})^2 \frac{E_z}{E_y}\right)(\varepsilon_x - \alpha_x \Delta T) + \frac{E_y}{h}\left((\vartheta_{xy}) + \vartheta_{xz}\vartheta_{yz}\frac{E_z}{E_y}\right)(\varepsilon_y - \alpha_y \Delta T) + \frac{E_z}{h}(\vartheta_{xz} + \vartheta_{yz}\vartheta_{xy})(\varepsilon_z - \alpha_z \Delta T) \quad (3.32)$$

$$\sigma_y = \frac{E_y}{h}\left(1 - (\vartheta_{xz})^2 \frac{E_z}{E_x}\right)(\varepsilon_y - \alpha_y \Delta T) + \frac{E_y}{h}\left((\vartheta_{xy}) + \vartheta_{xz}\vartheta_{yz}\frac{E_z}{E_y}\right)(\varepsilon_x - \alpha_x \Delta T) + \frac{E_z}{h}(\vartheta_{yz} + \vartheta_{xz}\vartheta_{xy}\frac{E_y}{E_x})(\varepsilon_z - \alpha_z \Delta T) \quad (3.33)$$

$$\sigma_z = \frac{E_z}{h}\left(1 - (\vartheta_{xy})^2 \frac{E_y}{E_x}\right)(\varepsilon_z - \alpha_z \Delta T) + \frac{E_z}{h}\left((\vartheta_{yz}) + \vartheta_{xz}\vartheta_{xy}\frac{E_y}{E_x}\right)(\varepsilon_y - \alpha_y \Delta T) + \frac{E_z}{h}(\vartheta_{xz} + \vartheta_{yz}\vartheta_{xy})(\varepsilon_x - \alpha_x \Delta T) \quad (3.34)$$

$$\sigma_{xy} = G_{xy}\varepsilon_{xy} \quad (3.34)$$

$$\sigma_{yz} = G_{yz}\varepsilon_{yz} \quad (3.35)$$

$$\sigma_{yz} = G_{yz}\varepsilon_{yz} \quad (3.36)$$

$$\sigma_{xz} = G_{xz}\varepsilon_{xz} \quad (3.37)$$

where $h = 1 - (\vartheta_{xy})^2 \frac{E_y}{E_x} - (\vartheta_{yz})^2 \frac{E_z}{E_y} - (\vartheta_{xz})^2 \frac{E_z}{E_x} - 2\vartheta_{xz}\vartheta_{yz}\vartheta_{xy}\frac{E_z}{E_x}$

when the shear modulus G_{xy}, G_{yz} and G_{xz} are same, i.e. for isotropic material. It reduces to:

$$G_{xy} = G_{yz} = G_{xz} = \frac{E_x}{2(1+\vartheta_{xy})}$$

3.2.2.2 Derivation of structural matrices

According to the principle of virtual work, a virtual (very small) change of the internal strain energy must be offset by an identical change in external work due to the applied loads, which can be stated as shown in Eq. (3.38).

$$\delta U = \delta V \tag{3.38}$$

where $U =$ strain energy, $V =$ external work and $\delta =$ virtual operator. The virtual strain energy is given in Eq. (3.39).

$$\delta U_1 = \int_{vol} \left(\{\delta\varepsilon\}^T [D] \{\varepsilon\} - \{\delta\varepsilon\}^T [D] \{\varepsilon^t\} \right) d(vol) \tag{3.39}$$

The strain vector is related to nodal displacement by:

$$\{\varepsilon\} = [B]\{u\} \tag{3.40}$$

where $[B]$= strain-displacement matrix, based on element shape functions and $\{u\}$ = nodal displacement vector.

Presuming all the effects are in global Cartesian system, Eq. (3.40) can be combined with Eq. (3.39) and noting that $\{u\}$ does not vary over the elemental volume (Ansys Inc 2002) it can be written as shown in Eq.(3.41).

$$\delta U_1 = \{\delta U\}^T \int_{vol} [B]^T [D][B] d(vol) \{u\} - \{\delta U\}^T \int_{vol} [B]^T [D] \{\varepsilon^t\} d(vol) \tag{3.41}$$

Another form of virtual strain energy when a surface moves against a distributed resistance may be written as shown in Eq. (3.42).

$$\delta U_2 = \int_{arear} \{\delta w_n\}^T \{\sigma\} d(arear) \tag{3.42}$$

where $\{w_n\} =$ motion normal to the surface, $\{\sigma\} =$stress carried by the surface and $arear =$ area of the distributed resistance.

Both $\{w_n\}$ and $\{\sigma\}$ have only one non-zero component. The point wise normal displacement is related to nodal displacements by:

$$\{w_n\} = [N_n]\{u\} \tag{3.43}$$

where $[N_n] =$ matrix of shape functions for normal motions at the surface.

$$\{\sigma\} = k_f\{w_n\} \tag{3.44}$$

where $k_f =$ foundation stiffness in units of force per length per unit area.

Combining Eq. (3.42) through Eq. (3.44) and assuming that k_f is constant over the area.

$$\delta U_2 = \{\delta u\}^T k_f \int_{arear} [N_n]^T [N_n] d(arear)\{u\} \tag{3.45}$$

By considering principle of virtual work it can be written as

$$\left([K_e] + \left[K_e^f\right]\right)\{u\} - \{F_e^t\} = [M_e]\{a\} + \left\{F_e^p\right\} + \{F_n^e\} \tag{3.46}$$

where $[K_e]$ is the element stiff matrix, $\left[K_e^f\right]$ is the element foundation stiffness matrix, $\{F_e^t\}$ is the element thermal load vector, $[M_e]$ is the element mass matrix, $\{u\}$ is nodal displacement vector, $\{a\}$ is acceleration vector, $\{F_e^n\}$ is the vector of nodal forces applied to the elements and $\left\{F_e^p\right\}$ is the element pressure vector.

3.2.2.3 Integration point stresses and strains

The element integration point stresses and strains are computed by combining Eq. (3.19) and Eq. (3.40) to get:

$$\{\varepsilon^e\} = [B]\{u\} - \{\varepsilon^t\} \tag{3.47}$$

$$\{\sigma\} = [D_e]\{\varepsilon^e\} \tag{3.48}$$

where $[B]$ =strain displacement matrix evaluated at the integration point.

3.2.2.4 Structural analysis with material non-linearities

This generally includes non-linear plasticity having a well-defined yield point and non-linear elasticity. In such cases the elastic strain vector is represented as:

$$\{\varepsilon^e\} = \{\varepsilon\} - \{\varepsilon^t\} - \{\varepsilon^p\} \tag{3.49}$$

where $\{\varepsilon^e\} =$ elastic strain vector, $\{\varepsilon\} =$ total strain vector, $\{\varepsilon^t\} =$ thermal strain vector and $\{\varepsilon^p\} =$ plastic strain vector.

Material non-linearity's exists due to the non-linear relationship between stress and strain. The stress is found to be a nonlinear function of the strain (Bezuhov 1968; Rao 1998 and Mandal2004). In the case of mild steel, the rate-independent plasticity, kinematic hardening, and bilinear von Mises yield criteria (Biswas and Mandal,2008; Alberg 2005; Cheng 2005 and Mandal 2004) are applicable. The above-mentioned formulations are derived with the help of reference books of the software (ANSYS Inc 2002), which is used in the analysis and from the standard FEM textbooks (Zienkiewicz 2001, Reddy 2003 and Chandrupatla 2002). The yield criteria, flow rule, hardening rule and plastic strain increment used in the analysis are described below:

3.2.2.4.1 Yield criteria

The yield criteria determine the stress level at which the yielding is initiated. For multi-component stresses, it is represented as a function of the individual components. Let us consider $f(\{\sigma\})$ be the equivalent stress, such that:

$$\sigma_e = f(\{\sigma\}) \tag{3.50}$$

where $\{\sigma\} =$ stress vector.

When the equivalent stress is equal to the material yield parameter σ_y such that:

$$f(\{\sigma\}) = \sigma_y \tag{3.51}$$

Then the material will develop plastic strains. If σ_e is less than σ_y, the material will remain in the elastic state and the stresses will develop according to the elastic stress-strain relations. It is

noted that the equivalent stress can never exceed the material yield stress. Since the plastic strain gets developed instantaneously, therefore the stress is maintained below the material yield stress.

3.2.2.4.2 Rate independent plasticity

The rate-independent plasticity is characterized by the irreversible straining that occurs in a material once the material reached to a certain level. The plastic strains are assumed to get develop instantaneously i.e. independent of time.

3.2.2.4.3 Flow rule

The flow rule determines the direction of plastic strain and is given as:

$$\{d\varepsilon^p\} = \lambda \left\{\frac{\partial Q_p}{\partial \sigma}\right\} \tag{3.52}$$

where $\lambda =$ plastic multiplier (which determines the amount of plastic strain) and $Q_p =$ function of stress, termed as plastic potential (which determines the direction of plastic strain).

Considering Q_p as a yielding function, the plastic strain occurs in a direction normal to the yield surface.

3.2.2.4.4 Hardening rule

The hardening rule describes the change of the yield surface with progressive yielding so that the conditions of subsequent yielding can be established. Kinematic hardening is used in the present analysis. It assumes that the yield surface remains constant in size and the surface translates in stress space with progressive yielding.

3.2.2.4.5 Plastic strain increment

If the equivalent stress computed using elastic properties exceeds the material yield stress, then the plastic strain occurs. Plastic strain reduces the state of stress so that it satisfies the yield criteria. The hardening rule states that the yield criteria changes with work hardening and kinematic hardening. Incorporating these dependencies in Eq. (3.50), it can be re-written into the following form as:

$$F(\{\sigma\}, k\{\alpha\}) = 0 \tag{3.53}$$

where $\{\alpha\} =$ translation of yield surface and $k =$ plastic work.

Hence k and $\{\alpha\}$ are internal variables. Plastic work is the sum of the plastic work done over the history of loading as shown in Eq. (3.54).

$$k = \int \{\sigma\}^T [M]\{d\varepsilon^p\} \tag{3.54}$$

And the translation of the yield surface is shown in Eq. (3.55).

$$\{\alpha\} = \int C\{d\varepsilon^p\} \tag{3.55}$$

where $C =$ material parameter and $\{\alpha\} =$ back stress (location of the center of the yield surface).

Eq. (3.53) can be differentiated to arrive at the consistency condition as:

$$dF = \left\{\frac{\partial F}{\partial \sigma}\right\}^T [M]\{d\sigma\} + \frac{\partial F}{\partial k} dk + \left\{\frac{\partial F}{\partial \alpha}\right\}^T [M]\{d\alpha\} = 0 \tag{3.56}$$

$$dk = \{\sigma\}^T [M]\{d\varepsilon^p\} \tag{3.57}$$

$$\{d\alpha\} = C\{d\varepsilon^p\} \tag{3.58}$$

Eq. (3.56) can be written as:

$$\left\{\frac{\partial F}{\partial \sigma}\right\}^T [M]\{d\sigma\} + \frac{\partial F}{\partial k}\{\sigma\}^T [M]\{d\varepsilon^p\} + C\left\{\frac{\partial F}{\partial \alpha}\right\}^T [M]\{d\varepsilon^p\} = 0 \tag{3.59}$$

3.3 Outline for the development of compound curved surface

The surfaces are classified into two categories: developable and non-developable surfaces. The developable surfaces are those surfaces, which exhibit zero Gaussian curvature throughout the surface. These surfaces are generally simple single curved surfaces. The development of developable surfaces is highly recommended because these surfaces can easily be formed from metal sheets. On the other hand, non-developable surfaces are those surfaces, which exhibit non-zero Gaussian curvature in some parts of the surfaces. These surfaces are generally doubly curved surfaces. Although the single curved shapes are highly desirable for the ease of production, there are surfaces associated with many engineering structures, which are commonly

fabricated as doubly curved shapes for fulfilling hydrodynamic, structural and functional requirements.

For the development of doubly curved shapes or compound curved shapes by the process of line heating, the strain distribution over the surface plays an important role. Based on the magnitude and direction of strains, the heating parameters and heating paths for the development of a particular curved shape is decided. A compound curved shape can be formed from numerous starting blank using a different amount of strain. So, the initial objective for the development of the desired shape is to determine the blank first for which the value of the strain has to be applied so that we get our desired shape. The steps carried out in the present work for the generation of the compound curved surface is represented in Fig.3.3.

3.3.1 Blank and strain field generation

In the present investigation two doubly curved shapes: pillow shape and saddle shape surfaces are studied. The shapes are developed by using the coordinate points as shown in Table 6.1 & 6.2, respectively. The first step in the laser forming process is the determination of the strain field required for forming the desired shape. The strain field is obtained by solving a large elastic deformation FEM model by flattening the desired shape under displacement constraints. The desired shape is placed between two flat rigid bodies and is compressed to form a planar shape for generating the strain field. The top rigid body is given a step by step displacement towards the bottom along the thickness directions until the gap between them is equal to the sheet thickness of the desired shape. It is assumed that friction is not considered between the rigid surface and the desired shape. The planar shape obtained after deformation is the desired blank obtained for the respective curved shape which has to be developed by the line heating process.

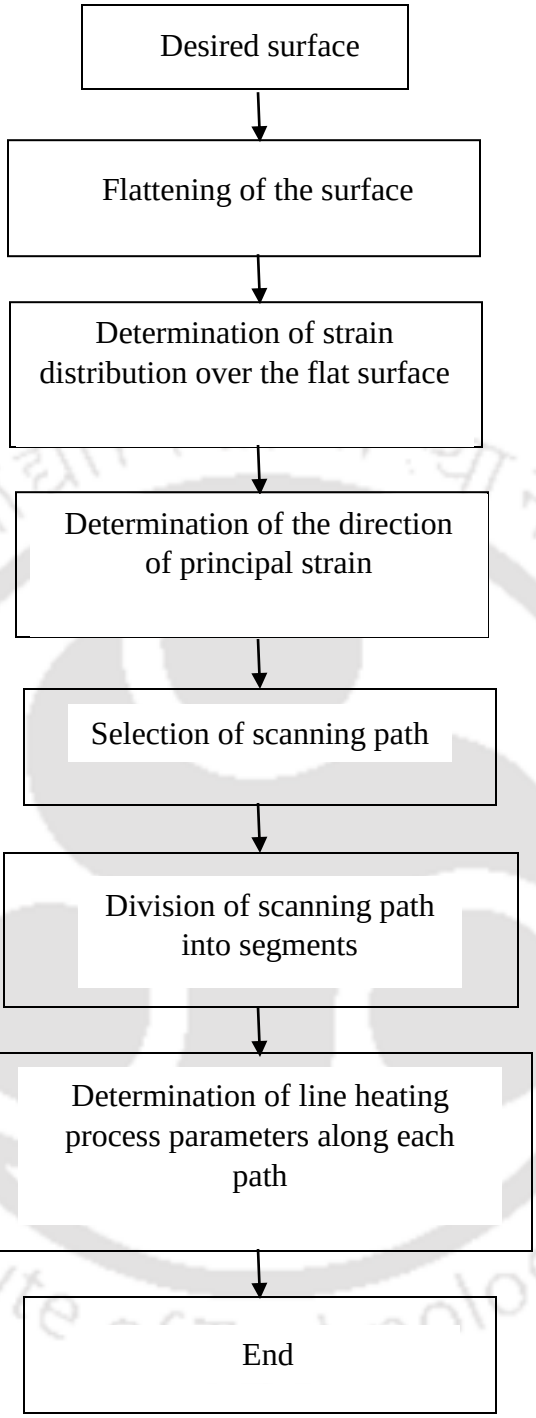

Fig. 3.3 Outline of process planning for the generation of compound curved surface

A large deformation model is considered because the desired shape considered for this analysis has a large deflection relative to its sheet thickness (Liu et al. 2005). Elastic FEM is applied instead of elastic/plastic FEM for this problem because few material properties need to be

specified in elastic FEM. In the case of small deflection, the normal displacement component of the mid-plane is small relative to the sheet thickness and thus the in-plane strain can be neglected. However, if the degree of deflection increases to a certain level, then the deflections are accompanied by stretching and contraction of the mid-plane which cannot be neglected. So for this reason the large deformation model is employed for carrying out the analysis.

The governing relations for elastic large deformation of a thin sheet are briefly summarized. It is considered that the sheet material is elastic, homogeneous and isotropic; the straight lines, initially normal to the middle surface before bending and after bending remain straight and normal to the middle surface during the deformation and the length of each element is unaltered. Deflection w_0 in the z(thickness) direction is assumed large relative to the sheet thickness h and therefore membrane forces (N_x,$N_y$and N_{xy}) become more significant. In the middle surface the strain displacement equation can be expressed as:

$$\varepsilon_{xx}^0 = \frac{\partial_{u_0}}{\partial x} + \frac{1}{2}\left(\frac{\partial w_0}{\partial x}\right)^2, \varepsilon_{yy}^0 = \frac{\partial_{v_0}}{\partial x} + \frac{1}{2}\left(\frac{\partial w_0}{\partial y}\right)^2, \gamma_{xx}^0 = \frac{\partial_{u_0}}{\partial y} + \frac{\partial v_0}{\partial x} + \frac{\partial w_0}{\partial x}\frac{\partial w_0}{\partial y} \quad (3.60)$$

where u_0,v_0 and w_0 are the displacement components and ε_{xx}^0, ε_{yy}^0 and γ_{xy}^0 are the strains at the middle surface respectively. The total strains acting in the layer of the sheet, which is parallel to the mid surface and a distance z from the middle surface can be written as:

$$\varepsilon_{xx} = \varepsilon_{xx}^0 - \frac{\partial^2 w_0}{\partial x^2} z, \varepsilon_{yy} = \varepsilon_{yy}^0 - \frac{\partial^2 w_0}{\partial y^2} z, \gamma_{xy} = \gamma_{xy}^0 - 2\frac{\partial^2 w_0}{\partial x \partial y} z \quad (3.61)$$

The equilibrium equation for the large deflection sheet analysis follows Hooks law and can be expressed in Eq. (3.62) as:

$$\frac{1}{Eh}\left[\frac{\partial^2}{\partial y^2}\left(N_x - vN_y\right) + \frac{\partial^2}{\partial x^2}\left(N_y - vN_x\right) - 2(1+v)\frac{\partial^2 N_{xy}}{\partial x \partial y}\right] = \left(\frac{\partial^2 w_0}{\partial x \partial y}\right)^2 - \frac{\partial^2 w_0}{\partial x^2}\frac{\partial^2 w_0}{\partial y^2} \quad (3.62)$$

where $\varepsilon_{xx}^0 = \frac{1}{Eh}\left(N_x - vN_y\right)$, $\varepsilon_{yy}^0 = \frac{1}{Eh}\left(N_y - vN_x\right)$ and $\gamma_{xy}^0 = \frac{N_{xy}}{GH}$; E and G are Young's modulus and shear modulus, respectively and v is Poisson's ratio.

The strains, membrane forces and displacement w_0, can be solved from the above set of equations, yielding two governing differential equations:

$$\frac{\partial^4 \varphi}{\partial x^4} + 2\frac{\partial^4 \varphi}{\partial x^2 \partial y^2} + \frac{\partial^4 \varphi}{\partial y^4} = h\left[\left(\frac{\partial^2 w_0}{\partial x \partial y}\right)^2 - \frac{\partial^2 w_0}{\partial x^2}\frac{\partial^2 w_0}{\partial y^2}\right] \tag{3.63}$$

$$\frac{\partial^4 w_0}{\partial x^4} + 2\frac{\partial^4 w_0}{\partial x^2 \partial y^2} + \frac{\partial^4 w_0}{\partial y^4} = \frac{1}{D'}\left[P' + \frac{\partial^2 \varphi}{\partial y^2}\frac{\partial^2 w_0}{\partial x^2} + \frac{\partial^2 \varphi}{\partial x^2}\frac{\partial^2 w_0}{\partial y^2} - 2\frac{\partial^2 \varphi}{\partial x \partial y}\frac{\partial^2 w_0}{\partial x \partial y}\right] \tag{3.64}$$

where $D' = \frac{h^3}{12(1-v^2)}$, $N_x = \frac{\partial^2 \emptyset}{\partial y^2}$, $N_y = \frac{\partial^2 \emptyset}{\partial x^2}$, $N_{xy} = -\frac{\partial^2 \emptyset}{\partial x \partial y}$, $\varphi = \emptyset/E$ and $P'(x, y)$ is the lateral load in the z direction $P(x, y)$ divided by E.

Once a desired shape is given, that is deflection w_0 and curvatures $\frac{\partial^2 w_0}{\partial x^2}$, $\frac{\partial^2 w_0}{\partial y^2}$ and $\frac{\partial^2 w_0}{\partial x \partial y}$ are known, φ and P' and in turn the in-plane strains, ε^0_{xx}, ε^0_{yy} and γ^0_{xy} can be calculated under appropriate boundary conditions and the calculation is independent of Young's modulus. However, Eq. (3.61) indicates that ε^0_{xx},ε^0_{yy} and γ^0_{xy} depends on Poisson's ratio v which is a geometric parameter. The total strain ε_{xx}, ε_{yy} and γ_{xy} can also be calculated from Eq. (3.61). The solution is obtained using ABAQUS FE package.

3.3.2 Decomposition of strains

Thin sheet is considered as assumption for the above formulation. So therefore, it involves only ε_{xx}, ε_{yy} and γ_{xy}, while the FEM implementation gives 3-D strains in terms of tensor. For obtaining the principal strains and the bending strains directly from the tensor E, the steps are outlined below. Ecan be expressed in terms of $\varepsilon_1 n_1 n_1^T + \varepsilon_2 n_2 n_2^T + \varepsilon_3 n_3 n_3^T$, where principal strains ε_1,ε_2 and ε_3 ($\varepsilon_1 \leq \varepsilon_2 \leq \varepsilon_3$) and the orientation of the principal strain n_1, n_2 and n_3 corresponding to the Eigen values and Eigen vectors of the strain tensor E at the material point. Therefore ε_1,ε_2 and ε_3 and n_1, n_2 and $n_3$can be obtained by solving the Eigen value problem:

$$En = \varepsilon n \tag{3.65}$$

where ε and n are principal strain and corresponding principal strain direction, respectively.

3.3.3 Significance of bending strain

The bending strain is generally caused by the non-uniform distribution of strain in the thickness direction. Given a (x, y) location, the bending strain at that location varies along the thickness direction and is generally defined as the difference between strain at that z value and the strain at the mid-plane of the sheet. For a thin sheet bending strain linearly increases with thickness and reaches the maximum value at sheet surfaces. The minimum principal bending strain at the top surface ($z = h/2$) is calculated based on the minimum principal strain found above.

$$\varepsilon_b = \varepsilon_1^{h/2} n_1^{h/2} - \varepsilon_1^0 n_1^0 \tag{3.66}$$

where $\varepsilon_1^{h/2}$ and $n_1^{h/2}$ are magnitude and direction of minimum principal strain at z and ε_1^0 and n_1^0 are magnitude and direction of the minimum principal strain at the mid-plane. The physical meaning of negative bending strain is that the top surface is subjected to more compressive strain than the middle. In the laser line heating process operating under temperature gradient mechanism, the sheet bends towards the laser beam. This indicates that the laser should be placed on the top surface of the sheet for this case. If the positive bending strains are much smaller than the negative ones and occur in much smaller regions, they can therefore be neglected as in case of pillow shape but not in the case of saddle shape.

3.3.4 Scanning path determination

Finally, the heating path is to be investigated. This depicts the path along which the laser heat source has to traverse on the blank to get the desired effect of heating and for obtaining the desired curved surface. The scanning path should be placed perpendicular to the minimum principal strain direction. The spacing between the heating paths should be appropriate in every region. No heating path should overlap with each other otherwise it may result in strain failure due to extra heating than necessary. The spacing between the two scanning paths should be more than the laser diameter. The detailed has been discussed in section 6.6.

3.3.5 Determination of heating parameters using artificial neural network (ANN)

The operating parameters needed for the process of laser line heating have been predicted with the help of an artificial neural network approach by using a back-propagation algorithm. The process parameters include laser power *P* (Watt), scanning velocity *V* (mm/min) and the number of passes considering the thickness of the sheet as constant. It is possible, in continuously varying the operating parameters to generate the required strain needed to form the desired shape. The different shapes that are needed to be developed, has its own minimum principal strain distribution over the surface. So, it is very much difficult to find the respective operating parameters corresponding to individual strains. To cater to the situation and to reduce the processing time, a suitable approach based on Artificial Neural Network (ANN) is followed. The basic reason is to model the minimum principal strain, which is the output with the input process parameters of laser line heating.

3.3.5.1 Artificial neural network

ANN is composed of multiple nodes that can simulate biological neurons of the human brain. The neurons are interconnected by links and they can interact with each other (Fausett 1994; Patterson 1995 and Tsoukals and Robert 1996). The nodes generally take the input data for performing simple operations on the data. The output of these operations is passed to other neurons. The output at each node is called as its activation or node value. A neural network consists of input, output, and hidden layers. These layers transform the input and transfers to the output layer. Each link of ANN is associated with weight. It acts as an excellent tool for finding the pattern by altering the weight values. It can recognize many complex patterns, which are very much difficult for recognition by the human program for machine learning applications. The illustration of a simple ANN is shown in Fig.3.4.

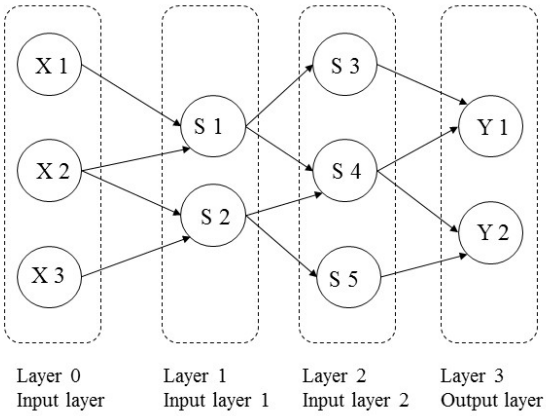

Fig. 3.4 Topology of a simple ANN network

3.3.5.2 Types of artificial neural network

There are two types of artificial neural network (ANN) topologies: feed forward and feedback ANN. In case of feed forward ANN, the flow of information is unidirectional. The feed-forward ANN topology is shown in Fig.3.5.

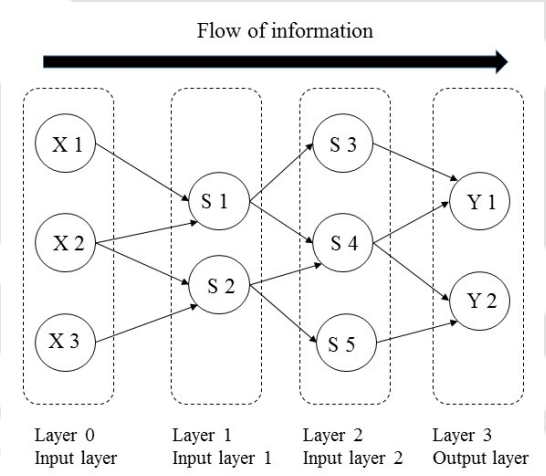

Fig. 3.5 Topology of Feed forward ANN

Here a unit conveys information to another unit from where it does not receive any information. There are no feedback loops. They have fixed inputs and outputs. Whereas in the case of Feedback ANN, feedback loops are allowed. The information is redirected to the specified or addressed location in the memories. The feedback ANN topology is shown in Fig.3.6.

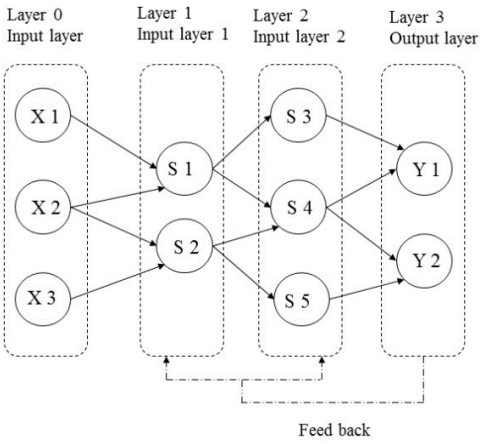

Fig.3.6 Topology of Feedback ANN

3.3.5.3 Working of ANN

In reference to the topology diagram as shown in Figs.3.5 & 3.6., each arrow represents the connection between two neurons and indicates the pathway for the flow of information. Each connection has weight, an integer number that controls the signal between two neurons. If the network generates good or deserved output, then the weights adjustment is not made. However, if the network generates a poor or undeserved output or an error, then the system alters the weight in order to improve the subsequent results.

3.3.5.4 Back propagation algorithm

The back-propagation training and learning algorithm is one of the most widely used algorithms in neural networks. In back propagation, the gradient vector of the error surface is calculated. The vector point in the direction of steepest descent from the current point indicating that moving along it in a short distance will decrease the error. Large steps may converge too quickly but may also overstep the solution. Small steps may go incorrect direction but require a large number of iterations. This is represented as a constant called a learning rate. The processing element may accept one or more signals which may be produced by other processing elements or applied externally. In the back-propagation network, each node resembles the connected network of a biological system (Parker 1985). The signals are amplified, weighted and summed together within the processing element. The hyperbolic tangent function is used as a transfer function. The function is easily defined as the ratio between the hyperbolic Sine and the Cosine functions as follows:

$$tanh(x) = \frac{Sinh(x)}{Cosh(x)} = \frac{e^x - e^{-x}}{e^x + e^{-x}} \tag{3.66}$$

where x is the sum of the node inputs. Hyperbolic function is similar to sigmoid function (Karlik et al. 2011). It ranges output between -1 to 1. The back-propagation process has two passes through the different layers of the network: a forward pass and a backward pass. In the forward pass, the input vector is applied to the sensory nodes of the network and its effect propagates layer-wise through the network. Finally, a set of output is obtained as the actual response of the network. During the forward pass, the synaptic weights of the network are all fixed. On the other hand, in the backward pass, the synaptic weights get adjusted by the error correction rule. Here the actual response of the network is subtracted from the desired response for producing an error signal. This error signal is then propagated backward through the network, against the direction of synaptic corrections. These synaptic weights are adjusted to make the actual response of the network closer to the desired response. Here each input or output parameter x_i is normalized as $(x_i)_n$ before being applied to neural network according to Eq. (3.67) given below.

$$(x_i)_n = \frac{(0.99 - 0.01)[x_i - (x_i)_{min}]}{[(x_i)_{max} - (x_i)_{min}]} + 0.01 \tag{3.67}$$

where $(x_i)_{max}$ and $(x_i)_{min}$ are the maximum and minimum values of parameter x_i. Before the starting of the application, the network is trained to perform the mapping between inputs to output parameters. The training of data is initiated by assigning small random values to the weights and the first set of input values are presented to the network, which in turn calculated the output values. As the initial weights are selected in random, the output values obtained are quite different from the desired output values. The difference between the desired and calculated outputs is obtained for getting the error output. That error output is then back propagated for adjustment of each weight for obtaining values closer to the desired ones. The weights preceding to each output node are updated according to the following Eq. (3.68)

$$Y_{ij}(t+1) = Y_{ij}(t) + kY_i(d - a) \tag{3.68}$$

Here Y_{ij} represents the weight connecting the i^{th} neuron of the input vector and j^{th}neuron of the output vector and k represents learning rate. The variable Y_i represents the i^{th}component of the input vector. The variable d represents the desired output of the neuron and the variable a represents the actual output of the neuron. This cycle is repeated until the calculated outputs

converge sufficiently close to the desired output. So, in reference to application point of view, new input data are presented to the network which results in prediction of new outputs based on the transfer characteristics learned during the training mode.

3.4 Mesh sensitivity analysis

The mesh sensitivity analysis plays a very predominant role in investigating the results obtained from FE analysis. The basis of doing the mesh sensitivity analysis is to know about the quality of mesh used for FE analysis. Correct mesh size results in obtaining the output results of an acceptable level, considering the inputs provided to the model are without error. Mesh density is a significant parameter, which is used for controlling the output results. Higher mess density results in the requirement of more computational time and with acquiring more memory as multiple iteration runs.

About the study of numerous investigations have been performed based on the variation of the element size, important conclusions have been drawn for the determination of the accuracy of results. Poor convergence of output results was observed for large element size. So, based on the observation it was noted that the selection of appropriate element size for the execution of finite element problems is very much necessary.

3.5 Taguchi method of Design of Experiment

The Taguchi method is employed for reducing the process variation by using the robust design of experiments. This method of experimental design offers an easy and effective approach for conducting experiments. This method has a potential evaluation of the variability of a specific process subjected to different operating parameters (Roy 1990). For achieving this in an effective and significant manner, the levels of operating parameters are significantly varied and corresponding outputs are evaluated. Based on the complete set of output results the critical operating parameters and their preferred levels are decided. Change in level of operating parameters will lead to a significant improvement in output result. In this present work, the Taguchi method is used for the determination of a minimum number of experiments are to be performed for the estimation of optimum operating parameters that results in maximum angular deformation.

Taguchi method has been classified into three stages and the steps for completing the experiment are listed below.

A. **The planning stage:** It includes: a) Conceptualization of problem, b) Formulation of the objective function, c) Evaluation of output, d) Recognition of operating parameters influencing the output, e) Selection of levels of the operating parameters, f) Selection of orthogonal array, g) Choosing of the interactions influencing the output, h) Allocation of the factors to the orthogonal array (OA) and detect the interaction.
B. **Performing stage:** Carrying out of experiments based on the orthogonal array (OA).
C. **Investigation stage:** It includes: a) Analysis and interpretation of results on the basis of signal to noise ratio (S/N) and analysis of variance (ANOVA), b) Carrying out of confirmation experiment.

3.5.1 Aim of the experiment

The aim of the experiment is to determine the optimized values of the operating parameters that will yield maximum angular deformation in the process.

3.5.2 Control factor and noise factor

The factors that can be controlled, while performing the experiment are called as control factors. The factors that cannot be controlled are called as noise factors. The list of noise factors and control factors associated with this work are shown in Table 3.1.

Table 3.1 Control and noise factors

Control factors	Noise factors
Laser power, traverse speed, number of pass, sheet thickness.	Operating environment temperature, material surface quality, position of work piece in machine work bed, internal residual stresses present in the blank, work piece alignment with fixture etc.

3.5.3 Selection of orthogonal array

It is selected based on the number of operating parameters and the number of levels for individual parameters. An orthogonal array is a type of experiment where the columns for the individual variables are 'orthogonal' to one another. Taguchi has established OAs for describing a large number of experimental situations. The symbolic representation of arrays carries the key information on the size of the experiment. Every array is represented by L (number). The 'number' indicates the number of trials required. For situations demanding more number of factors, higher levels as well as mixed levels, several other OAs are also available.

Experiment designs by OAs are very much fascinating because of experimental efficiency. The experiments based on orthogonal array (OA) works well when there is minimum interaction between the factors. The outcome is directly proportional to the linear combination of individual factor main effects. It distinguishes the optimum condition and estimates performance at this condition accurately. If the factors interact with each other and influence the outcome in a non-linear manner, the optimum conditions are identified with higher accuracy.

3.5.4 Signal noise ratio

In Taguchi's method, the "signal" depicts the desired value and the "noise" depicts the value which is undesirable of the process output, respectively. The analysis of the signal to noise ratio is performed to develop a process that is not sensitive to any of the noise factors as listed in Table 3.1. There are three categories of performance characteristics in Taguchi's method for analysis of signal to noise ratio. They are: i) lower the better, ii) nominal the better and iii) higher the better.

The objective of the present work is to maximize the angular deformation. Thus, higher the better characteristics are used in this work. The signal to noise ratio belongs to 'higher the better' characteristics is calculated using Eq. (3.67). In Taguchi's method, a higher signal to noise ratio corresponds to better performance with minimum process variation. Thus, optimum combination of parameters is the one with highest signal to noise ratio.

$$S/N = -10\log_{10}\left(\frac{1}{n}\sum_{i=1}^{n}\frac{1}{y_i^2}\right) \quad (3.67)$$

where y_i is the i^{th} result of the experiment or observation.

3.5.5 Analysis of Variance (ANOVA)

There is a standard statistical technique called Analysis of Variance (ANOVA) which has been used for providing a measure of confidence. This technique does not directly analyze the data, but rather determines the variability or variance of the data. Confidence is measured from the variance. This technique is generally employed to interpret the experimental data and make decisions on control factors that affect the process output characteristics. The basic equation of analysis of variance is given below.

Total sum of squares (SS_{Total}) = Sum of squares due to mean (SS_{mean}) + Sum of squares due to error (SS_{error}).

Mean square or variance is a measure of dispersion of data scattered from the mean. Variance of any factor is given by its sum of squares divided by its degree of freedom.

3.6 Summary

In this chapter the formulation and detailed methodologies used to achieve the objectives of the thesis. The chapter starts with prediction of thermal history of laser line heating. The Equations in section 3.2.1 are used for the development of 3-D FE heat source model which are used in Chapter 5. The thermal model is followed by 3-D FE model for non-linear structural analysis, which is used to analyze the residual deformation, thermal residual stresses and thermal residual strains which is discussed in Chapter 5. The mesh sensitivity analysis mentioned in section 3.3 is used in Chapters 5 and 6. The procedure for development of compound curved surface generation is mentioned in section 3.3 along with the artificial neural network (ANN) mentioned in section 3.3.5 is used in Chapter 6. The Taguchi method of DOE and ANOVA which are discussed in section 3.5 are used in Chapter 4 for the determination of the effect of operating parameters related to laser line heating process.

Chapter 4

Effect of Operating Parameters of Laser Line Heating

4.1 Introduction

In this chapter, an experimental study was conducted for obtaining the optimized values of operating parameters which include: laser power, traverse speed, number of passes and sheet thickness with their effect on angular deformation based on temperature gradient mechanism (TGM). The output results obtained were suitably analyzed under Taguchi analysis and ANOVA and with the development of the relationship between the operating parameters suitable optimum parameters were obtained.

4.2 Experimental details

A CO_2 gas laser machine (Orion 3015, LVD make) was used for the experiments. Rectangular mild steel blanks of dimension 100 mm × 100 mm and thickness 3 mm and 4 mm were taken as working specimens. For the experiment to be started the specimens were put on the machine work table with the help of clamp, with job holding attachment as shown in Fig.4.1 about 5 mm to 6 mm gap was maintained between the work table and the specimen so that there should be no constraints for the specimen while undergoing counter bending.

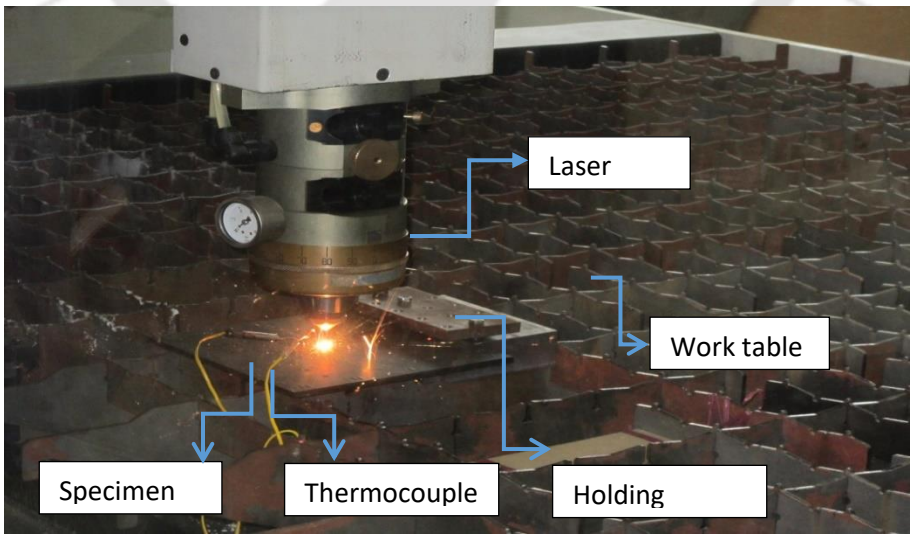

Fig.4.1 Experimental set up for straight line bending

Numerous numbers of experiments were carried out by altering the operating parameters. The angular deformation of the sheet was determined with the help of a coordinate measuring machine (CMM) for an individual set of experiments. As in the present study, the temperature gradient mechanism (TGM) is to be maintained throughout the process. For establishing the TGM throughout the process, the laser operating parameters are selected based on a dimension less parameter known as Fourier number (F_0). The Fourier number (F_0) can be expressed as follows:

$$F_0 = \frac{\Psi d}{s^2 V} \tag{4.1}$$

where Ψ is thermal diffusivity and t is the thickness of sheet. Fourier number is used for characterizing the nature of heat conduction for a given laser material interaction time, equal to beam diameter divided by traverse speed ($^{d}/_{V}$) . For the thin sheet section, the lower value of F_0 i.e. less than unity recommends TGM will be the dominant mechanism with BM (Buckling mechanism) and UM (Upsetting mechanism) at higher value of F_0 (Griffiths 2012; Li and Lawrence 2001). For establishing TGM, the laser diameter has to be maintained of the order of sheet thickness. So, estimation of suitable stand-off distance (SOD) is an important part of the process. The strategy taken for the estimation of SOD is shown in Figs.4.2.

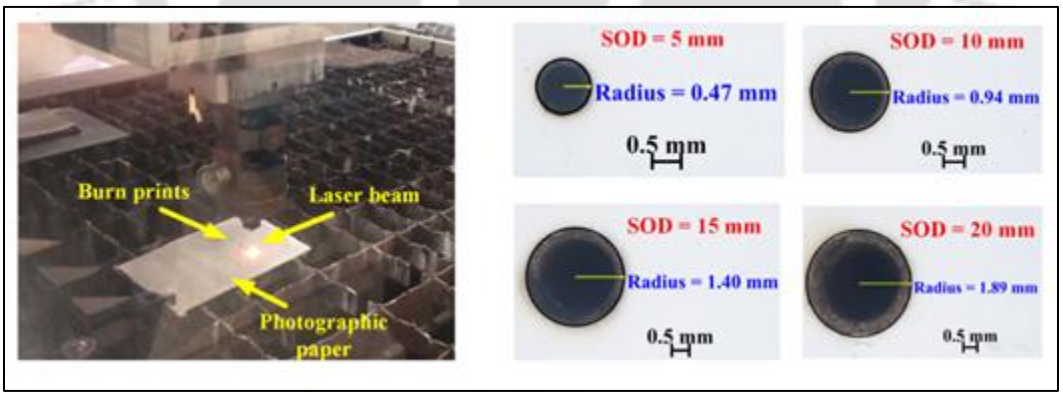

Fig.4.2 Experimental set up for estimation of stand-off distance

The laser beam was allowed to fall on a photographic paper as shown in Fig.4.2. Due to the laser-material interaction, a dark spot was seen on the surface of the photographic paper. The experiment was repeated for different stand-off distance and the burn prints were collected. It

was observed that with the increase in stand-off distance the diameter of burn print varies, it increases with an increase in stand-off distance as shown in Fig.4.2. Based on this above procedure the relation between the standoff distance and the laser diameter was determined. As the present work deals with the usage of TGM, the selection of laser diameter is performed by the above procedure based on the thickness of the sheet material. The laser power was selected such that, it will burn the region confined to laser diameter only. It was also observed that the burn impressions are found to be elliptical with a very minute difference in the major and minor axis of the ellipse as shown in Fig.4.2.

4.3 Material properties

The material used for the investigation is mild steel. The mechanical properties associated with the material used have been determined experimentally. The stress-strain plot of the material used in the experiment and the mechanical properties associated with the material are shown in Fig.4.3 and Table 4.1 respectively.

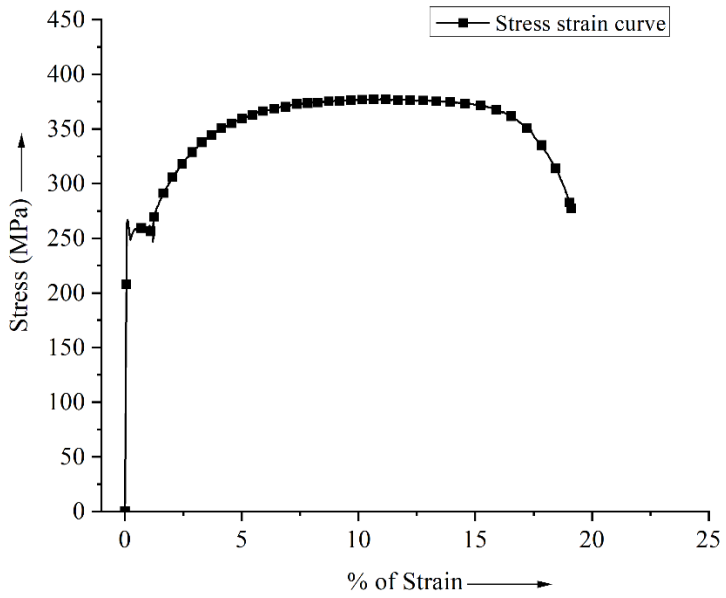

Fig.4.3 Experimentally obtained stress-strain plot

Table 4.1 Material properties used in analysis

Density	7800 kg/mm^3
Poisson's ratio	0.3
Young's Modulus	200 GPa
Yield stress	281 MPa

4.4 Taguchi method of Design of Experiment

Design of experiment is a method where the experiments were performed according to a fixed system or plan. This is necessary for solving any problem related to engineering in principles, techniques and data collection stage, so that in ensuring in getting some logical and justifiable conclusions. It also enables the designs for the determination of individual and interactive effect of many factors, which could affect the output results in any design. Here in this case Taguchi method of design of experiment is taken into consideration before performing the experiments and analysis.

Taguchi method (Roy 1990) has been designed for obtaining of improved quality processes and outputs where the performance of the output depends on several factors. It can be thought that for carrying out any test and development, simple logic is sufficient for establishment of possible combination of several factors along with the ranges to be taken into consideration. Taguchi has developed a set of designs for applications. The special features of this type of designs are the usage of orthogonal arrays. These arrays help in performing minimum number of experiments required for a given set of parameters. Here we have used Taguchi design of experiment for optimizing the operating parameters.

4.4.1 Selection of the level of parameters

For the selection of the level of parameters, first the number of operating parameters involves in the process are to be selected and then the level of individual parameters is to be defined. If it happens that the number of levels is not uniform for all, then mixed level design is to be taken into consideration. By considering both the values (number of parameters and levels) the suitable

orthogonal array has to be chosen from the manuals or handbook (Roy 1990). The design should be extracted from the listed designs and it is to be used.

Here the experimental design for multi pass line heating was taken into consideration by selecting four laser operating parameters, they are: traverse speed, laser power, sheet thickness and number of scans. All the parameters were varied in four levels except the sheet thickness which is varied in two levels. L-16 orthogonal array was incorporated for the design of experiment as shown in Table 4.2. The operating parameters and the output results obtained from the experiment were put based on the L-16 design pattern and the S/N analysis was performed. As in this case the main aim is to obtain large bend angle with change in operating parameters, so higher values of S/N ratio give better result corresponding to optimal process parameter.

Table 4.2 Operating parameters and their selected levels (under Taguchi DOE L-16 array)

Experiment no.	Traverse speed (mm/min)	Power (W)	Number of pass	Sheet thickness (mm)
1	500	300	1	3
2	500	400	2	3
3	500	500	3	4
4	500	600	4	4
5	400	300	2	4
6	400	400	1	4
7	400	500	4	3
8	400	600	3	3
9	300	300	3	3
10	300	400	4	3
11	300	500	1	4
12	300	600	2	4
13	200	300	4	4
14	200	400	3	4
15	200	500	2	3
16	200	600	1	3

4.5 Results and discussion

4.5.1 Single pass line heating

A series of experiments were performed for obtaining the angular deformation of the mild steel sheets of dimension 100 mm × 100 mm with varying thickness. The experiments were carried out by changing the laser power and traverse speed, keeping the laser diameter constant, which is maintained of the order of sheet thickness. The peak temperatures obtained from the experimental study at different locations are shown in Fig.4.4 and the values are tabulated in Table 4.3.

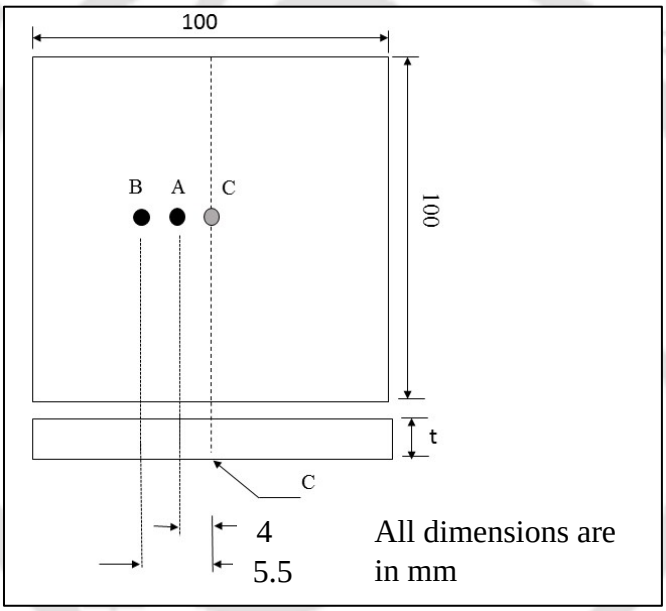

Fig.4.4 Position of thermocouples

Table 4.3 Peak temperatures obtained at measured locations under single pass line heating

Sl. no.	Power (W)	Traverse speed (mm/min)	Temperature at position 'A' (°C)	Temperature at position 'B' (°C)	Temperature at position 'C' (°C)
1	400	500	142.02	99.66	146.96
2	400	400	164.92	121.17	168.71
3	400	300	207.06	157.59	215.56

4	400	200	262.97	223.14	300.51
5	500	500	220.82	139.48	224.79
6	500	400	226.86	182.36	343.54
7	600	500	147.45	146.77	380.80
8	600	200	372.53	309.37	523.17

A temperature study was conducted by using thermocouples (K-type) which were placed on the upper and lower side of the mild steel sheet. The thermocouple A and B were placed at the top side of the mild steel sheet (laser traversing side) at varying distance from the laser heating line and the thermocouple C was placed just beneath of the laser heating path. The thermocouples A and B were placed at a distance of 4 mm and 5.5 mm from the heating line, respectively as shown in Fig. 4.4. The thermocouples were connected with computer with the help of Agilent 34970A data logger and the temperature data for the eight combinations of laser operating parameters as mentioned in Table 4.3 were recorded.

The angular deformation for different set of operating parameters under single pass line heating process for mild steel sheet of 3 mm sheet thickness are shown in Fig.4.5 and Table 4.4, respectively.

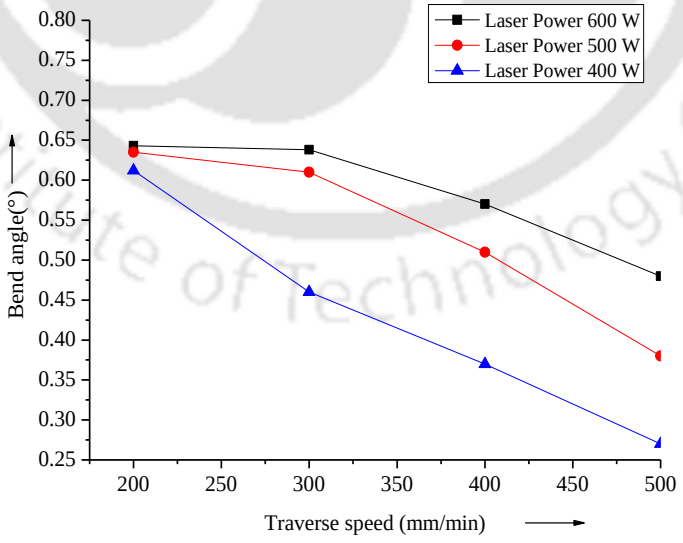

Fig.4.5 Effect of traverse speed on bend angle for different laser power

Table 4.4 Results for experiments under single pass line heating

Sl. no.	Laser Power (W)	Traverse speed (mm/min)	Angular deformation (°)
1	600	200	0.643
2	600	300	0.638
3	600	400	0.570
4	600	500	0.480
5	500	200	0.635
6	500	300	0.610
7	500	400	0.510
8	500	500	0.380
9	400	200	0.612
10	400	300	0.460
11	400	400	0.370
12	400	500	0.270

From Fig.4.5 it is seen that for constant laser power and increase in traverse speed, the angular deformation value reduces. The reduction pattern is non-uniform in nature. Another study was performed based on the trend line which was obtained from the values of angular deformation under different heat input per unit length for sheet thickness of 3 mm is shown in Fig.4.6.

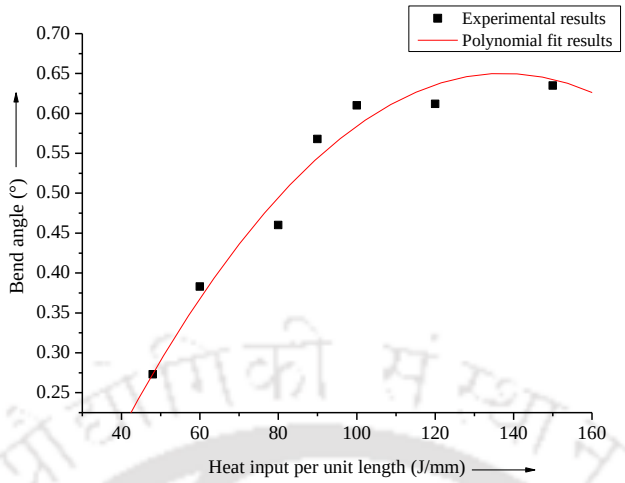

Fig.4.6 Effect of heat input per unit length on angular deformation

It is seen from the Fig.4.6 that with the increase in line heat input, the angular deformation increases. But the rate of increase of angular deformation increases with lower values of line heat input. After certain line heat input of approximately 120 J/mm, the rate of increase in angular deformation becomes low. So, from Fig. 4.6 it can be concluded that the line heating should be carried out within the line heat input value of 120 J/mm.

4.5.2 Multi-pass line heating

On the basis of L-16 orthogonal array as shown in Table 4.2, the experiments were performed by changing the operating parameters for obtaining the results of angular deformation. The results of angular deformation are shown in Table 4.5.

Table 4.5 Experimental results on the basis of Taguchi L-16 array DOE

Experiment no.	Traverse Speed (mm/min)	Power (W)	Number of pass	Sheet thickness (mm)	Resultant angular deformation (°)
1	500	300	1	3	0.210
2	500	400	2	3	0.480

3	500	500	3	4	0.460
4	500	600	4	4	0.971
5	400	300	2	4	0.012
6	400	400	1	4	0.057
7	400	500	4	3	1.482
8	400	600	3	3	1.166
9	300	300	3	3	0.869
10	300	400	4	3	1.372
11	300	500	1	4	0.209
12	300	600	2	4	0.420
13	200	300	4	4	0.816
14	200	400	3	4	0.822
15	200	500	2	3	0.994
16	200	600	1	3	0.643

4.5.3 Analysis of DOE results

The obtained experimental results were investigated under Taguchi method of analysis. Taguchi analysis incorporates the basic three objectives, which are: (i) For the determination of the optimum condition, (ii) factors contributing to the results and determination of percentage contribution of the operating parameters to the output results, (iii) Expected results at the optimum condition.

Identification of the optimum condition can be obtained by simple arithmetic calculations (Roy 1990). On determination of optimum parameters, trial run must be performed for checking and confirmation of the output results. The combination of optimum parameters may not be in the set of experiment that has been obtained under suitable set of orthogonal arrays.

4.5.3.1 Signal to Noise ratio and its significance

The “Signal” depicts the useful information and the “Noise” represents the value which is undesirable (Kolahan et al. 2011). From the Taguchi analysis we obtain the plot for S/N ratio in

Fig. 4.7. The values of the graph indicate the optimal parameters based on the bend angle as an output for the process.

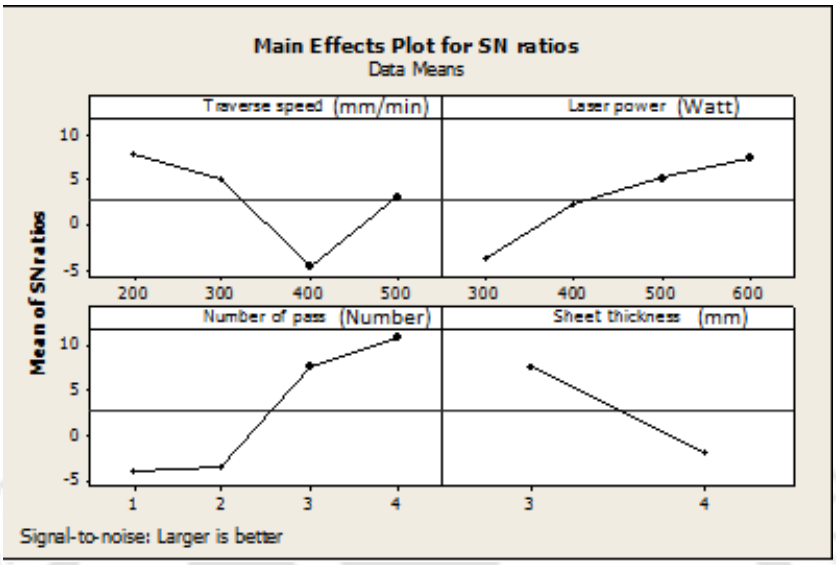

Fig.4.7 Mean S/N ratio for the input parameters

From Fig.4.7 it has been observed that, with the usage of the values of the parameter having negative mean S-N ratio will lead in obtaining poor quality of output (bend angle). For obtaining the optimum bend angle the parameters which are having higher positive value are to be selected. It is seen that optimum bend angle can be obtained by using laser power = 600 W, traverse speed = 200 mm/min, number of pass = 4 and sheet thickness = 3 mm.

4.5.3.2 Analysis of Variance

It is a technique which has been used for providing measure of confidence. This technique has been applied to the experimental results for the determination of the effectiveness of the parameters which are responsible for the required output. This technique helps in providing confidence on the basis of variance of the data (Kolahan et al. 2011).

Table 4.6 ANOVA table for bend angle

Source	DF	Seq SS	Adj SS	Adj MS	F	P	Percentage Contribution
Traverse Speed	3	0.794	0.794	0.264	1	0.465	2.629

Laser Power	3	1.647	1.647	0.549	2.07	0.223	5.450
Number of Pass	3	21.415	21.415	7.138	26.94	0.002	70.874
Sheet thickness	1	5.034	5.034	5.034	19	0.007	16.660
Residual error	5	1.324	1.324	0.265	-----	------	4.384
Total	15	30.216	------	------	------	------	----------

From the above analysis as shown in Table 4.6 the R-Squared and the adjustable R-squared is found to be about 95.62% and 86.85%, respectively which indicates the wellness of data to fit into a statistical model.

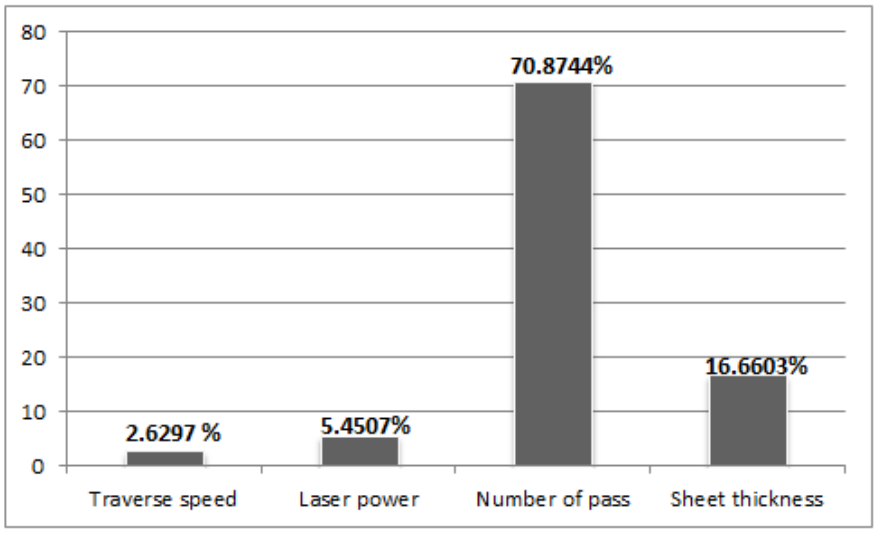

Fig.4.8 Percentage contribution of individual operating parameters

From Fig.4.8 it can be observed that the bend angle has a significant influence on sheet thickness and number of pass (scans) than the rest of other parameters. It is also observed from the values of percentage contribution both scanning speed and number of pass is dominant with respect to all other parameters.

4.5.3.3 Regression analysis

A multivariable regression analysis has been done for obtaining a relationship between the angular deformation with that of the input parameters (i.e. laser power, traverse speed, sheet thickness and number of pass). The equation obtained based on the regression analysis is shown in Eq. (4.1).

$$\emptyset = 1.28 - 0.000901V + 0.00107P + 0.300N - 0.431t \quad (4.1)$$

where $\emptyset$ =bend angle (°), V =traverse speed (mm/min), P = laser power (W), N =number of pass, and t = sheet thickness (mm).

Table 4.7 Regression table

Predictor	**Coef**	**SE Coef**	**T**	**P**
Constant	1.2783	0.2351	5.44	0.000
Traverse speed	-0.0009015	0.0002336	-3.86	0.003
Laser power	0.0010710	0.0002336	4.58	0.001
Number of pass	0.29965	0.02336	12.83	0.000
Sheet thickness	-0.43075	0.05224	-8.25	0.000
S = 0.104472 , R-Sq = 96.1 % , R-Sq(adj) = 94.6%				

Here R-Sq act as a measure of accuracy of the result to be obtained as output in relation to that of the input parameters with the experimental results. Higher the value of R-Sq indicates that the empirical relation obtained i.e. Eq. (4.1) above has the better predicting capability of the output (bend angle), there will be less mismatch between the experimental output with that of the output obtained from Eq. (4.1). As per Table 4.7, which is the regression table for the above Eq. (4.1), the value of R-Sq is found to be 96.1%, which shows that the model can be used with sufficient accuracy. A test run has been performed based on the parameters tabulated in Table 4.8

Table 4.8: Values of the bend angle obtained from the regression equation

Experiment No.	Traverse speed (mm/min)	Laser power (W)	No. of pass	Sheet thickness (mm)	Bend angle from experiment (°)	Bend angle from regression analysis equation (°)	% error
1	400	400	1	3	0.370	0.354	4.32
2	300	400	1	3	0.460	0.444	3.47
3	500	600	1	4	0.437	0.478	9.23
4	500	600	4	4	0.971	0.947	2.47

It is seen that the experimental output obtained validates well with that of the output obtained from the regression Eq. (4.1). The results obtained are of great accuracy with minimum amount of percentage error. Thus, this model can be used for predicting the bend angle by altering the input parameters within the range.

4.6 Summary

In this chapter, bending of mild steel sheet is carried out with the process of laser line heating with the input process parameters considered as traverse speed, laser power, number of pass and sheet thickness and the response obtained is bend angle as output.

- The line heating process parameters are optimized with respect to multiple performances in order to achieve best quality of angle of bend.
- Optimization of the process parameters are carried out using Taguchi method of analysis and a statistical technique called ANOVA.
- ANOVA statistics revealed that number of pass is the most influencing parameter in achieving good results followed by sheet thickness, laser power and traverse speed.
- A suitable co-relationship has been obtained between the laser power, traverse speed, sheet thickness and number of pass with bend angle by using multiple regression analysis. The expression validates well with the experimental results.

- Thus, it is concluded that the procedure proposed in this chapter for the optimization of laser line heating process parameters will significantly improve the angle of bend for mild steel sheets and plates.

Chapter 5

Thermo-Mechanical Analysis of Laser Line Heating

5.1 Introduction

For the generation of doubly curved surface by the process of laser line heating, the selection of suitable operating parameters was found to be an important part of the process. The operating parameters were selected on the basis of strain development. In this chapter, the process of laser line heating was simulated with the development of a 3D-FE model and a transient elasto-plastic thermo-mechanical analysis was carried out. The temperature distribution and the residual deformation were obtained for a combination of different operating parameters and the results were validated with the experimental ones. The validated FE model was then used for the prediction of stress and strain distribution associated with the laser line heating process. The results obtained from the thermo-mechanical analysis have been presented in this chapter.

5.2 Material properties

For accomplishing thermal and structural analysis for the process, the temperature dependent material properties for mild steel (Brown and Song 1992) are to be taken into consideration. The variation of material properties with change in temperature are listed in Table 5.1.

Table 5.1 Temperature dependent material properties of mild steel

Temperature (°C)	**Thermal expansion coefficient (10^{-6}/°C)**	**Specific heat (J/kg K)**	**Thermal conductivity (W/mK)**	**Modulus of elasticity (GPa)**	**Poisson's ratio**
0	10	450	51.9	200	0.278
100	11	499.2	51.1	200	0.309
300	12	565.2	46.1	200	0.331
450	13	630.5	41	250	0.338
550	14	705.5	37.5	110	0.357

600	14	773.3	35.6	88	0.373
720	14	1080.4	30.6	20	0.373
800	14	931	26	20	0.423
1450	15	437.9	29.4	2	0.473

The variation of enthalpy and yield strength of mild steel with temperature is presented in Table 5.2 and Table 5.3, respectively.

Table 5.2 Temperature dependent enthalpy of mild steel

Temperature (°C)	0	100	200	300	400	500	600	700	800	900
Enthalpy (MJ/m^3)	0	360	720	1100	1500	1980	2500	300	3700	4500

Table 5.3 Temperature dependent yield strength of mild steel

Temperature (°C)	0	100	300	450	550	600	720	800
Yield strength (MPa)	290	260	200	150	120	110	9.8	9.8

5.3 FE-model for laser line heating

A 3-D FE-modeling was executed for carrying out thermal and structural analysis for the process. The models were developed using APDL (Ansys Parametric Design Language). The sheet size of 100 mm × 100 mm with variable sheet thickness was considered along with a CO_2 laser heat source that was used for carrying out the analysis. Here in this process, the sheet was modeled using a three-dimensional brick element SOLID 70. Fine meshing was made in the region along the heating line, whereas coarse meshing was made in the region aside from the heating line as shown in Fig.5.1.

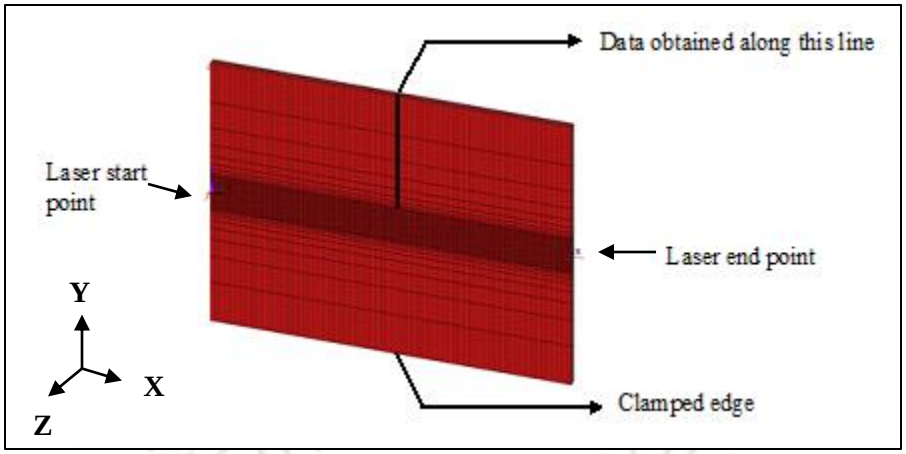

Fig.5.1 Model and meshing view

One side of the edge of the sheet was fully constrained for simulating the clamped edge condition. The heat flux distribution on the surface of the metal sheet exposed to laser heat source follows Gaussian distribution which is given in chapter 3, section 3.1.1.3. The absorption coefficient of the material subjected to the laser heat source, laser power, focal length, and effective beam diameter was used and the heat flux distribution was calculated. In the model fine mesh was made in the region where the rate of change of output data is very high, therefore more data points are required for evaluation of the results and the coarser mesh was used in the region where the rate of change of results is low. The thermal analysis was performed first for obtaining the temperature field and the results of the thermal analysis were used as input for carrying out the structural analysis. The boundary conditions which were used for carrying out the analysis are as follows:

5.3.1 Thermal boundary condition

The heat transfer in the boundary was modeled by natural convection and radiation. The convection follows Newton's law, where the heat loss per unit area i.e. W/m^2 is given by equation (5.1):

$$q_c = h_c(T_s - T_a) \tag{5.1}$$

where h_c= Coefficient of convective heat transfer, T_s = Surface temperature of the irradiated surface, T_a= Ambient temperature. The heat loss takes place due to radiation in W/m^2 is given by equation (5.2):

$$q_r = 5.67 \times 10^{-8} \epsilon (T_s^4 - T_a^4) \qquad (5.2)$$

where ϵ = emissivity of the surface. The magnitude of the emissivity depends on the surface condition and the sheet temperature. The temperature dependent emissivity value for mild steel is given in Table 5.4 (Brown and Song 1992).

Table 5.4 Temperature dependent emissivity of mild steel

Temperature (°C)	0	100	200	300	500	750	1000	1590
Emissivity	0.2	0.4	0.45	0.47	0.54	0.58	0.59	0.60

5.3.2 Structural boundary condition

In structural analysis, a one-sided clamped boundary condition was used as a constraint. While performing the structural analysis, SOLID 45 elements were used in this analysis. The sheet was generally considered to be flat and free from residual stresses. Simulations were carried out for different operating parameters and were matched with the experimental results. In structural analysis kinematic hardening and bilinear, von Mises yield criteria were considered (Biswas & Mandal 2008) in this thesis.

5.4 Experimental details

The experiments were carried out on mild steel sheets, which were used as a working specimen of dimension 100 mm × 100 mm with varying thicknesses. A CO_2 gas laser machine (Orion 3015, LVD make) was used for the experimental purpose. While performing the experiments, the specimens were held on the machine work table with the help of a fixture as shown in Fig.5.2. A space of about 5 mm to 6 mm is maintained between the work table and the specimen so that there should not be any restriction to the specimen during counter bending. Numerous

experiments were carried out and the results were obtained by changing the operating parameters. The angular deformation in the specimen after each experiment was evaluated with the help of a coordinate measuring machine (CMM). The temperature data were recorded by fixing thermocouple (K-type) at measured distances from the center of the heating line. The stand-off distance was maintained of 3 mm for sheet thickness of 3 mm for maintaining the TGM in the whole process.

Fig.5.2 Experimental set up for laser line heating process

5.5 Verification of FE-model

It is very much necessary in acquiring an idea of temperature distribution across and over the sheet surface subject to laser beam line heating over the sheet. So, for achieving perfection in the analysis, the FEM is validated with the experimental results by correlating with the predicted temperature distribution with the experimental ones. The comparison of FEM and experimental single pass temperature distribution on the top surface at a location of 4 mm away from the heating line is shown in Fig.5.3. The heating parameters selected for the single-pass laser line heating process are laser power: 500 W, traverse speed: 300 mm/min and sheet thickness: 3mm.

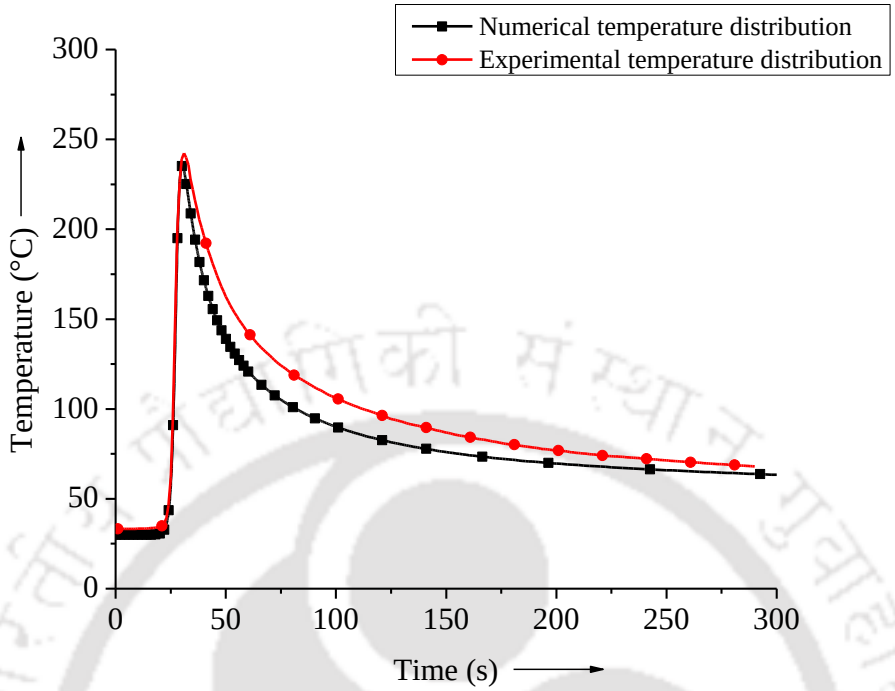

Fig.5.3 Comparison of temperature profiles for 3 mm thick sheet,4 mm away from the heating line

The peak temperature results were also obtained at a distance of 4.5 mm away from the heating line for 3 mm sheet thickness and the results are shown in Table 5.5.

Table 5.5 Peak temperature recorded at a distance of 4.5 mm away from the heating line

Laser Power (W)	Traverse speed (mm/min)	Experimentally obtained peak temperature (°C)	FE-model peak temperature (°C)	Percentage of error (%)
350	300	155.55	146.06	6.10
450	300	195.85	182.85	6.63
500	300	209.37	197.48	5.67

By comparing the temperature results obtained from the experiment and the FE-model, it is observed that all the results of the FE-model matched well with the experimental ones, with a

maximum percentage of error of 6.63 % as shown in Fig.5.5. This shows the effectiveness of the FE-model. The results of angular deformation were also evaluated using the above FE-model. A comparison between numerical and experimental results for 3 mm sheet thickness is listed in Table 5.6.

Table 5.6 Results of angular deformation obtained from experimental and FE-model

Laser Power (W)	Traverse speed (mm/min)	Experimental angular deformation (°)	Numerical angular deformation (°)	Percentage of error (%)
500	300	0.610	0.633	3.77
600	300	0.638	0.617	3.29

From Table 5.6 it is observed that the angular deformation results obtained from the experiment validates with the results obtained from the FE-model with a maximum percentage of error of 3.77 %. Thus, the results of temperature and angular deformation obtained from the FE-model validates well with the experimental ones. This shows the effectiveness of the FE-model and the model can be used for further investigation purpose.

5.6 Results and discussion

After validation of the FEM model, the analysis was carried out with the different combinations of laser line heating process parameters. The sheet dimension of 100 mm × 100 mm with variable sheet thickness was used for carrying out the FEM analysis. The effect of individual operating parameters on temperature distribution, residual deformation, and stress-strain distribution were studied.

5.6.1 Thermal history

The single-pass line heating temperature distribution for a laser power: 300 W, traverse speed: 300 mm/min and sheet thickness: 3 mm are shown in Figs.5.4 - 5.6. The temperature distribution contour on the surface of the sheet and the temperature distribution along the through-thickness direction of the sheet perpendicular to the heating line is shown in Figs.5.4 & 5.5 respectively.

The transient temperature distribution at various distances perpendicular to the heating line is shown in Fig.5.6.

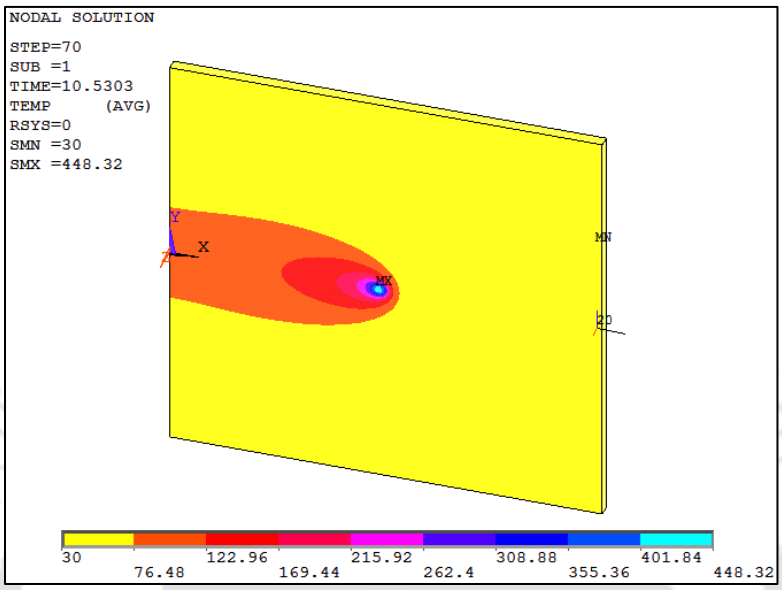

Fig.5.4 3-D contour of temperature distribution at mid-position of the sheet

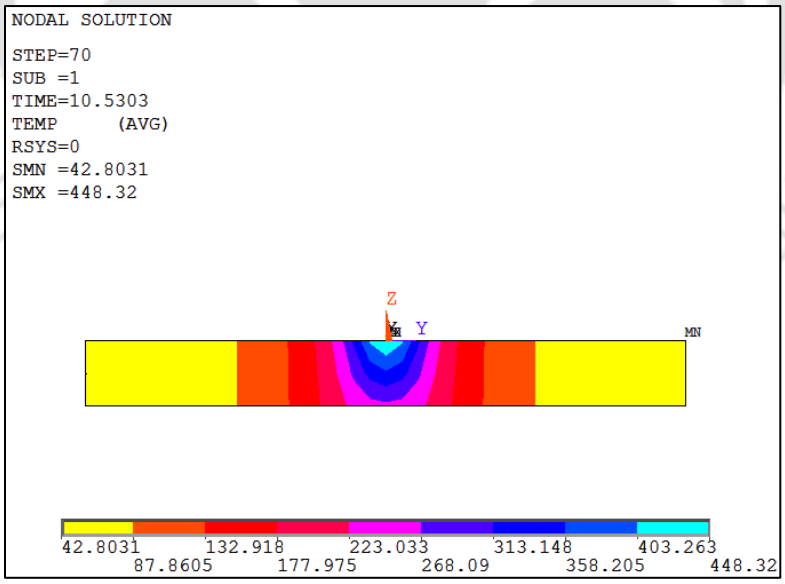

Fig.5.5 3-D contour of temperature distribution along through thickness direction

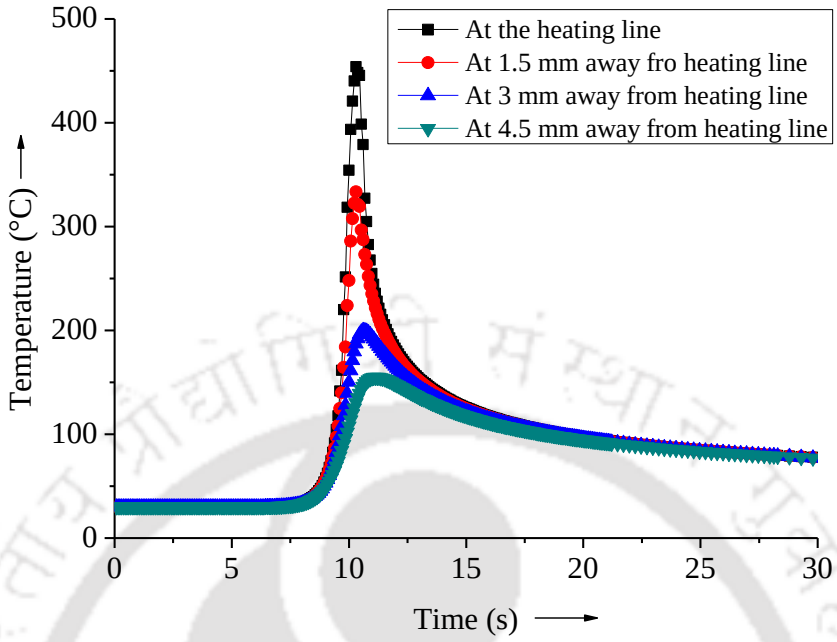

Fig.5.6 Transient temperature distribution at different points away from heating line

From Fig.5.6, it is seen that the heating and cooling curves on the top surface of the heating line show a very rapid rate of heating and cooling. From Figs.5.4 - 5.6 it is observed that the peak temperature gradually decreases from the center of the heating line to away from the heating line. From Fig.5.5 it can be seen that there is the presence of a sharp temperature gradient in the through-thickness direction. The effects of individual laser operating parameters on temperature distribution were studied and are presented below.

5.6.1.1 Thermal history in reference to variation of laser power

The temperature distribution for different laser power of 300 W, 350 W, 400 W, 450 W, 500 W, 550 W, and 600 W under constant traverse speed: 300 mm/min for a mild steel sheet having a sheet thickness of 3 mm under single-pass laser line heating has been presented in Figs.5.7 – 5.9. The variation of peak temperature with different laser power can be seen in Fig.5.7. It is seen that with an increase in laser power along the heating line the surface peak temperature increases gradually. It is also observed from Fig.5.9 that the peak temperature exists for a very short period and progressively the temperature cools down with time.

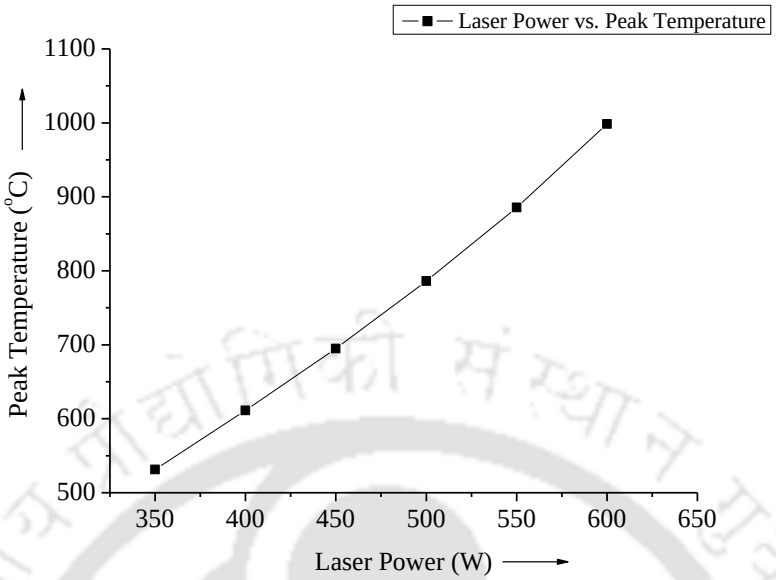

Fig.5.7 Effect of peak temperature on variation of laser power

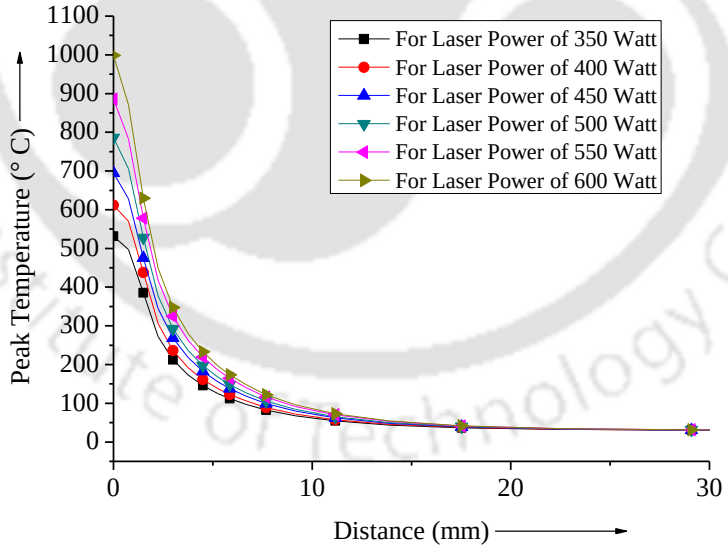

Fig.5.8 Effect of peak temperature with distance perpendicular to the heating line

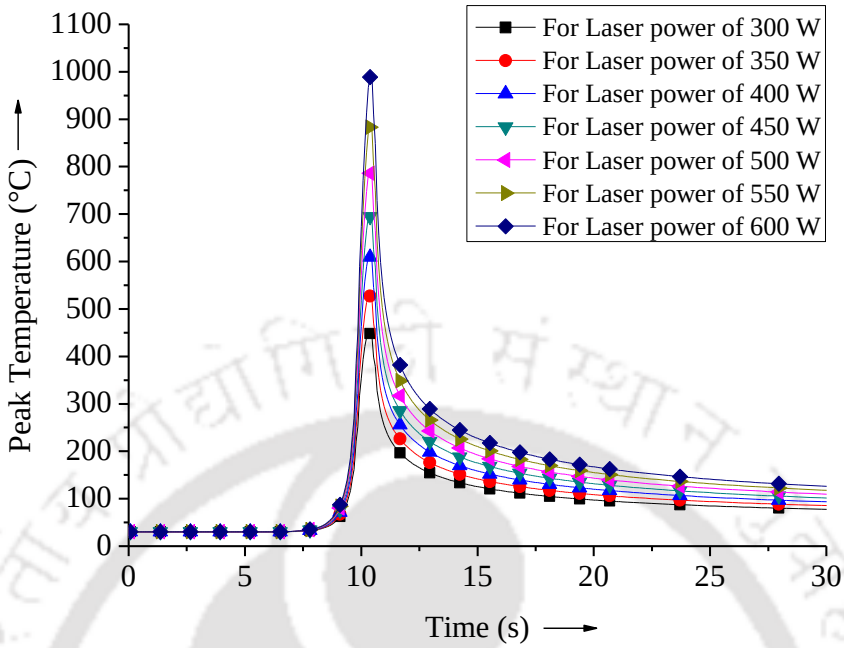

Fig.5.9 Peak temperature variation with respect to time with variation in laser power

This can also be seen that the cooling rate decreases with an increase in laser power. The peak temperature distribution perpendicular to the heating line is shown in Fig.5.8. It is seen that the temperature value decreases along the distance perpendicular to the heating line. Considering traverse speed in the lower range, with an increase in laser power the peak temperature rises beyond the recrystallization temperature of the mild steel sheet. So, for selecting the appropriate laser heating parameters proper combination of laser power and traverse speed is necessary to keep the surface temperature below the recrystallization temperature of the sheet material.

5.6.1.2 Effect of traverse speed on thermal history

The thermal history for different traverse speeds of 200, 300, 400, 500 and 600 mm/min under constant laser power: 350 W for a mild steel sheet having a sheet thickness of 3 mm under a single pass has been presented in Figs.5.10 - 5.12.

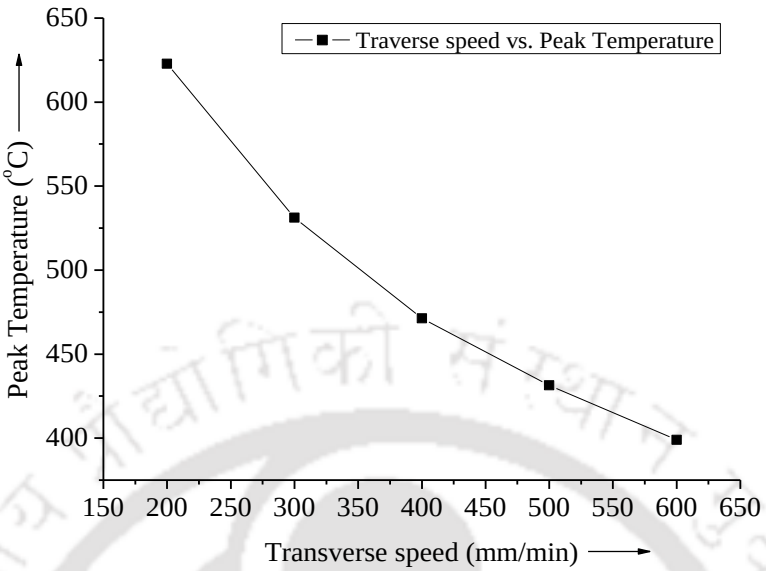

Fig.5.10 Effect of peak temperature with variation in traverse speed

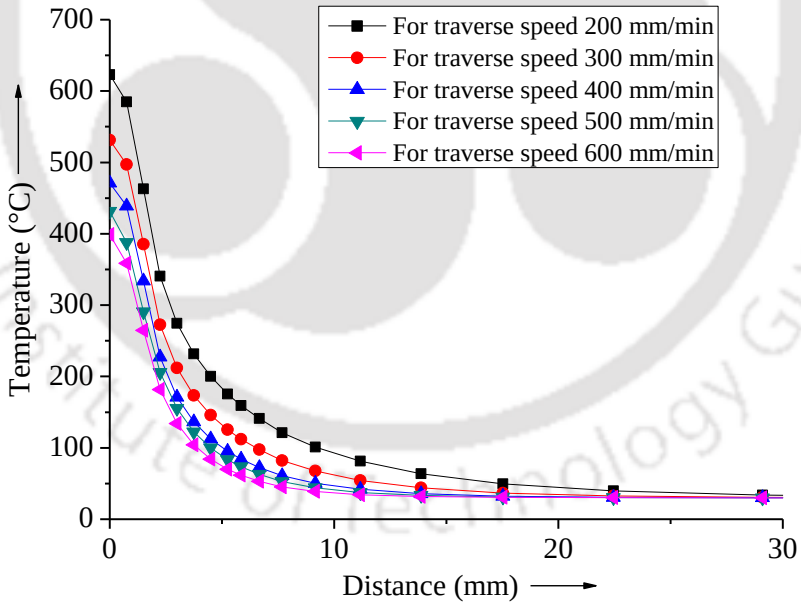

Fig. 5.11 Effect of peak temperature with distance perpendicular to the heating line

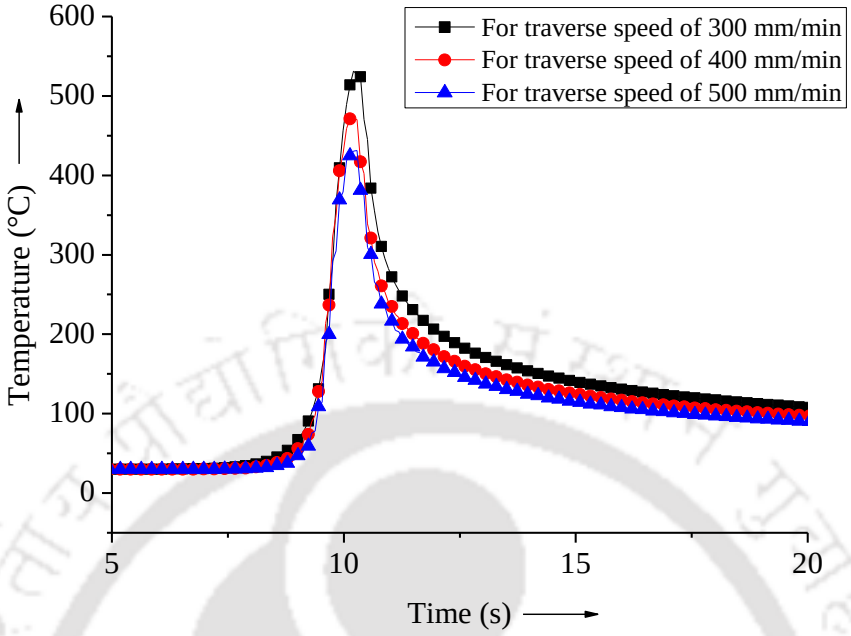

Fig.5.12 Transient temperature distribution with variation in traverse speed

It can be observed from Fig.5.10 that with an increase in traverse speed for constant laser power, constant sheet thickness there is a fall in sheet surface temperature. The sheet peak temperature perpendicular to the heating line is shown in Fig.5.11. It is seen that temperature value decreases along the distance perpendicular to the heating line. Fig.5.12 shows the temperature distribution with respect to time at a particular point for different traverse speed. The cooling rate enhances with enhancement of traverse speed.

5.6.1.3 Effect of sheet thickness on thermal history

Temperature distribution due to single-pass laser line heating for different sheet thickness of 2 mm, 3 mm and 4 mm under constant laser power and constant traverse speed of 300 W and 300 mm/min, respectively are shown in Figs.5.13 - 5.15.

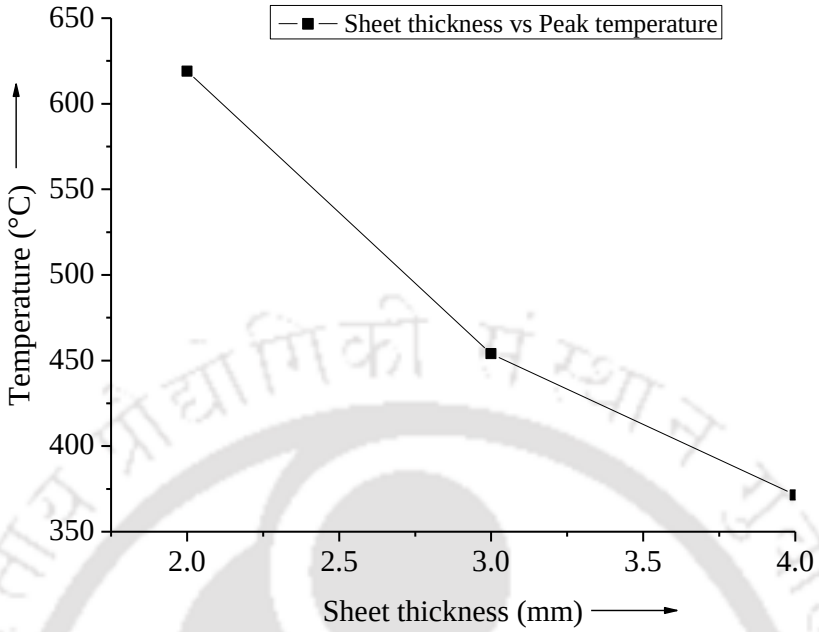

Fig.5.13 Effect of peak temperature with variation in sheet thickness

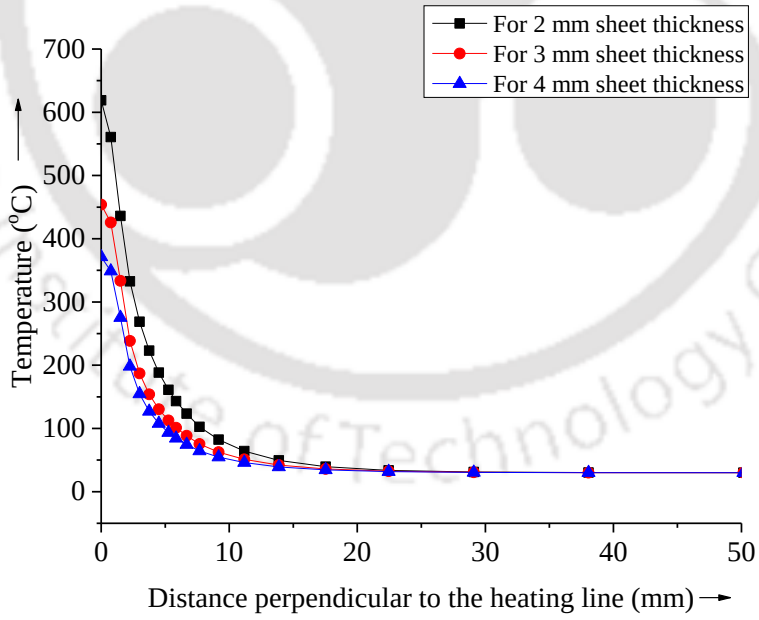

Fig.5.14 Effect of peak temperature with distance perpendicular to the heating line

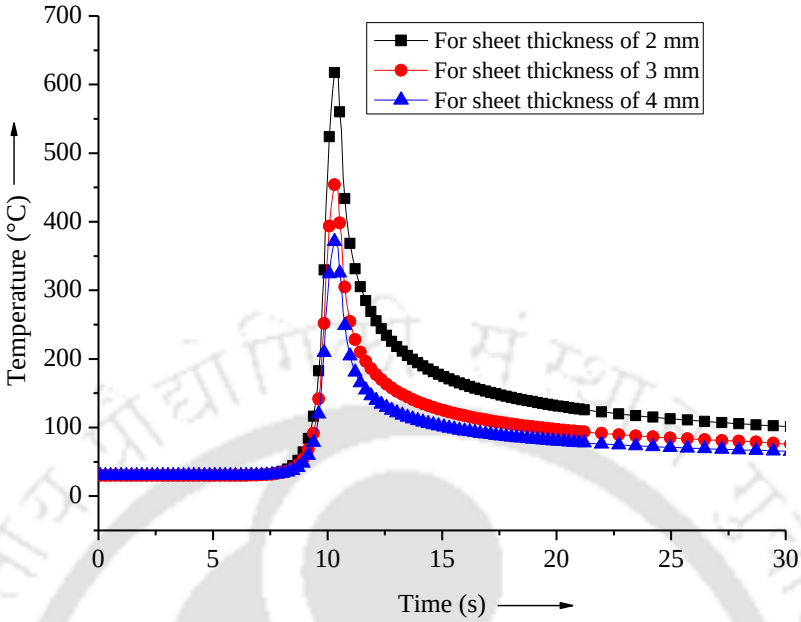

Fig.5.15 Transient temperature variation for different sheet thickness

For the above figures, it is seen that like laser power and traverse speed, the sheet thickness also has a significant effect on temperature distribution. It can also be seen from Fig.5.13 that the sheet surface temperature is significantly dependent on sheet thickness of the sheet. It is seen that for a constant value of traverse speed and laser power, with the enhancement of sheet thickness the surface peak temperature value reduces. The reduction in the temperature value is because of the increasing heat sink effect. The heat sink effect increases with the increase in sheet thickness. Fig.5.15 shows the temperature distribution with respect to time at a particular point for different sheet thicknesses. It is seen that the temperature gradient is found to be more for higher sheet thickness and it decreases with lesser sheet thickness value. Due to the presence of more temperature gradient, rapid heat flow occurs due to conduction in the material which results in a decrease in sheet surface temperature. Fig. 5.14 shows variation of surface peak temperature of the sheet at measured distances perpendicular to the heating line for different sheet thicknesses. For constant power and constant traverse speed, the increase in peak temperature value is high for lesser thickness and it gradually decreases along a perpendicular direction to the heating line. The cooling rate is found to be less for material having lesser sheet thickness than that of the material having higher sheet thickness.

5.6.1.4 Effect of line energy on thermal history

The thermal history for constant sheet thickness of 3 mm under different line energy have been presented in Figs. 5.16 - 5.18.

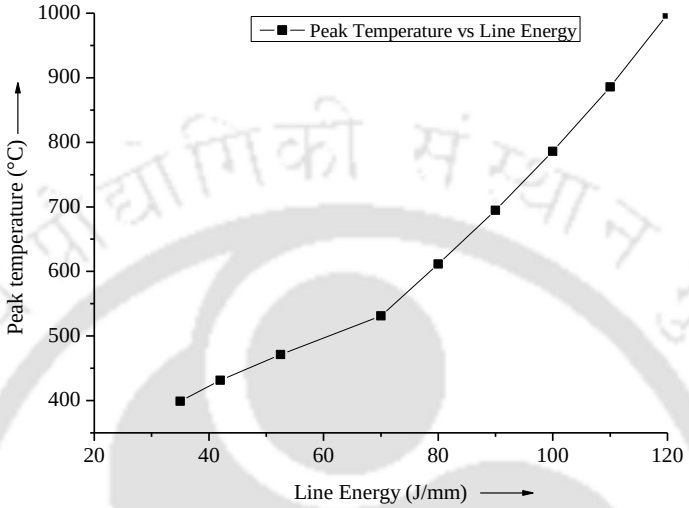

Fig.5.16 Effect of peak temperature on variation in line energy

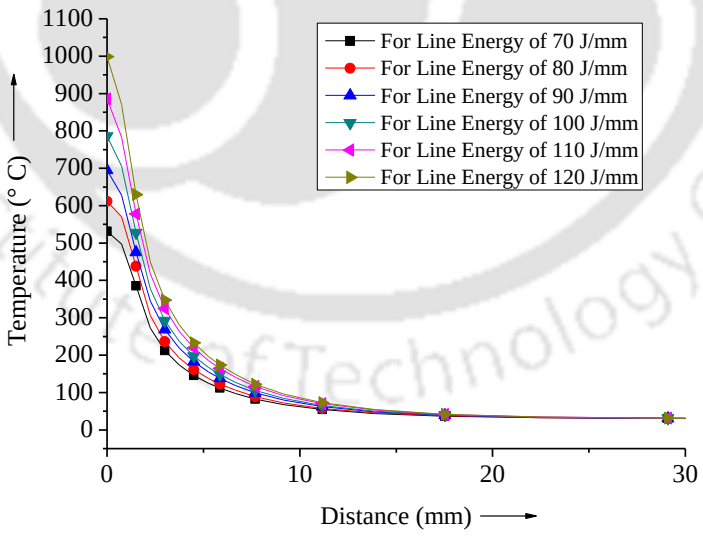

Fig.5.17 Effect of peak temperature with distance perpendicular to the heating line

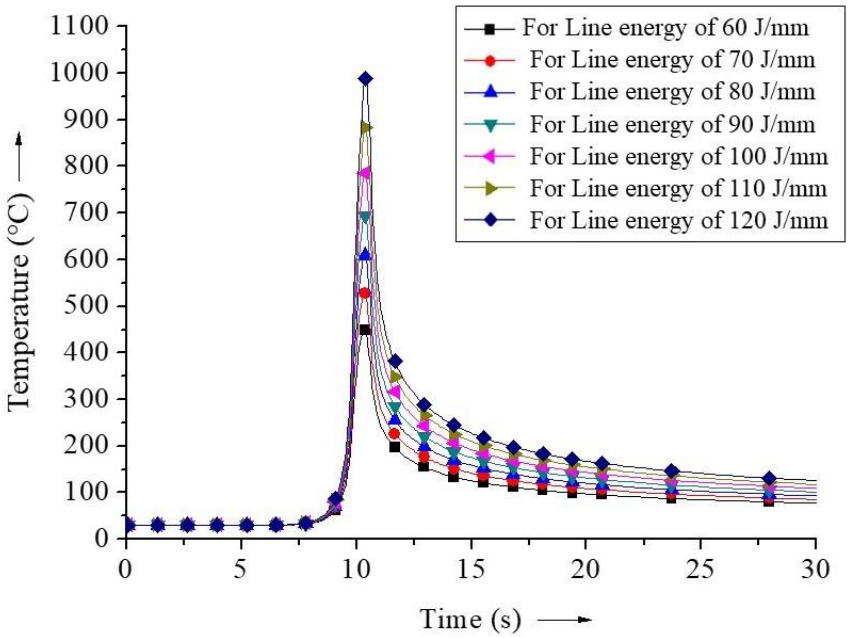

Fig.5.18 Transient temperature variation for different line energy

The line energy is described by heat input per unit length. It is obtained from the combined effect of laser power and traverse speed. With an increase in line energy the surface peak temperature value increases as shown in Fig.5.16. It can also be seen from Fig.5.18 that the cooling rate decreases with an increase in line energy. The peak temperature distribution perpendicular to the heating line is shown in Fig.5.17. It is seen that the temperature value decreases along the distance perpendicular to the heating line. Considering line energy in the higher range the peak temperature rises beyond the recrystallization temperature of the mild steel. The selection of line energy in the proper range will enable to maintain the sheet surface temperature below the recrystallization range.

5.6.2 Residual deformation

The laser beam act as a thermal load that incorporates residual deformation in the sheet. In the process the sample was clamped on one side and laser is allowed to traverse along the x-direction as shown in Fig.5.19. Here transient elasto-plastic thermo-mechanical structural analysis was executed by considering transient temperature distribution which was obtained from transient thermal analysis.

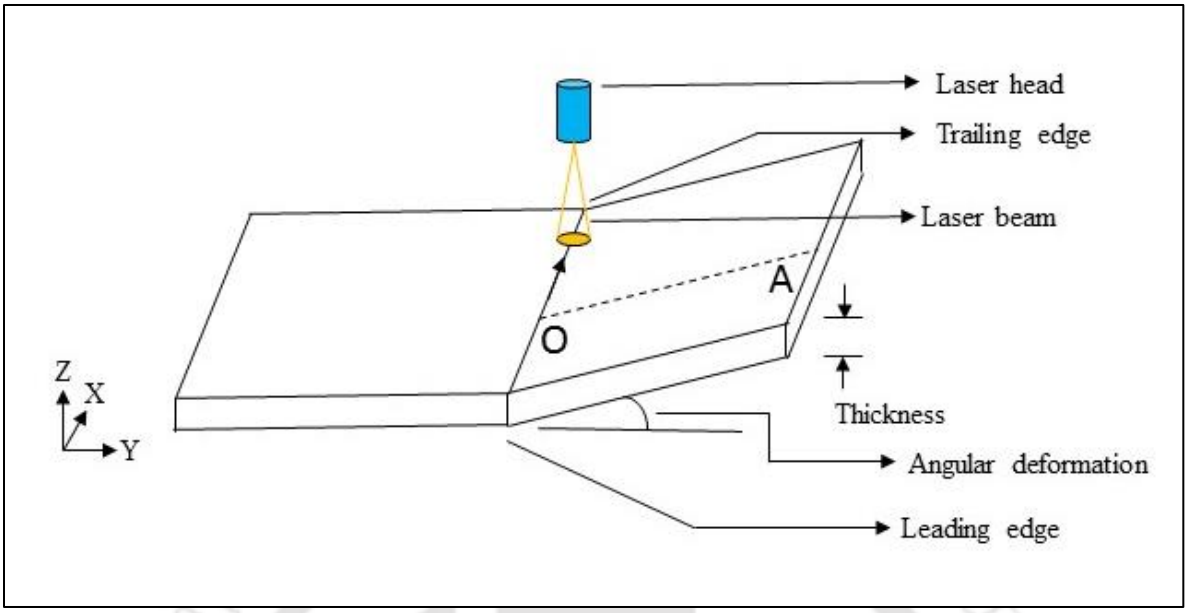

Fig.5.19 Schematic of laser line heating process for bend angle prediction

The residual deformation for individual specimen is obtained as:

$$\propto = tan^{-1}\frac{(Z_A - Z_O)}{(Y_A - Y_O)} \tag{5.3}$$

where O is a point taken on the heating line and point A is taken at a distance perpendicular to the heating line on the deformed part of the sheet. z_A and z_o are the Z-component of displacement at point A and O respectively. $(Y_A - Y_O)$ represents the horizontal distance between point A and O along Y- component. $\propto$ is the value of angular deformation in degrees as shown in Fig.5.19.

The residual deformation can be expressed in terms of angular deformation as shown in Eq. (5.3). The variation of Z-component of displacement for a laser power: 350 W, traverse speed: 200 mm/min and sheet thickness: 3 mm are shown in Figs. 5.20 & 5.21, respectively.

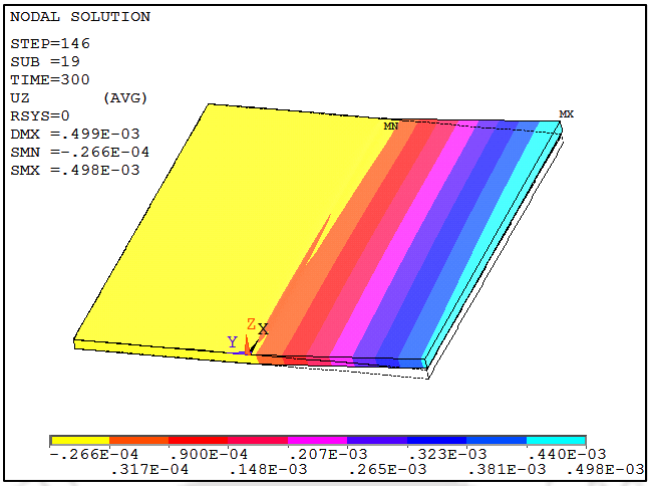

Fig.5.20 3-D contour plot of residual deformation

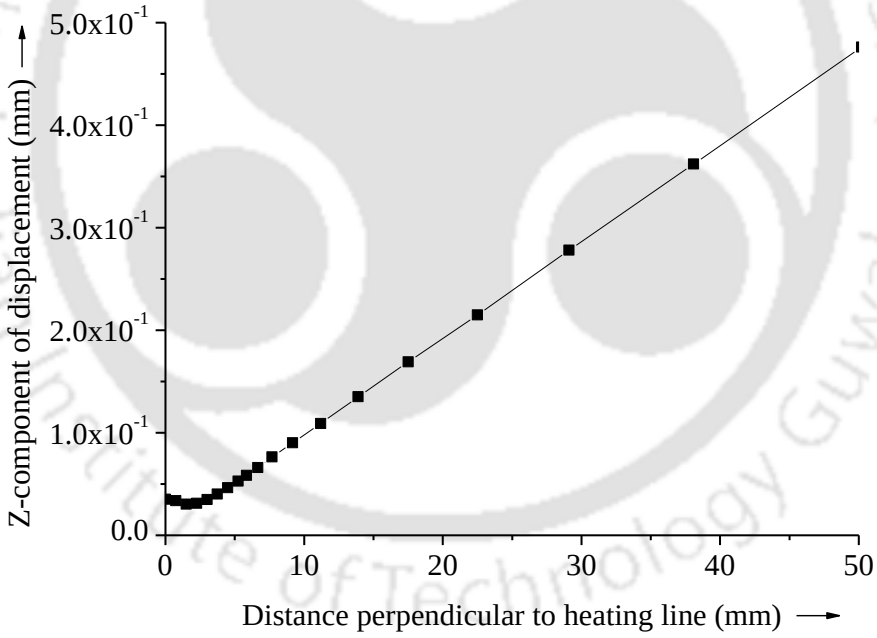

Fig.5.21 Z- component of displacement perpendicular to the heating line

The residual deformation results for different set of operating parameters are presented below.

5.6.2.1 Effect of laser power on residual deformation

The residual deformation over the sheet for different laser power of 300 W, 350 W, 400 W, 450 W, 500 W, 550 W and 600 W under constant traverse speed: 300 mm/min for mild steel sheet having a sheet thickness of 3 mm under single pass line heating are presented in Figs.5.22 & 5.23.

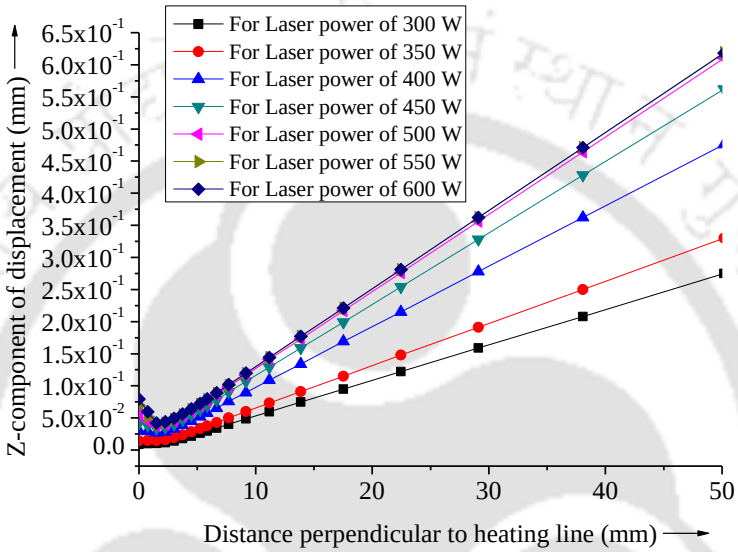

Fig.5.22 Z-component of displacement perpendicular to the heating line

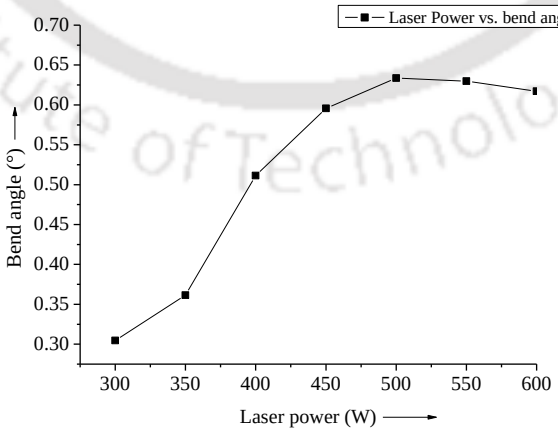

Fig.5.23 Angular deformation of mild steel sheet for different laser power

It can be observed that using constant traverse speed, constant sheet thickness with an increase in laser power the Z-component of displacement and angular deformation increases. It is also seen from Fig.5.23 that with the enhancement of laser power beyond 500 Watt there is no substantial increase in the value of displacement in the Z-direction which results in the decrement of angular deformation. So, to obtain maximum angular deformation maintaining all other parameters constant the magnitude of laser power should be used within the range of 500 W.

5.6.2.2 Effect of traverse speed on residual deformation

The residual deformation over the sheet for different traverse speed under constant laser power: 350 W for a mild steel sheet having a sheet thickness of 3 mm under single pass heating have been presented in Figs.5.24 & 5.25. It is seen that using constant laser power the angular deformation increases with the decrease in traverse speed. A decrease in traverse speed allows greater heat absorption over the sheet. An increase in heat absorption allows the sheet material across the thickness to get more expansion and contraction and allows in getting a higher bend angle.

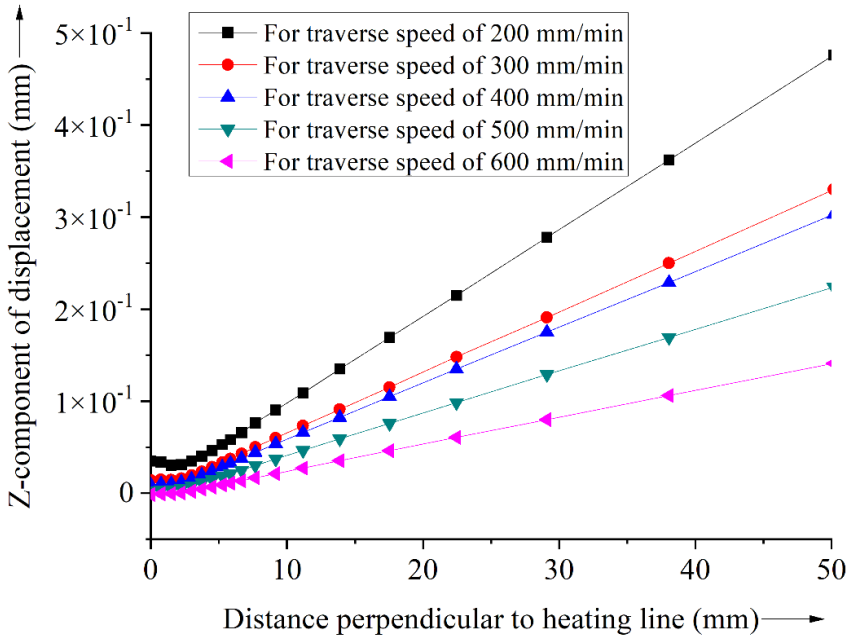

Fig.5.24 Z-component of displacement perpendicular to the heating line

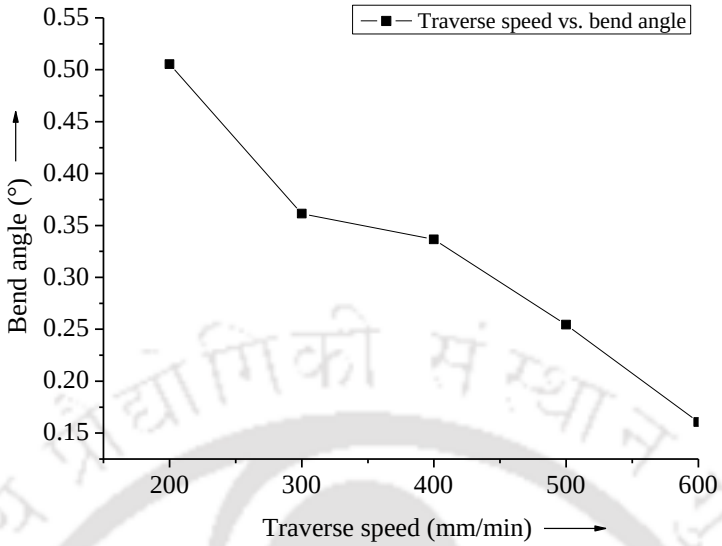

Fig.5.25 Angular deformation of mild steel sheet for different traverse speed

5.6.2.3 Effect of sheet thickness on residual deformation

The residual deformation over the sheet for different sheet thickness of 2 mm, 3 mm and 4 mm under constant laser power: 300 W for a constant traverse speed of 300 mm/min under single pass line heating have been presented in Figs.5.26 & 5.27, respectively.

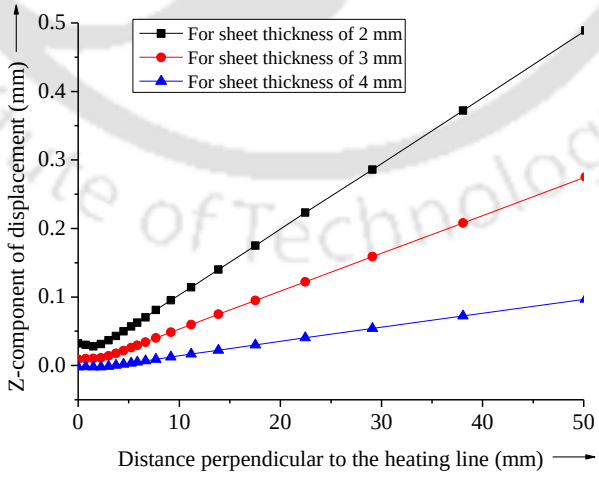

Fig.5.26 Z-component of displacement perpendicular to the heating line

It can be seen that with an increase in sheet thickness under the same operating parameters the residual deformation decreases. The residual deformation is dependent on heat dissipation across the sheet. It has been observed that there is a decrease in peak temperature at the top surface of the work piece with an increase in sheet thickness, while the temperature at the bottom end remains almost the same. With an increase in sheet thickness the heat sink effect increases, this results in the reduction in temperature gradient across the through-thickness direction is responsible for the reduction in residual deformation for higher thickness sheet.

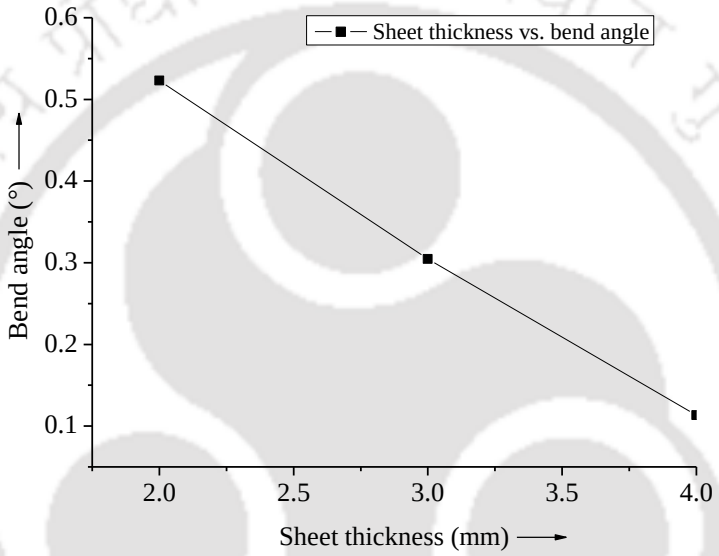

Fig.5.27 Angular deformation of mild steel sheet for different sheet thickness

5.6.2.4 Effect of line energy on residual deformation

The residual deformations over the sheet for constant sheet thickness of 3 mm under different line energy for single pass have been presented in Figs.5.28 & 5.29, respectively.

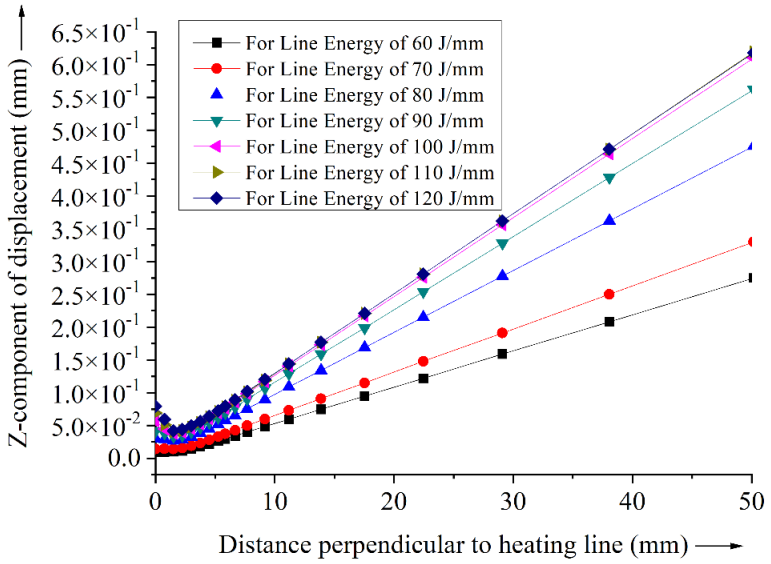

Fig.5.28 Z-component of displacement perpendicular to the heating line

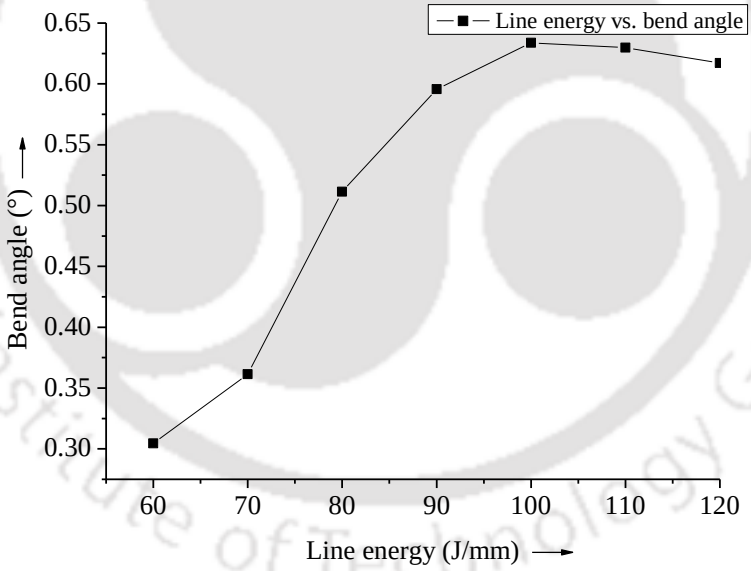

Fig.5.29 Residual deformation of mild steel for different line energy

With the increase in line energy, the heat dissipation rate will increase and will result in an increment of residual deformation. The change in line energy is made by increasing the laser power by maintaining the traverse speed constant or by decreasing the traverse speed and maintaining the laser power constant.

It has been observed from the Fig.5.28 that with the increase in line energy, the residual deformation increases. It is also seen that for a 3 mm sheet thickness, with the increase in line energy beyond 100 J/mm, the slope of the curve decreases as shown in Fig.5.29. The residual deformation is produced due to fast heating of the surface and slow heat conduction into the sheet a steep temperature gradient along the thickness is set and thus result in differential thermal expansion. For creating a large temperature gradient, the laser power and traverse speed are to be selected such that the thermal diffusion depth to be small compared to work piece thickness. So the reduction in slope of bend angle beyond 100 J/mm can also be improved by selecting the proper combination of laser power and traverse speed.

5.6.3 Residual stresses

The temperature field from the combination of various operating parameters induces residual stresses in the sheet material. The stress analysis was carried out for the laser line heating process. The longitudinal, transverse and von- Mises stress distribution in the sheet after the sheet cools down to the climate temperature are presented in this section. The stress response of the sheet subjected to laser line heating for laser power: 500 W, traverse speed: 300 mm/min with 3mm sheet thickness under single pass line heating are presented in Figs.5.30 to 5.33.

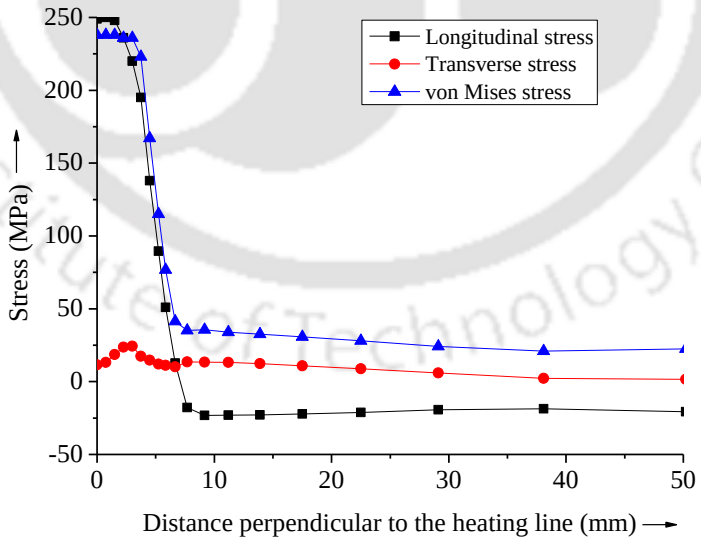

Fig.5.30 Different stresses distribution perpendicular to the heating line

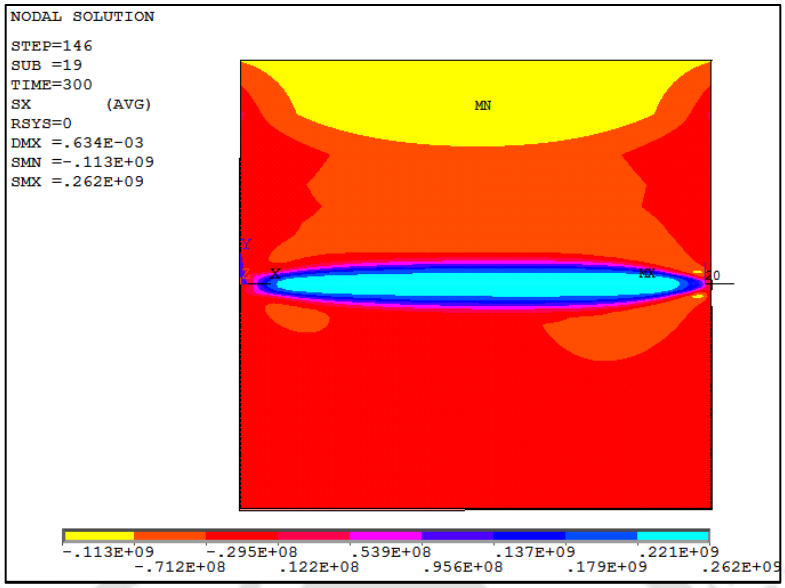

Fig.5.31 3-D contour plot of longitudinal residual stress distribution of the sheet

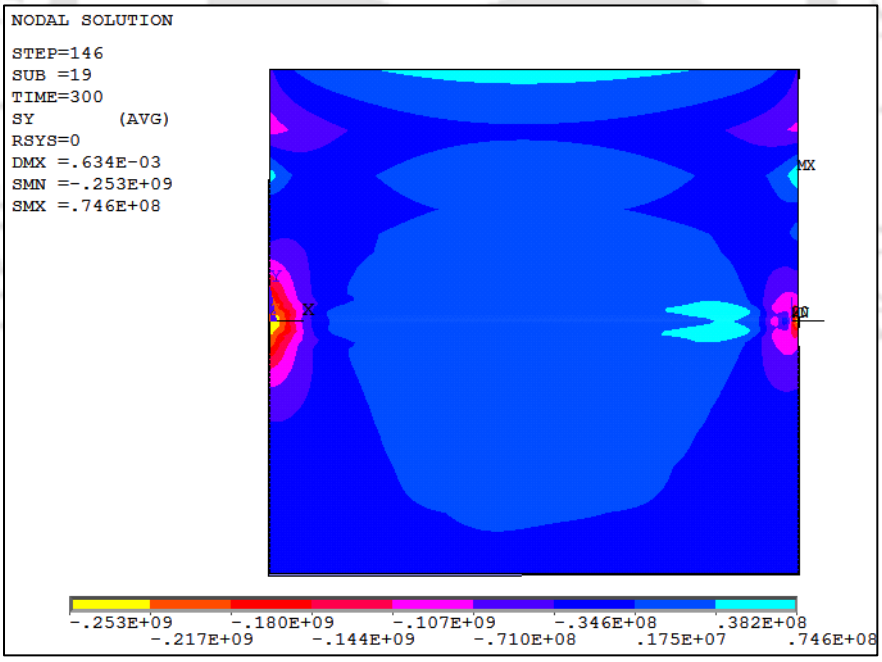

Fig.5.32 3-D contour plot of transverse stress distribution of the sheet

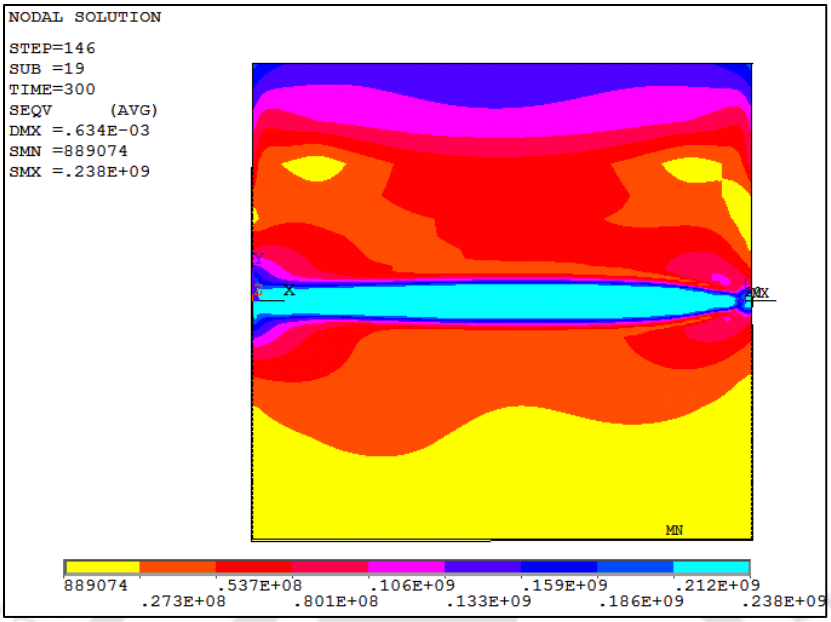

Fig.5.33 3-D contour plot of von Mises stress distribution of the sheet

The value of longitudinal residual stress is much higher than the transverse residual stress. It can be observed from Fig.5.30 that the transverse residual stress acting perpendicular to the laser heating direction is almost negligible. The longitudinal residual stress acting parallel to the laser heating line was subjected to large tensile stress near the heating line and then decreases gradually and become compressive away from the heating line. The longitudinal residual stress is found to be very large in the heating region. The von Mises stress reached the maximum value of about 240.26 MPa near the heating line and then the value decreases.

The effects of individual laser operating parameters on stress distribution were studied with respect to change in laser operating parameters and the results are listed below.

5.6.3.1 Effect of laser operating parameters on longitudinal residual stress

The longitudinal residual stress distribution over the sheet for different laser power of 300 W, 400 W, 500 W and 600 W under constant traverse speed: 300 mm/min for a mild steel sheet having a sheet thickness of 3 mm under single pass have been presented in Fig.5.34. It can be observed from Fig.5.34 that the highest value of longitudinal residual stress is closer to the range of yield stress value within this laser power range. It is seen that the reduction in laser power reduces the longitudinal residual stress distribution width along the perpendicular direction of the heating line.

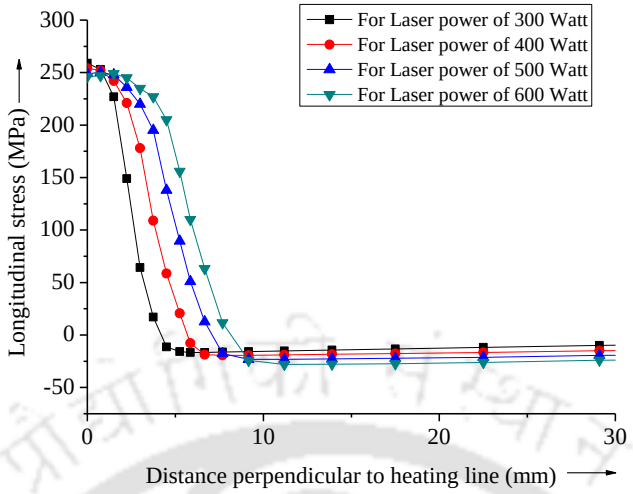

Fig.5.34 Longitudinal stress distribution with variation in laser power

Along and near the heating line the longitudinal residual stresses are tensile in nature and gradually decrease away from the heating line. The longitudinal residual stress away from the heating zone is compressive in nature. The longitudinal stress distribution over the sheet for different traverse speed of 200,300,400,500 and 600 mm/min under constant laser power: 350 W and the sheet thickness of 3 mm under single pass line heating are shown in Fig.5.35.

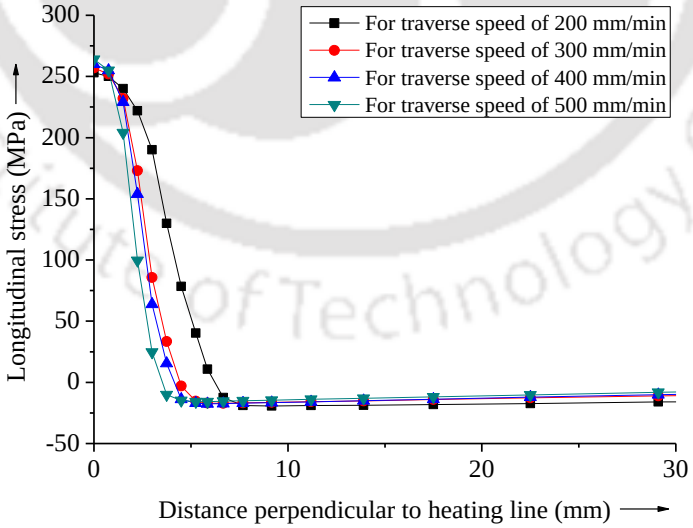

Fig.5.35 Longitudinal stress distribution with variation in traverse speed

It can be observed from the Fig.5.35 that for a constant laser power and variation in traverse speed, there is very small change in the magnitude of longitudinal residual stress in the heating line. However, with increase in distance perpendicular to the heating line the zone of longitudinal residual stress is found to be more with increase in traverse speed. The longitudinal residual stress distribution over the sheet for different sheet thickness of 2 mm, 3 mm and 4 mm under constant laser power: 300 W for a constant traverse speed of 300 mm/min under single pass line heating has been presented in Fig.5.36.

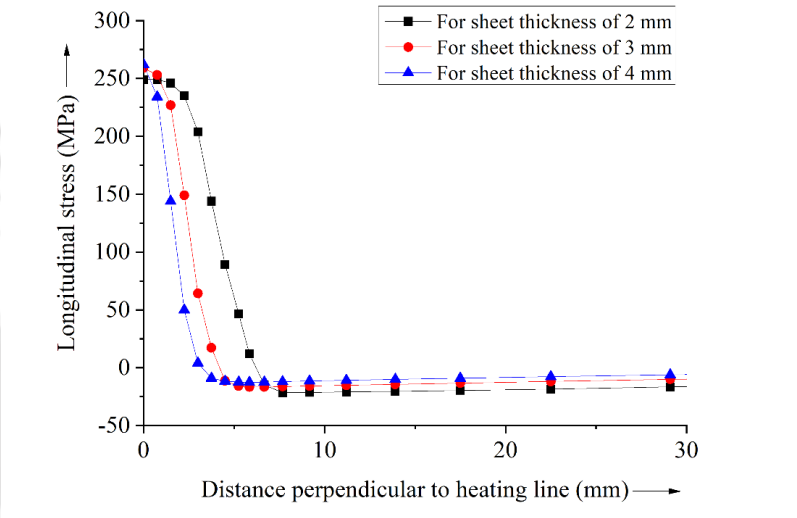

Fig.5.36 Longitudinal stress distribution with variation in sheet thickness

It can be observed from the Fig.5.36 that with the increase in sheet thickness, there is decrease in the value of longitudinal stress in the heating line. The rate of decrease of longitudinal stress value along the distance perpendicular to the heating line was found to be lesser for the sheet having lesser sheet thickness. It can be also observed that the sheet having lesser sheet thickness experiences a large zone of tensile stress near to the region of the heating line. The longitudinal stress distribution over the sheet for constant sheet thickness of 3 mm under different line energy for single pass has been presented in Fig.5.37.

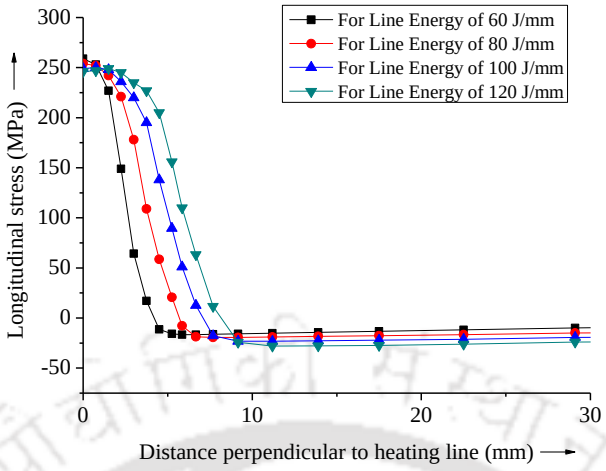

Fig.5.37 Longitudinal stress distribution with variation in line energy

It can be observed from the Fig.5.37 that with the increase in line energy the longitudinal residual stress magnitude decreases along the heating line. It is also observed that with the increase in line energy for constant sheet thickness the zone of tensile longitudinal stress also increases along perpendicular direction of the heating line.

5.6.3.2Effect of laser operating parameters on transverse residual stress

The transverse residual stress distribution over the sheet for different laser power of 300 W, 400 W, 500 W and 600 W under constant traverse speed: 300 mm/min for a mild steel sheet having a sheet thickness of 3 mm under single pass has been presented in Fig.5.38.

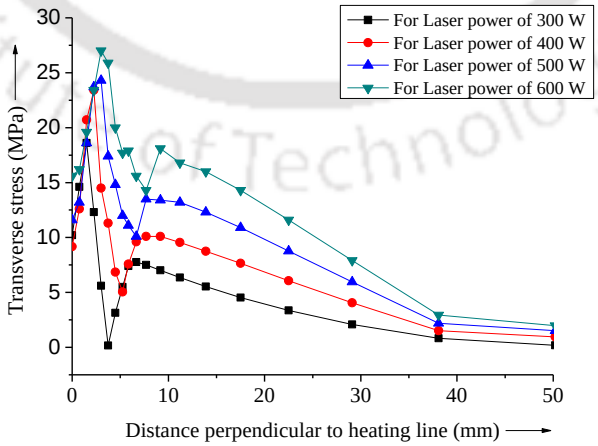

Fig.5.38 Transverse stress distribution with variation in laser power

The transverse residual stresses are taken perpendicular to the heating line direction. It is observed that the longitudinal stresses are of higher magnitude than the transverse residual stresses across the heating line. It can be noticed from Fig.5.38 that the region which gets heated more experiences more transverse residual stress. Due to the conduction of heat, the surface material near to the heating line is stretched by thermal expansion. It can also be seen that the thermal expansion is obstructed by the non-heated region, which results in a decrease in the stress value in that region. With the progressive increase in distance perpendicular to the laser heating path, the sheet surface temperature equalizes with the sheet ambient temperature (non-heated region of the sheet), due to this there develops the tensile stress in the region and after that region, the stress reduces progressively. It is observed that with an increase in laser power at constant traverse speed, the peak surface temperature of the sheet increases which results in an increase in more transverse residual stress. The transverse stress distribution over the sheet for different traverse speeds of 200, 300, 400, 500 and 600 mm/min under constant laser power: 350 W for a mild steel sheet having a sheet thickness of 3 mm under single pass has been presented in Fig.5.39.

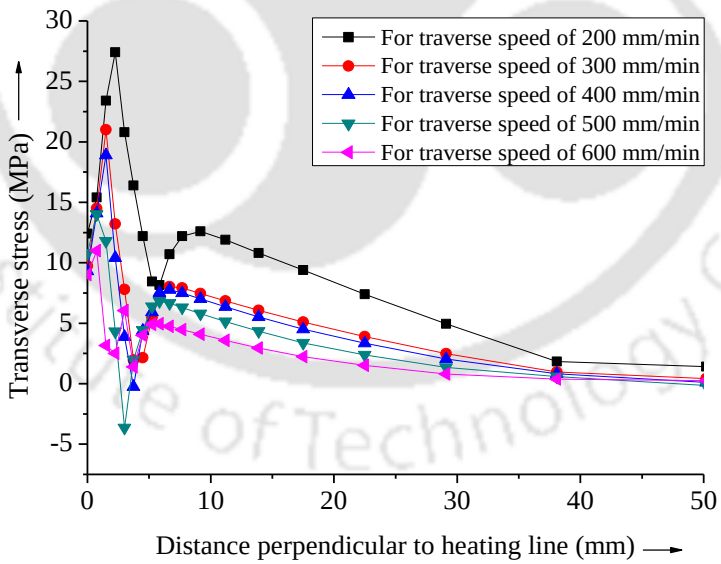

Fig.5.39 Transverse stress distribution with variation in traverse speed

It can be observed from Fig.5.39 that under constant laser power, with an increase in traverse speed the transverse residual stress decreases along the perpendicular direction of the heating

line. It is seen that with a decrease in traverse speed under constant laser power, the heat energy absorbed on the sheet surface is more. It results in an increase in surface temperature. Increase in surface temperature yields more tensile stress along and near the heating line. Thus, from Fig.5.39, it is observed that for lesser traverse speed under constant laser power the magnitude of transverse residual stress is more and it decreases with an increase in traverse speed.

The transverse residual stress distribution over the sheet for different sheet thickness of 2 mm, 3 mm and 4 mm under constant laser power: 300 W for a constant traverse speed of 300 mm/min under single pass has been presented in Fig.5.40.

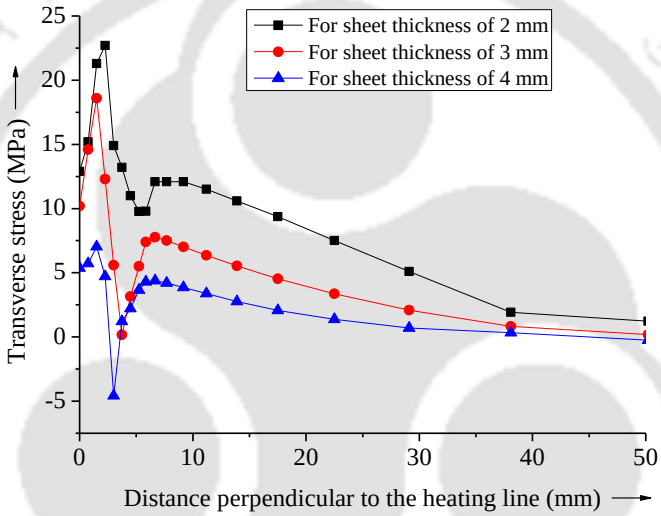

Fig.5.40 Transverse stress distribution with variation in sheet thickness

It can be observed from Fig.5.40 that under constant laser power and constant traverse speed, with the increase in sheet thickness the transverse residual stress value reduces along the heating line. An increase in sheet thickness reduces sheet surface temperature due to the effect of the heat sink. The stress value increases with an increase in thermal expansion of the material near the heating line and then decreases progressively with the surface temperature of the sheet. The transverse stress distribution over the sheet for constant sheet thickness of 3 mm under different line energy for single pass has been presented in Fig.5.41.

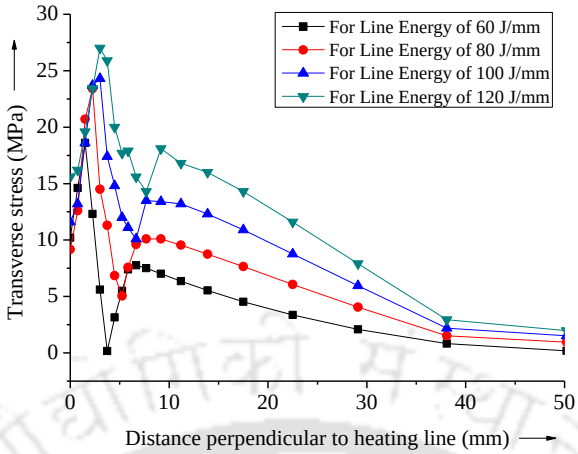

Fig.5.41 Transverse stress distribution with variation in line energy

It can be seen from the Fig.5.41 that the region experiencing more line energy experiences more transverse residual stress. The transverse residual stress pattern on the surface near to the heating line is dependent on the heat conduction into the surface. It is observed that with an increase in line energy the zone of transverse residual stress increases. The magnitude of transverse residual stress is tensile in nature and gradually increases away from the heating line. With the progressive increase in distance perpendicular to the heating path, the surface temperature of the sheet reduces and it reduces progressively till it reaches the ambient temperature of the sheet.

5.6.3.3Effect of laser operating parameters on von Mises residual stress

The von Mises residual stress distribution over the sheet for different laser power of 300 W, 400 W, 500 W and 600 W under constant traverse speed: 300 mm/min, having a sheet thickness of 3 mm under single pass has been presented in Fig.5.42.

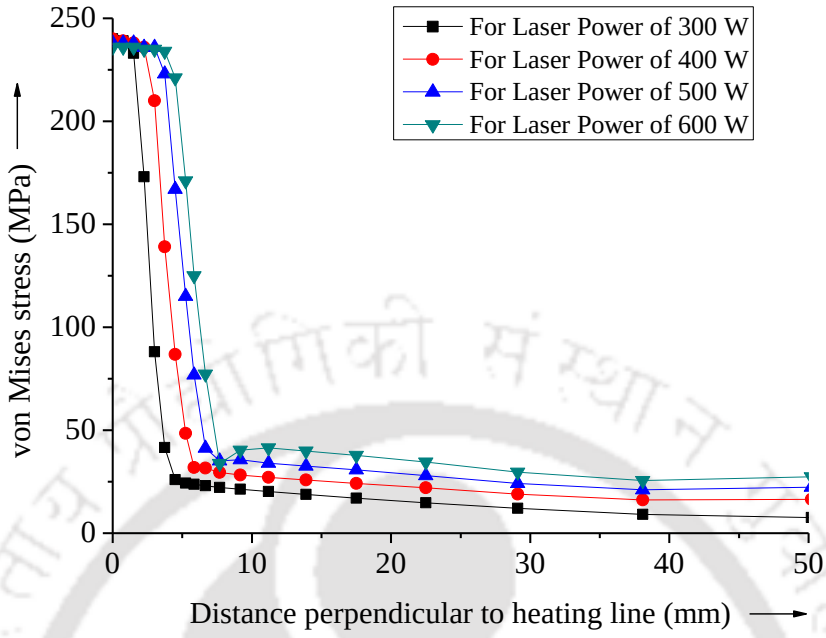

Fig.5.42 von Mises stress distribution with variation in laser power

It can be seen from Fig.5.42 that with an increase in laser power under constant traverse speed the maximum magnitude of von Mises stress on the surface of the sheet remains almost the same along the heating line. The von Mises stress is found to be tensile in nature. There is a decrement in the value of von Mises residual stress along the perpendicular direction from the heating line. The rate of decrement of stress is found to be more for the lower range of laser power and progressively it increases for higher laser power. After sudden decrement in stress value till a certain distance, the rate of decrease of stress becomes slow and gets nullified with the increase in distance. The width of the von Mises residual stress distribution along the perpendicular direction of the heating line increases as the laser power increases.

The von Mises stress distribution for different traverse speed of 200,300,400,500 and 600 mm/min under constant laser power: 350 W for a mild steel sheet having a sheet thickness of 3 mm under single pass line heating has been presented in Fig.5.43.

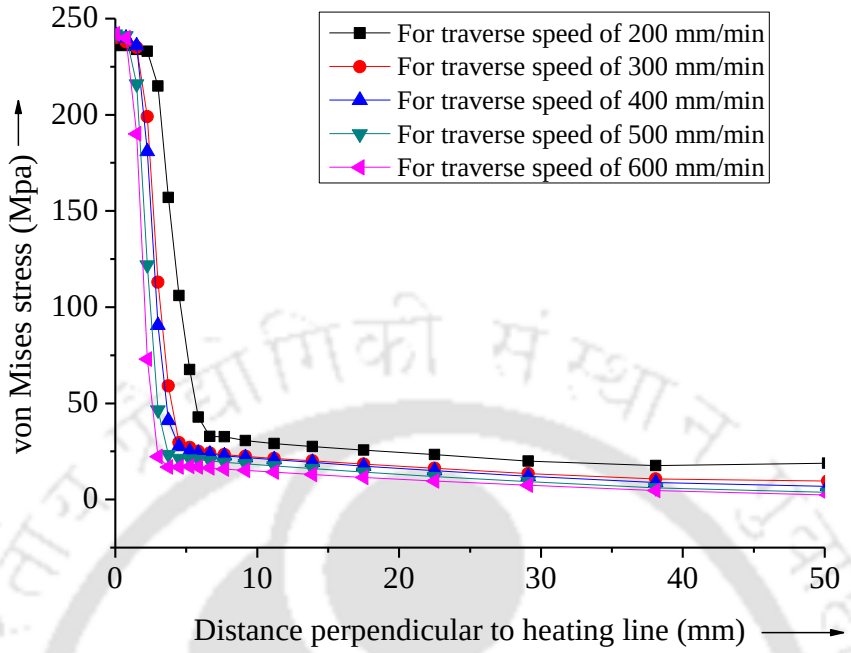

Fig.5.43 von Mises stress distribution with variation in traverse speed

It is observed from Fig.5.43 that for a constant laser power and variation in traverse speed, there is no significant change in the magnitude of maximum von Mises residual stress along and near the heating line. This stress is tensile and it gradually decreases away from the heating line. With an increase in distance perpendicular to the heating line, the zone of von Mises residual stress is found to be more with a decrease in traverse speed. The rate of decrement is found to be more for higher traverse speed to a certain distance. Progressively the rate of decrease becomes slow and it gets nullified with an increase in distance.

The von Mises residual stress distribution over the sheet for different sheet thickness of 2 mm, 3 mm and 4 mm under constant laser power: 300 W for a constant traverse speed of 300 mm/min under single pass has been presented in Fig.5.44. With higher sheet thickness under constant laser power and constant traverse speed, the von Mises stress value remains almost the same along the heating line and is of tensile in nature.

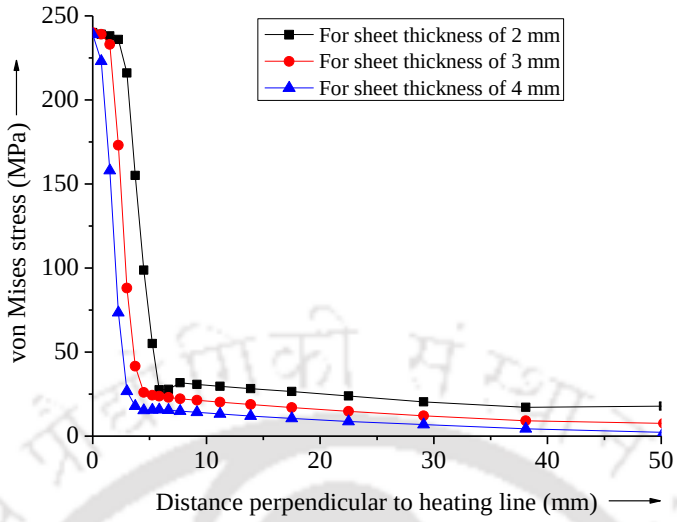

Fig.5.44 von Mises stress distribution with variation in sheet thickness

However, with a decrease in sheet thickness, the zone of von Mises residual stress is found to be more with an increase in distance perpendicular to the heating line. With the increase in sheet thickness, the von Mises residual stress decreases progressively and gets nullified with an increase in distance. The von Mises stress distribution over the sheet for constant sheet thickness of 3 mm under different line energy for single pass has been presented in Fig.5.45.

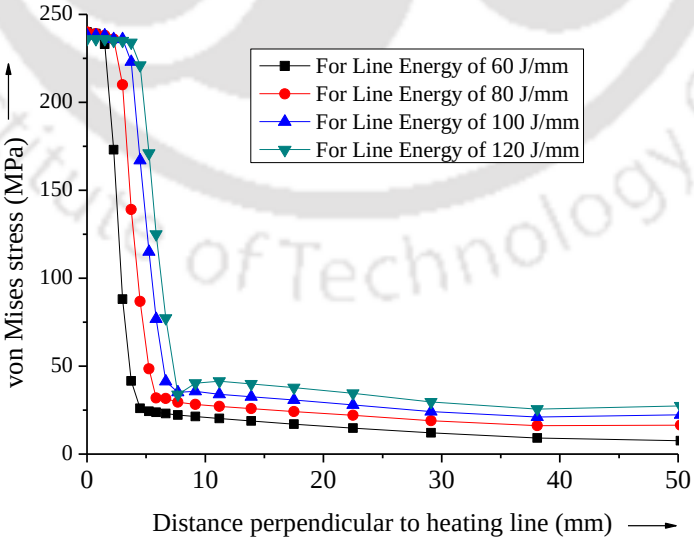

Fig.5.45 von Mises stress distribution with variation in line energy

It is seen from Fig.5.45 that with an increase in line energy the zone of von Mises residual stress increases. With a decrease in line energy, the von Mises residual stress decreases. The rate of decrement is more for heating lines experiencing lower line energy. Progressively the rate of decrement becomes slow after a certain distance and gets nullified with an increase in distance.

5.6.4 Strain distribution due to laser line heating

For obtaining the effect of operating parameters on residual plastic strains the strain analysis was carried out for the process. The plastic strain distribution on the sheet subjected to laser line heating for laser power: 300 W, traverse speed: 300 mm/min with 3mm sheet thickness under single pass are presented in Figs.5.46 - 5.49.

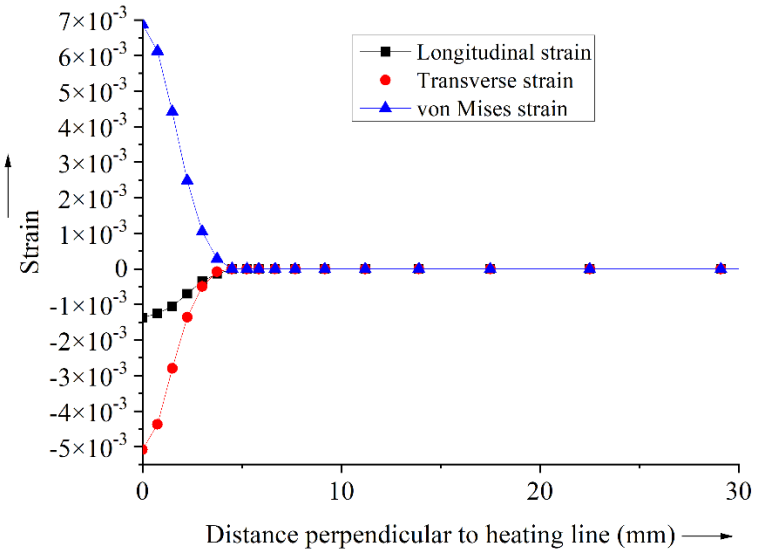

Fig.5.46 Strain result for single pass line heated sheet

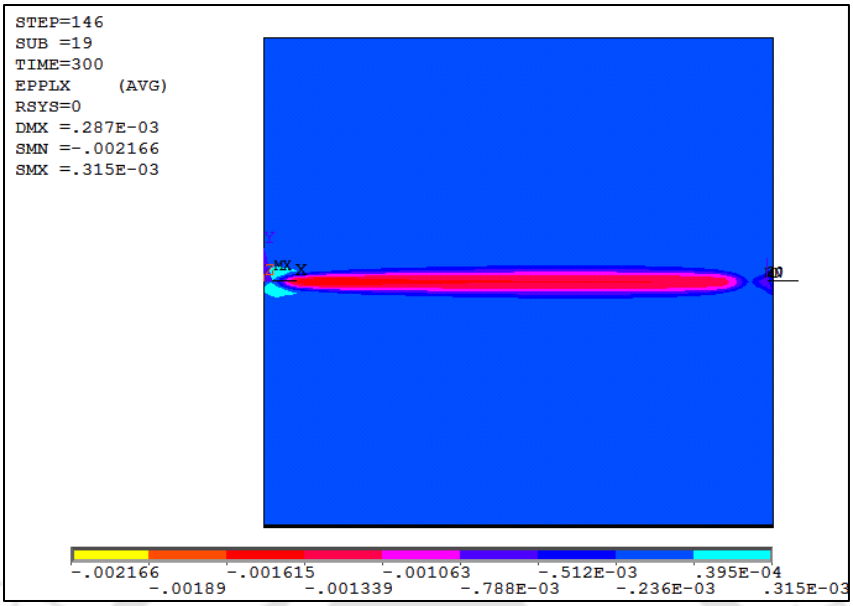

Fig.5.47 3-D contour plot of longitudinal strain distribution on the sheet

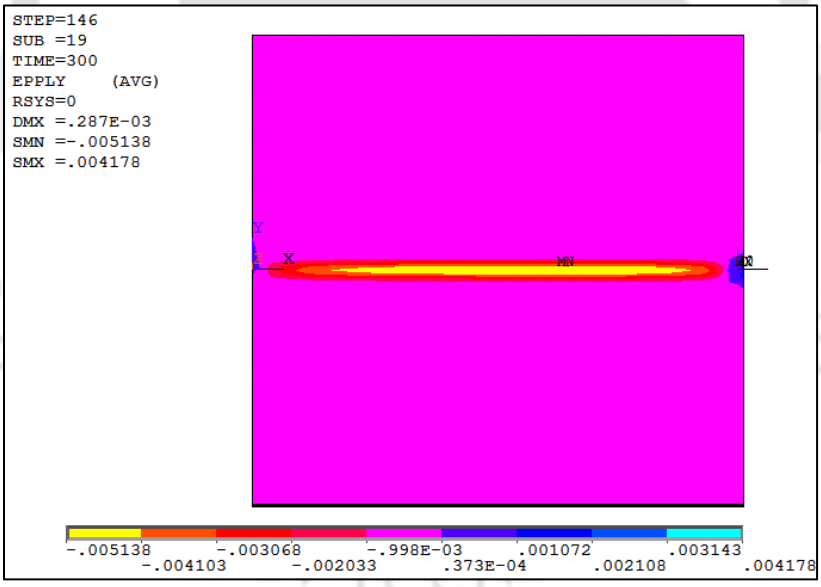

Fig.5.48 3-D contour plot of transverse strain distribution on the sheet

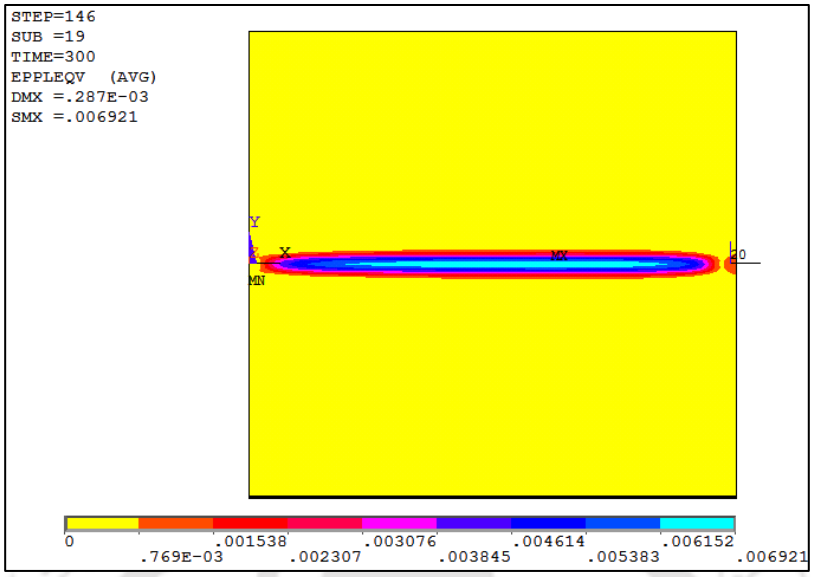

Fig.5.49 3-D contour plot of von Mises strain distribution on the sheet

It can be observed from Fig.5.47 that both the longitudinal and transverse strain follows a similar pattern. It starts with initial compressive plastic strains on the heating line and the compressive plastic strain value reduces with the increase in distance in the perpendicular direction of the heating line. The magnitude of longitudinal residual plastic strain is less compared to transverse residual plastic strain. The von Mises strain is found to be tensile on the heating region and its value reduces with the increase in distance along the perpendicular direction of the heating line.

The effects of individual laser operating parameters on plastic strains distribution were studied and the results are listed below.

5.6.4.1 Effect of operating parameters on strains distribution

The longitudinal strain distribution over the sheet for different laser power of 300 W, 400 W, 500 W and 600 W under constant traverse speed: 300 mm/min having a sheet thickness of 3 mm under single pass has been presented in Fig.5.50.

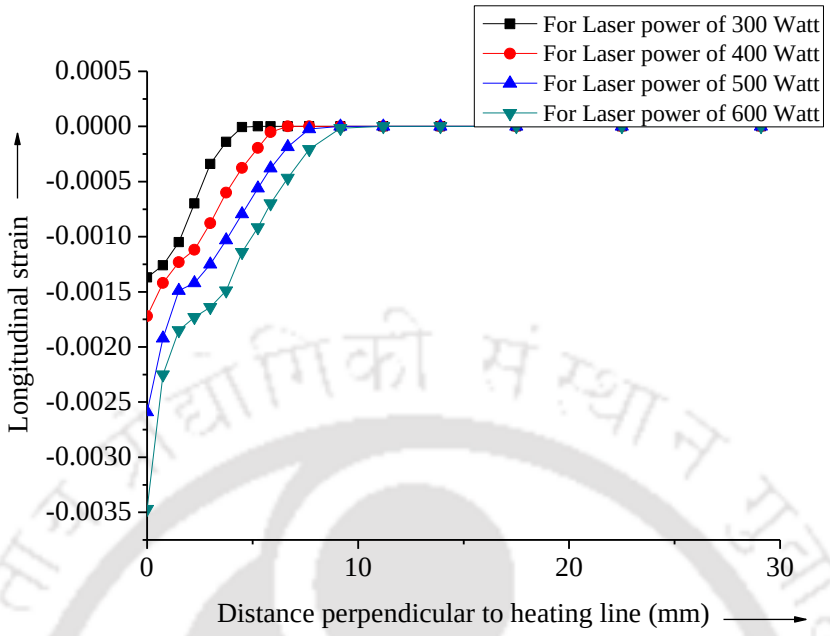

Fig.5.50 Longitudinal residual strain distribution with variation of laser power

It can be observed from the Fig.5.50 that with an increase in laser power increases the longitudinal residual strain along the heating line. The longitudinal strain value reduces along the perpendicular direction of the heating line. The longitudinal residual strain is compressive in nature and gradually decreases away from the heating line. It can be seen that a reduction in laser power reduces the longitudinal residual strain distribution width along the perpendicular direction of the heating line. The longitudinal strain distribution over the sheet for different traverse speed of 200,300,400,500 and 600 mm/min under constant laser power: 350 W for a mild steel sheet having a sheet thickness of 3 mm under single pass has been presented in Fig.5.51.

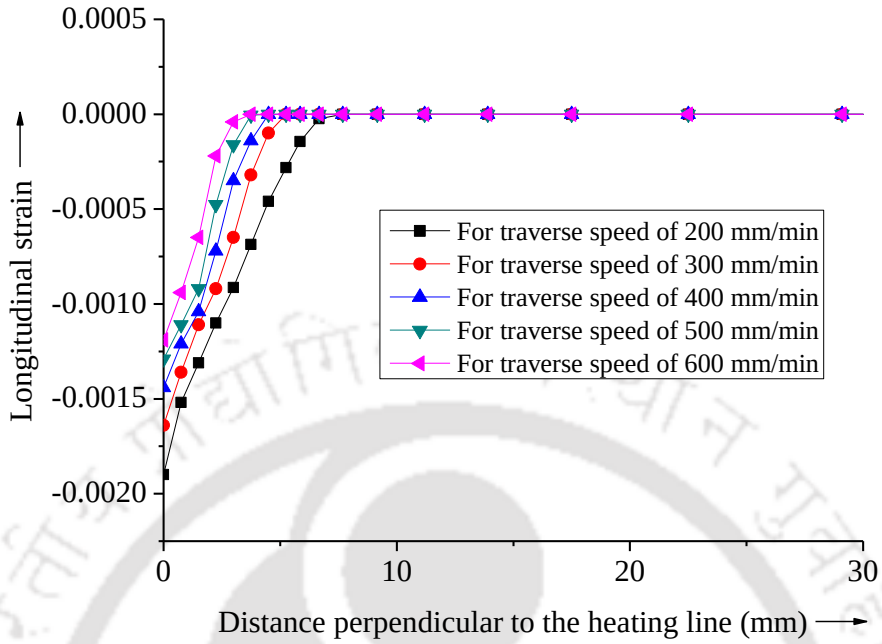

Fig.5.51 Longitudinal residual strain distribution with variation of traverse speed

It can be observed from the Fig.5.51 that under different traverse speed, with constant laser power the longitudinal residual strain decreases along the perpendicular direction of the heating line with increase in traverse speed. It is seen that with an increase in traverse speed under constant laser power, the heat energy absorbed on the surface of the sheet is less. With a decrease in temperature, the magnitude of compressive longitudinal strain is less on the heating line and the value decreases with the increase in distance perpendicular to the heating line. With an increase in distance perpendicular to the heating line, the zone of compressive residual strain is found to be more with a decrease in traverse speed. The longitudinal strain distribution over the sheet for different sheet thickness of 2 mm, 3 mm and 4 mm under constant laser power: 300 W for a constant traverse speed of 300 mm/min under single pass has been presented in Fig.5.52.

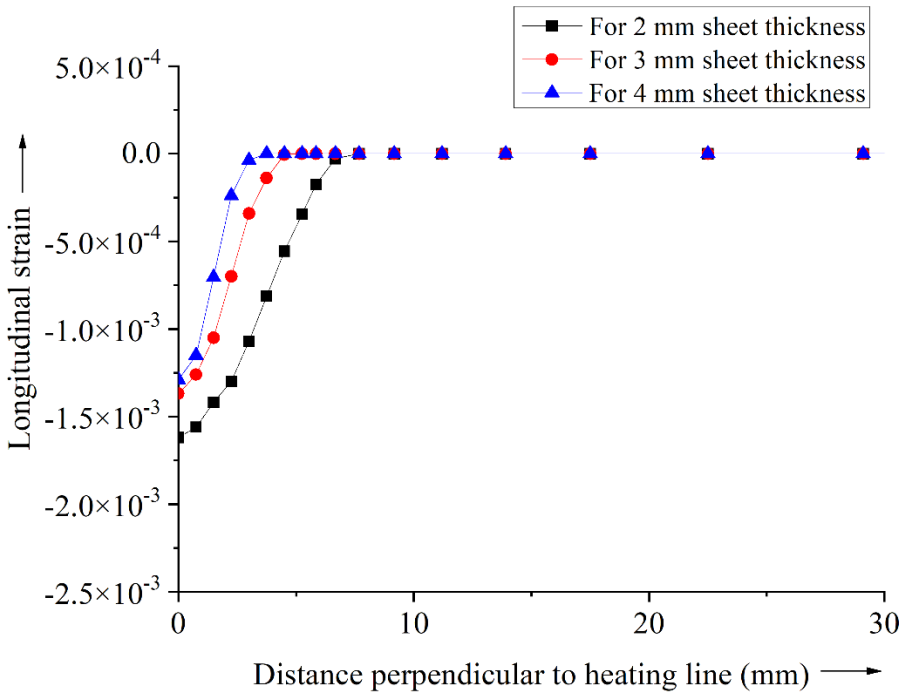

Fig.5.52 Longitudinal residual strain distribution with variation in sheet thickness

It can be seen from Fig.5.52 that under constant traverse speed, constant laser power and variation in sheet thickness the longitudinal residual strain increases along the heating line in compressive direction. It is also seen that the value of longitudinal strain decreases along the perpendicular direction of the heating line. The rate decrement of the strain is more for material having higher sheet thickness. It is also observed that sheet having lesser sheet thickness experiences a large zone of compressive strain near to the region of heating line.

The longitudinal strain distribution over the sheet for constant sheet thickness of 3 mm under different line energy for single pass has been presented in Fig.5.53. It can be seen that for the same sheet thickness the longitudinal strain increases with an increase in line energy. It is seen that with higher line energy the zone of compressive longitudinal residual strain increases. The magnitude of longitudinal residual strain decreases away from the heating line.

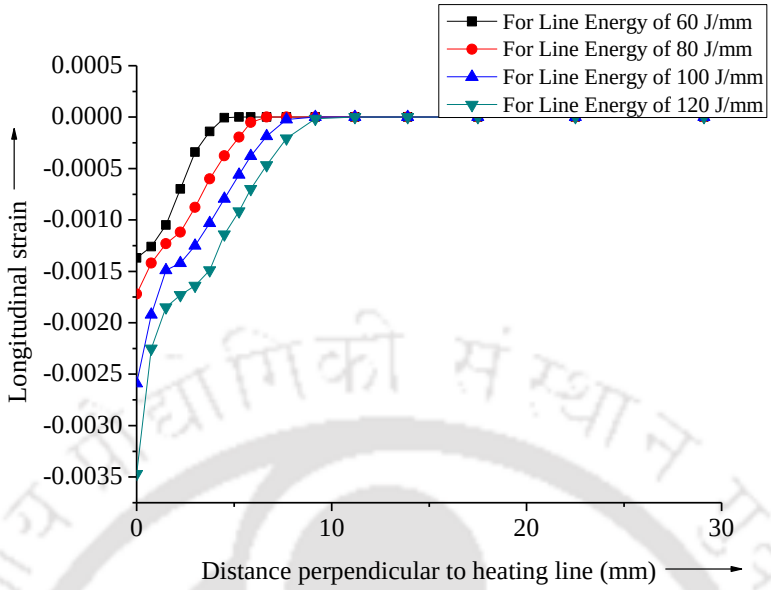

Fig.5.53 Longitudinal residual strain distribution with variation in line energy

The transverse strain distribution over the sheet for different laser power of 300 W, 400 W, 500 W, and 600 W under constant traverse speed: 300 mm/min for a mild steel sheet having a sheet thickness of 3 mm under single pass has been presented in Fig.5.54.

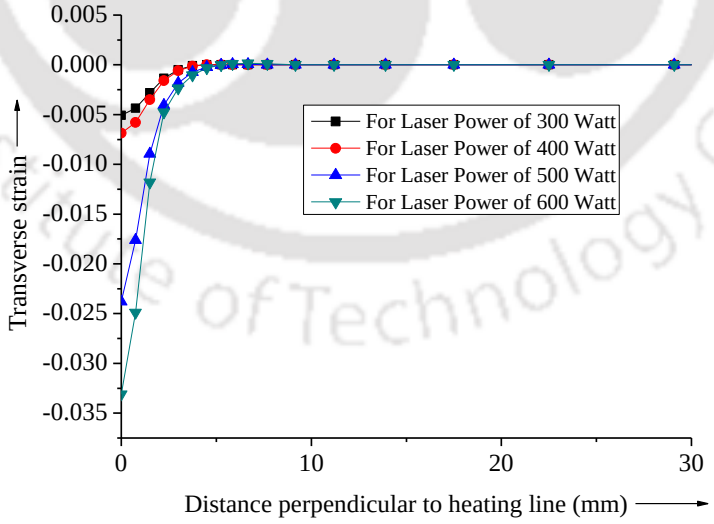

Fig.5.54 Transverse residual strain distribution with variation in laser power

It can be observed from Fig. 5.54 that with an increase in laser power there is an increase in transverse residual strain along the heating line. The strain is compressive in nature. It is observed that with an increase in the distance along the perpendicular to the heating line direction the zone of transverse residual strain is found to be more with an increase in laser power. It is also observed that with increase in distance perpendicular to heating line the strain value get decreases and get nullified.

The transverse strain distribution over the sheet for different traverse speed of 200,300,400,500 and 600 mm/min under constant laser power: 350 W for a mild steel sheet having a sheet thickness of 3 mm under single pass has been presented in Fig.5.55.

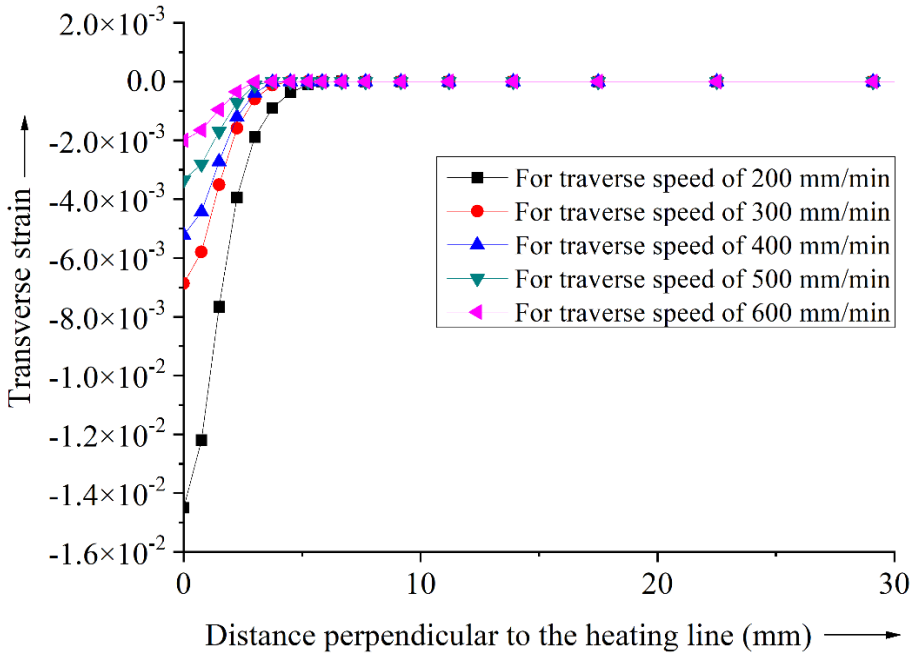

Fig.5.55 Transverse residual strain distribution with variation in traverse speed

It can be seen from Fig.5.55 that with an increase in traverse speed there is a reduction in transverse residual strain along the heating line direction. The strain is compressive in nature. With a decrease in traverse speed under constant laser power increases the sheet surface temperature. With the rise in temperature the magnitude of compressive transverse strain increases. It is observed that the reduction in traverse speed increases the transverse strain distribution width along the perpendicular direction of the heating line. With an increase in

distance perpendicular to the heating line, the strain value gets decreases and gets nullified. The transverse strain distribution over the sheet for different sheet thickness of 2 mm, 3 mm and 4 mm under constant laser power: 300 W for a constant traverse speed of 300 mm/min under single pass has been presented in Fig.5.56.

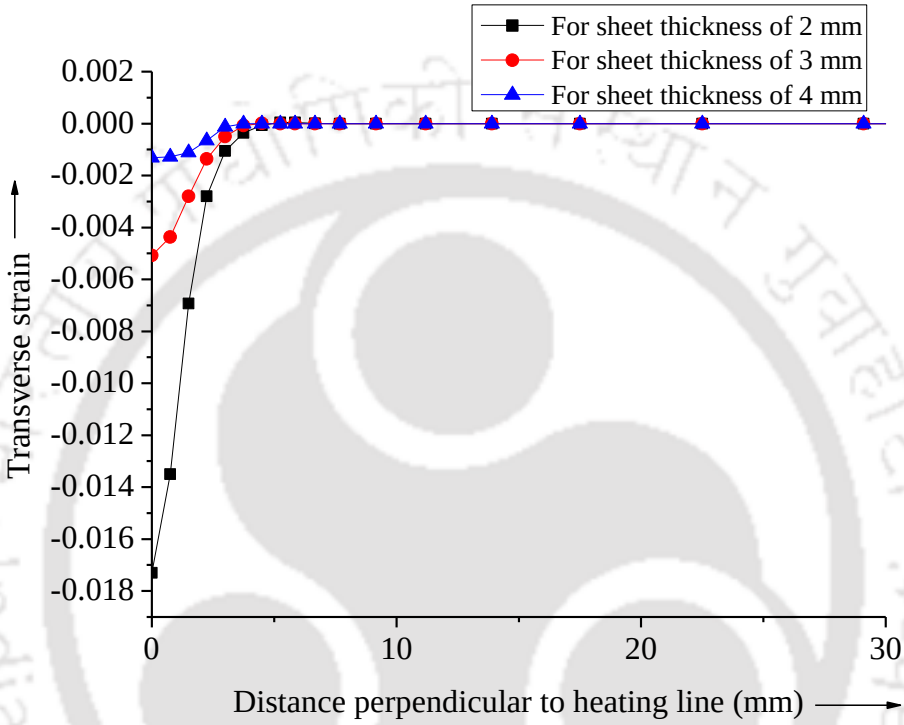

Fig.5.56 Transverse residual strain distribution with variation in sheet thickness

It can be seen from Fig.5.56 that with an increase in sheet thickness, the transverse residual strain decreases. It is observed that under constant laser power and traverse speed, with an increase in sheet thickness the surface peak temperature of the sheet decreases. The magnitude of transverse residual strain is dependent on the temperature of the sheet surface. It is seen that the zone of transverse residual strain decreases along the perpendicular direction of the heating line, with an increase in sheet thickness. With an increase in distance perpendicular to the heating line, the strain value gets decreases and gets nullified. The transverse strain distribution over the sheet for constant sheet thickness of 3 mm under different line energy for single-pass has been presented in Fig.5.57.

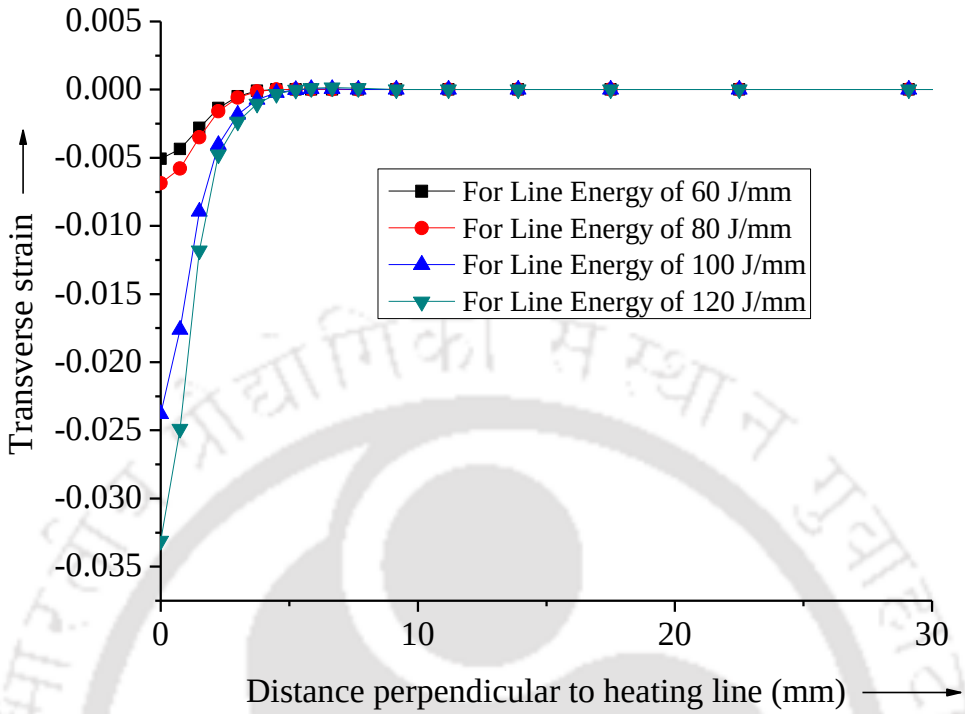

Fig.5.57 Transverse residual strain distribution with variation in line energy

It can be seen from Fig.5.57 that with an increase in line energy the magnitude of compressive transverse residual strain increases along the heating line. With the increase in line energy, the surface temperature of the sheet increases. An increase in temperature results in an increase in transverse strain along the heating line in the compressive direction. It is seen that with an increase in line energy the zone of transverse residual strain increases along the perpendicular direction of the heating line. It is observed that with an increase in distance perpendicular to the heating line the strain value gets decreases and gets nullified. The von Mises strain distribution over the sheet for different laser power of 300 W, 400 W, 500 W, and 600 W under constant traverse speed: 300 mm/min having a sheet thickness of 3 mm under single pass has been presented in Fig.5.58.It can be observed that the von Mises strain increases with the increase in laser power. With an increase in laser power under constant traverse speed the surface peak temperatures of the sheet material increase.

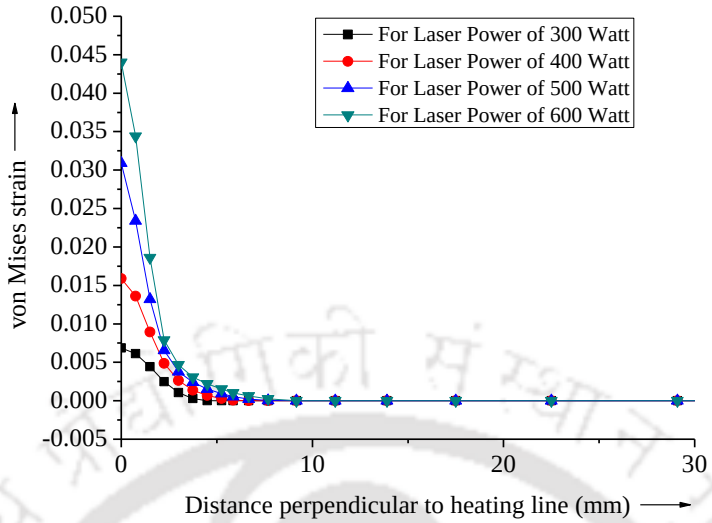

Fig.5.58 von Mises residual strain distribution with variation in laser power

The strain obtained is tensile in nature. With a decrease in temperature perpendicular to the heating line, the strain value reduces and gets nullified. For higher laser power the von Mises residual strain distribution width increases along the perpendicular direction of the heating line. The von Mises strain distribution over the sheet for different traverse speed of 200, 300, 400, 500 and 600 mm/min under constant laser power: 350 W having a sheet thickness of 3 mm under single pass has been presented in Fig.5.59.

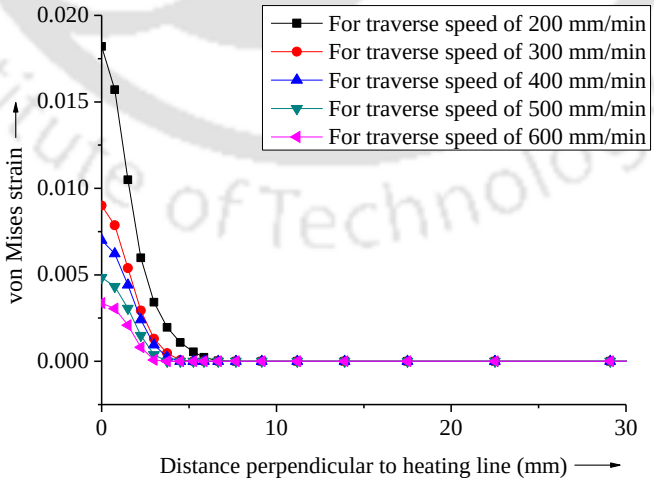

Fig.5.59 von Mises residual strain distribution with variation in traverse speed

It can be observed from Fig.5.59 that with an increase in traverse speed under constant laser power the magnitudes of von Mises strain decrease. With higher traverse speed the sheet surface temperature reduces. As the von Mises strain is temperature-dependent, its value get reduces and gets nullified when the sheet surface temperature reaches the ambient temperature. For lesser traverse speed the von Mises residual strain distribution width increases along the perpendicular direction of the heating line. The von Mises strain distribution over the sheet for different sheet thickness of 2 mm, 3 mm and 4 mm under constant laser power: 300 W for a constant traverse speed of 300 mm/min under single pass has been presented in Fig.5.60.

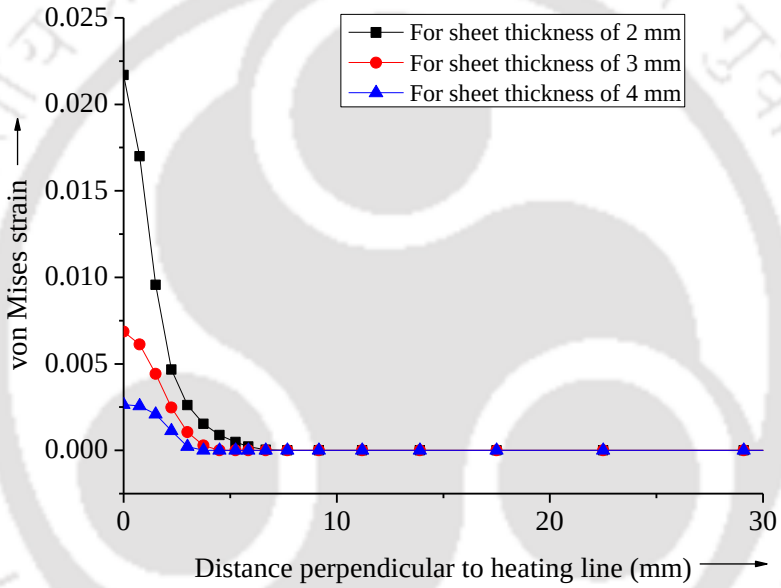

Fig.5.60 von Mises residual strain distribution with variation in sheet thickness

It can be seen from Fig.5.60 that the magnitude of von Mises residual strain decreases with an increase in sheet thickness. It can also be observed from the Fig.5.60 that the von Mises strain experienced by higher sheet thickness experiences a very low magnitude of the strain compared to that of sheet having lesser thickness value. As the von Mises strain is temperature-dependent, so the peak temperature of the sheet having lesser thickness is more compared to the sheet having higher thickness value. This increases the von Mises strain value of the sheet having lesser thickness. The von Mises strain is found to be tensile in nature and it reduces progressively with the reduction in temperature in the direction perpendicular to the heating line. With an

increase in distance perpendicular to the heating line, the zone of von Mises residual strain is found to be more with a reduction in sheet thickness along the direction perpendicular to the heating line. The von Mises strain distribution over the sheet for constant sheet thickness of 3 mm under different line energy for single-pass has been presented in Fig.5.61.

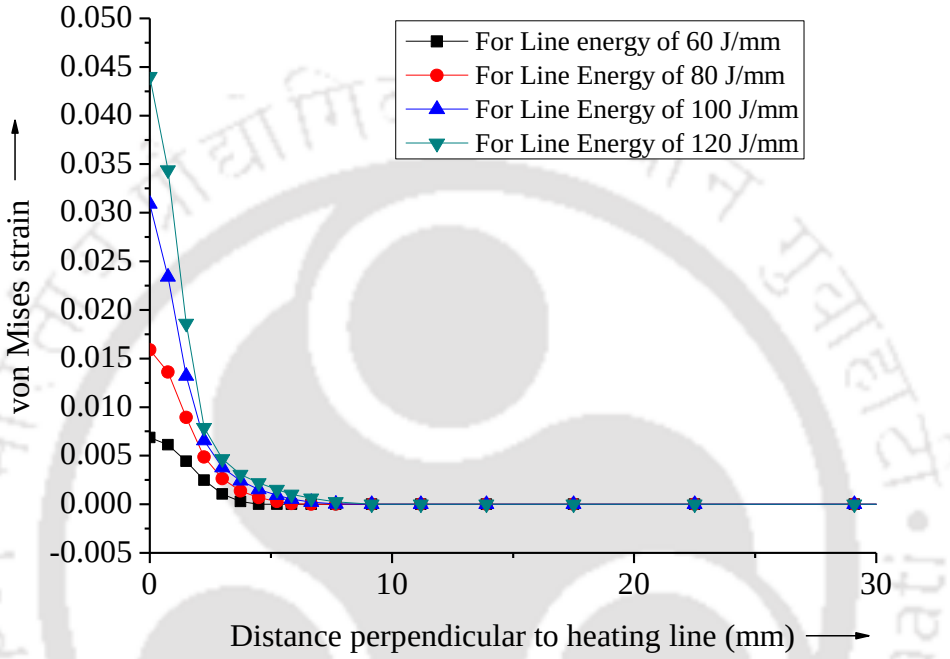

Fig.5.61 von Mises strain distribution with variation in line energy

It can be observed from the Fig.5.61 that with increase in line energy, the von Mises strain value increases. The von Mises strain is tensile in nature. With the increase in line energy, the sheet surface temperature increases. An increase in temperature results in an increase in von Mises strain along the heating line in the tensile direction. It is observed that with an increase in distance perpendicular to the heating line the strain value gets decreases and gets nullified. It is seen that with an increase in line energy the zone of von Mises residual strain increases along the perpendicular direction of the heating line. The maximum principal strain distribution over the sheet for different laser power of 300 W, 400 W, 500 W, and 600 W under constant traverse speed: 300 mm/min having a sheet thickness of 3 mm under a single pass has been presented in Fig.5.62.

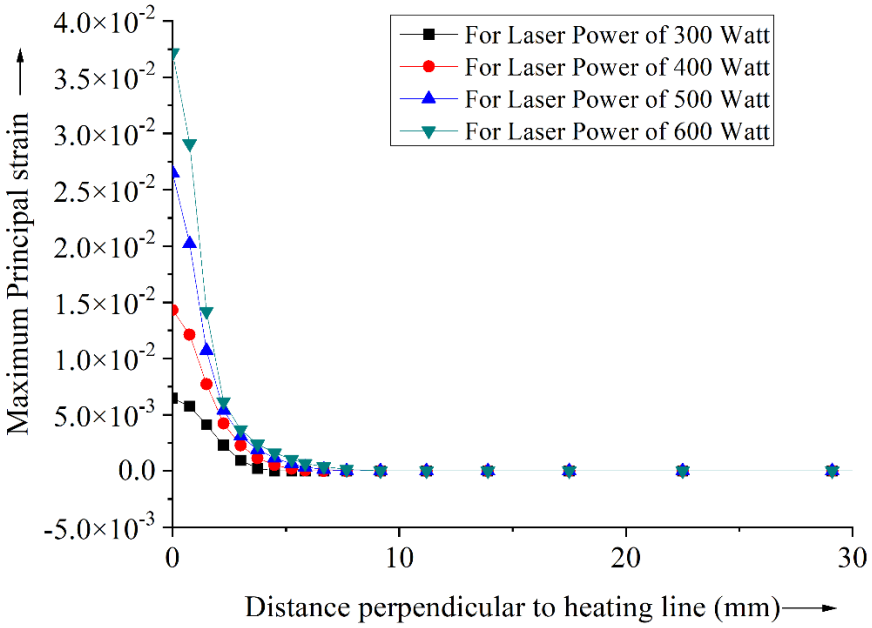

Fig.5.62 Maximum principal strain distribution with variation in laser power

It can be observed from Fig.5.62 that with the increase in laser power under constant traverse speed, the maximum principal strain value increases. The maximum principal strain is tensile in nature. With increase in laser power the surface peak temperature increases. An increase in temperature results in an increase of maximum principal strain on the heating surface of the sheet. It is also observed that with an increase in distance perpendicular to the heating line, there is a decrement in the value of maximum principal strain. It can be observed that reduction in laser power reduces the magnitude of maximum principal residual strain distribution width along the perpendicular direction of the heating line. The maximum principal strain distribution over the sheet for different traverse speed of 200, 300, 400, 500 and 600 mm/min under constant laser power: 350 W having a sheet thickness of 3 mm under single pass has been presented in Fig.5.63.

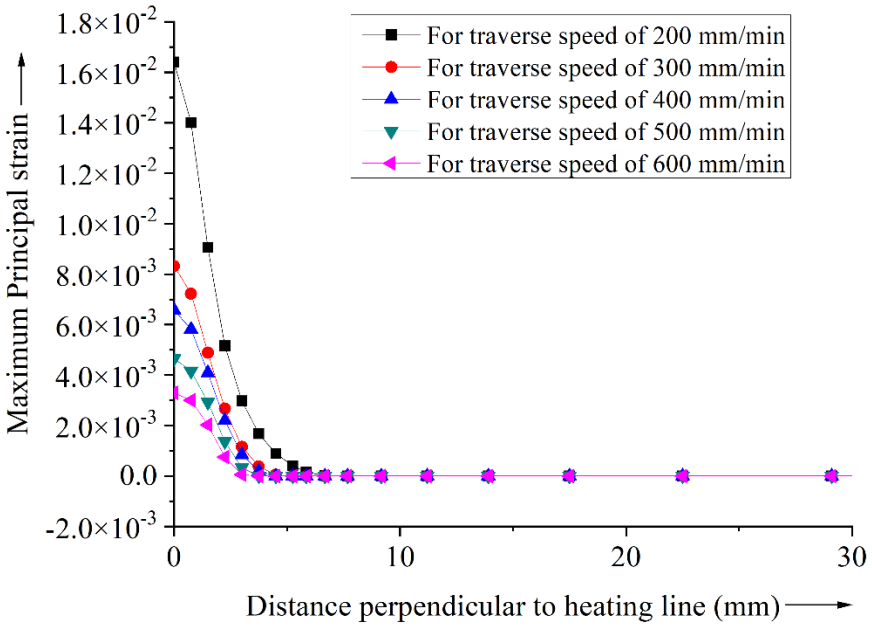

Fig.5.63 Maximum principal strain distribution with variation in traverse speed

It can be seen from the Fig.5.63 that with the increase in traverse speeds under constant laser power, the magnitude of maximum principal strain decreases. An increase in traverse speed reduces heat absorption time on the sheet surface. The decrease in the value of the maximum principal strain is due to less heat input on the sheet surface, resulting in fewer rises in surface temperature. The magnitude of maximum principal strain reduces with progressive reduction of sheet surface temperature along the perpendicular direction of the heating line. It is seen that with an increase in distance perpendicular to heating line the zone of maximum principal strain distribution is found to be more with a decrease in traverse speed. The maximum principal strain distribution over the sheet for different sheet thickness of 2 mm, 3 mm and 4 mm under constant laser power: 300 W for a constant traverse speed of 300 mm/min under single pass has been presented in Fig.5.64.

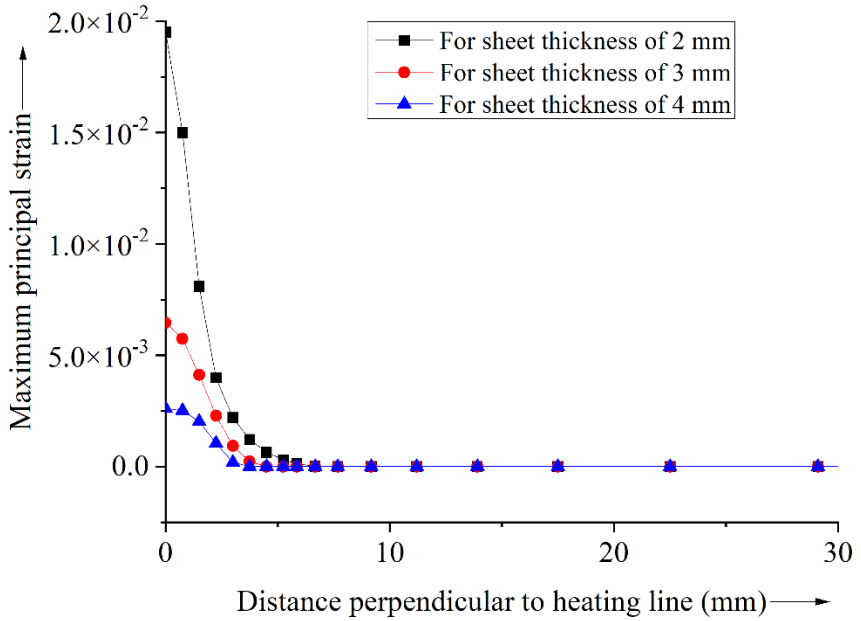

Fig.5.64 Maximum principal strain distribution with variation in sheet thickness

It can be observed from the Fig.5.64 that with the increase in sheet thickness under constant laser power and traverse speed, the magnitude of maximum principal strain decreases. The decrement is due to the lesser rise in the surface temperature of the sheet material. With the increase in sheet thickness the surface temperature decreases due to the heat sink effect. The magnitude of maximum principal strain reduces with progressive reduction in the surface temperature of the sheet surface along the perpendicular direction of the heating line. It can also be seen that sheet having lesser sheet thickness experiences a large zone of maximum principal strain near to the region of heating line.

The maximum principal strain distribution over the sheet for constant sheet thickness of 3 mm under different line energy for single-pass has been presented in Fig.5.65.

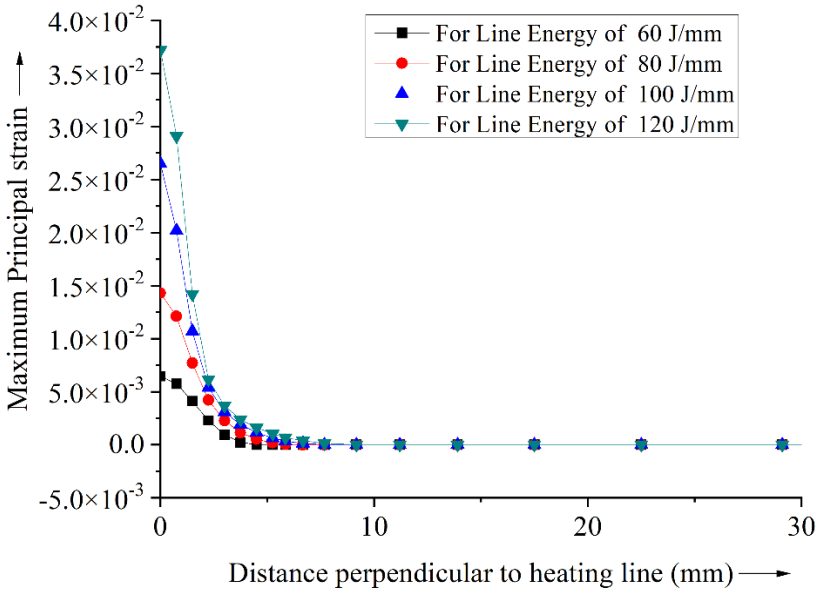

Fig.5.65 Maximum principal strain distribution with variation in line energy

It can be seen from the Fig.5.65 that with increase in line energy, the value of maximum principal strain increases. The maximum principal strain is tensile in nature. With the increase in line energy, the surface temperature of the sheet increases. An increase in temperature results in an increase in maximum principal strain along the heating line in the tensile direction. It is observed that with an increase in distance perpendicular to the heating line the strain value gets decreases till the temperature of the sheet reaches ambient temperature. It can also be seen that with an increase in line energy the zone of maximum principal strain increases along the direction perpendicular to the heating line. The minimum principal strain distribution over the sheet for different laser power of 300 W, 400 W, 500 W, and 600 W under constant traverse speed: 300 mm/min having a sheet thickness of 3 mm under a single pass has been presented in Fig.5.66.

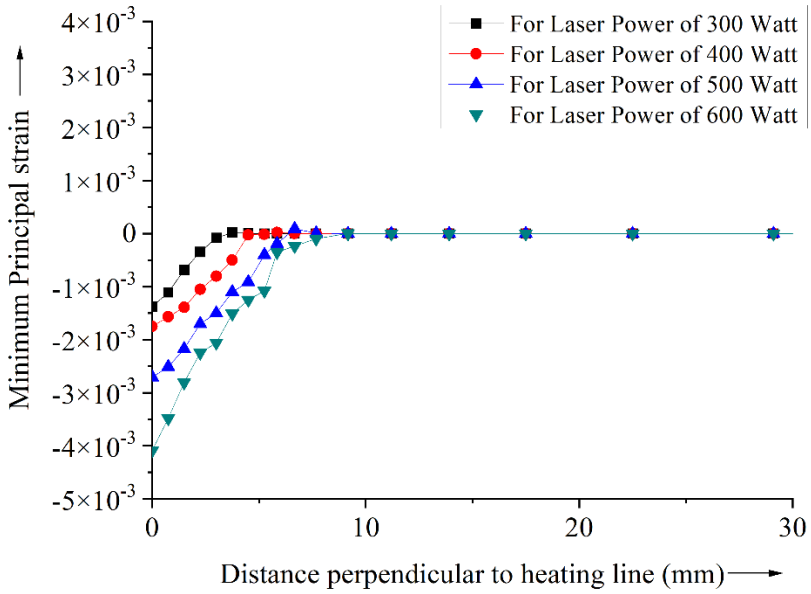

Fig.5.66 Minimum principal strain distribution with variation in laser power

It can be seen from Fig.5.66 that with an increase in laser power the minimum principal strain increases along the heating line. The minimum principal strain is compressive in nature. With an increase in laser power, the surface temperature of the sheet increases. An increase in temperature results in an increase in minimum principal strain along the heating line in the compressive direction. It is observed that with an increase in distance perpendicular to the heating line the strain value gets decreases till the temperature of the sheet reaches ambient temperature. It can be seen that an increase in laser power increases the minimum principal strain width along the perpendicular direction of the heating line. The maximum principal strain distribution over the sheet for different traverse speeds of 200, 300, 400, 500 and 600 mm/min under constant laser power: 350 W for a mild steel sheet having a sheet thickness of 3 mm under single pass has been presented in Fig.5.67.

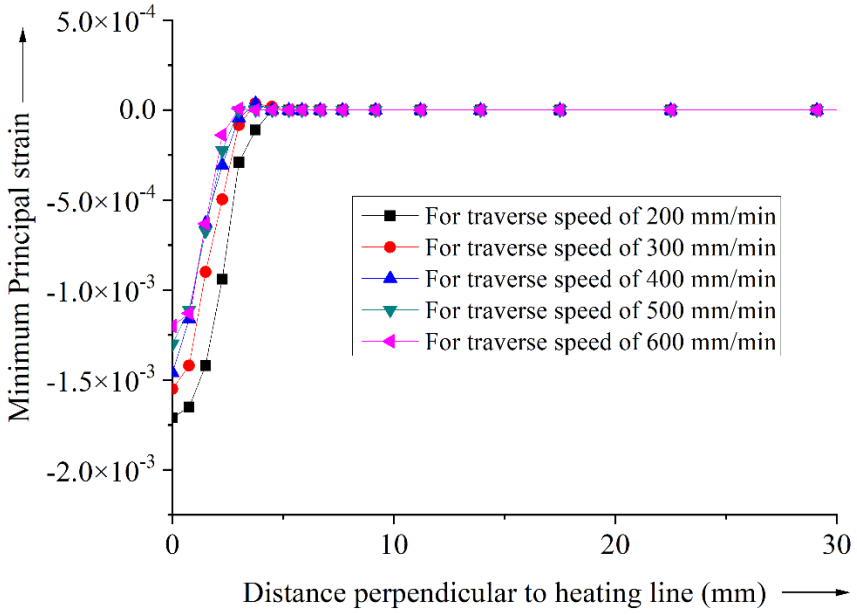

Fig.5.67 Minimum principal strain distribution with variation in traverse speed

It can be observed from Fig.5.67 that with an increase in traverse speed under constant laser power the magnitudes of minimum principal strain decrease. An increase in traverse speed reduces heat absorption time on the surface of the sheet. The decrease in the magnitude of the minimum principal strain is due to less heat input on the sheet surface, resulting in fewer rises in surface temperature. The magnitude of minimum principal strain reduces with progressive reduction of sheet surface temperature along the perpendicular direction of the heating line. It is seen that with an increase in distance perpendicular to heating line the zone of minimum principal strain is found to be more with a decrease in traverse speed. The minimum principal strain distribution over the sheet for different sheet thickness of 2 mm, 3 mm and 4 mm under constant laser power: 300 W for a constant traverse speed of 300 mm/min under single pass has been presented in Fig.5.68.

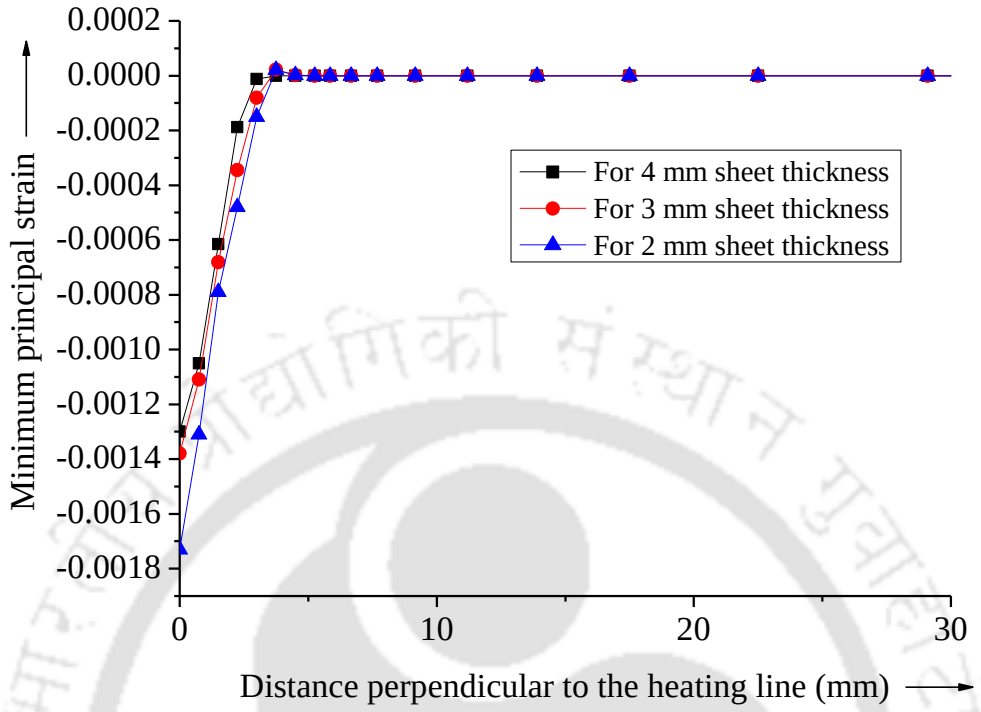

Fig.5.68 Minimum principal strain distribution with variation in sheet thickness

It can be observed from Fig.5.68 that with an increase in sheet thickness the magnitude of minimum principal strain decreases. The decrement is due to the lesser rise in the surface temperature of the sheet material. The magnitude of minimum principal strain reduces with progressive reduction of sheet surface temperature along the perpendicular direction of the heating line. It can be also observed that the sheet having lesser sheet thickness experience a large zone of minimum principal strain near to the region of heating line.

The minimum principal strain distribution over the sheet for constant sheet thickness of 3 mm under different line energy for single pass has been presented in Fig.5.69. It can be seen that with increase in line energy, the magnitude of minimum principal strain increases. The minimum principal strain is compressive in nature. With the increase in line energy, the sheet surface temperature increases. An increase in temperature results in an increase in minimum principal strain along the heating line in the compressive direction.

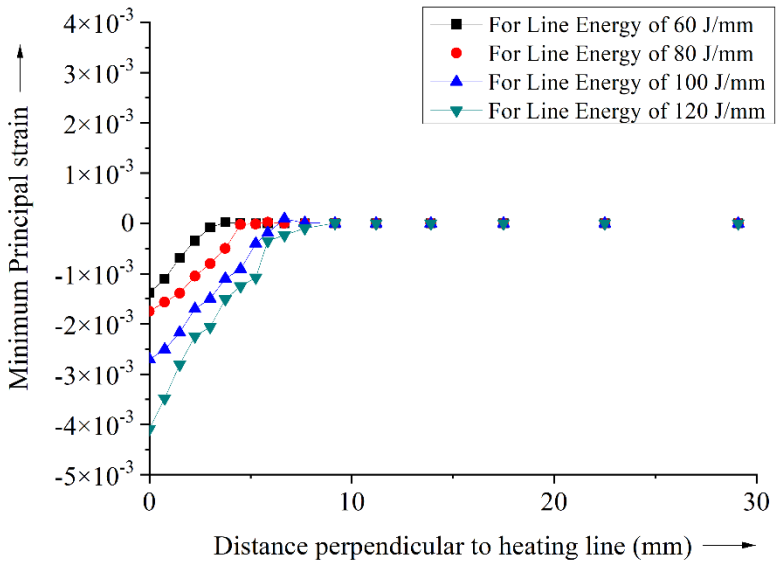

Fig.5.69 Minimum principal strain distribution with variation in line energy

It is observed that with an increase in distance perpendicular to the heating line the strain value gets decreases till the temperature of the sheet reaches ambient temperature. It is observed that with an increase in line energy the zone of minimum principal strain increases along the direction perpendicular to the heating line.

As the present thesis mainly focuses on the development of a 3-D compound curved surface, the evaluation of principal strain is found to be an essential part of the process. On the basis of the results obtained from the thermo-mechanical stress-strain analysis, the magnitude of minimum principal strain was taken into consideration for the determination of the heating parameters. The maximum values of minimum principal strain are compressive in nature which is shown in Table 5.6.

Table 5.7 Minimum principal strains for different laser operating parameters

Sl. no.	Laser Power (W)	Traverse speed (mm/min)	Sheet thickness (mm)	Minimum Principal strain
1	300	300	3	-0.00138
2	350	300	3	-0.00155
3	400	300	3	-0.00175
4	450	300	3	-0.00211
5	500	300	3	-0.00271
6	550	300	3	-0.0034
7	600	300	3	-0.00409
8	350	200	3	-0.00171
9	350	400	3	-0.00146
10	350	500	3	-0.0013
11	350	600	3	-0.0012

5.7 Summary

- A 3-D FE-model was successfully developed for the estimation of thermal history, residual deformation, stresses and strains. The results obtained from the FE-model were validated with the results obtained experimentally with a maximum percentage error of 6.63 % and 3.77% with the thermal history and residual deformation respectively.
- With the enhancement in laser power and line energy there is an increase in surface peak temperature of the sheet. Keeping all other operating parameters constant with increase in traverse speed and sheet thickness the peak temperature of the sheet reduces.
- In this study the surface temperature of the material is to be maintained within the recrystallization range. So the effect of operating parameters on temperature was studied and proper combination of laser power and traverse speed was identified for carrying out the process, so that the maximum temperature remains within recrystallization temperature.

- It is found that with the enhancement in laser power the angular deformation increases. If the peak temperature of the material moves closer to the melting temperature of the material, then there occurs substantial decrease in angular deformation.
- Angular deformation of the sheet decreases with increase in traverse speed.
- From the stress analysis results it was found that along the heating line, the longitudinal stress, transverse stress and von Mises stresses are found to be tensile in nature.
- The value of the transverse stress increases with the increase in laser power and line energy and decreases with increase in sheet thickness and traverse speed.
- There is no substantial increment in the magnitude of von Mises stress along the heating line. The rate of decrement with distance of the magnitude of von Mises stress increases with higher sheet thickness and traverse speed. The decrement of the magnitude of von Mises stress reduces with increase in laser power and line energy.
- From strain analysis results it was observed that the longitudinal plastic strain and the transverse plastic strain along the heating line are compressive in nature and the von Mises strain along the heating line is tensile in nature.
- The longitudinal strain, transverse strain and von Mises strain value increases with enhancement in laser power and line energy and decreases with increase in sheet thickness and traverses speed.
- The maximum principal strain along the heating line is tensile in nature and its value increases with increase in laser power and line energy. The magnitude of maximum principal strain decreases with increase in traverse speed and sheet thickness.
- The minimum principal strain along the heating line is compressive in nature and its value increases with increase in laser power and line energy.
- The magnitude of minimum principal strain decreases with increase in traverse speed and sheet thickness.

Chapter 6

Development of Compound Curved Surface by Laser Line Heating

6.1 Introduction

For the generation of 3-D compound curved surface, the evaluation of principal strain distribution is found to be one of the essential part of the process. On the basis of the magnitude and the direction of the principal strains, the position of the heating line and the heating parameters are decided. The present work mainly focuses on the determination of heating path, estimation of heating parameters along the path and blank generation for the development of a particular surface patch. A Finite Element Model (FEM) was developed for the determination of principal strain distribution along with the bending strain distribution for the desired surface patch. For the generation of compound surface patches, in this study, both pillow and saddle shape surface patches were taken into consideration which are shown in Fig.6.1 & Fig.6.2, respectively.

6.2 FE modeling details of pillow and saddle patches

The pillow and the saddle shape patches were generated by using the coordinate points as shown in Tables 6.1 and 6.2, respectively. In this study, the thickness of both pillow and the saddle patches were taken to be 3 mm. The pillow shape was generated by FE Abaqus software which is shown in Fig.6.1.

Table 6.1 Control points for pillow shape surface patch

X (mm)	Y(mm)	Z (mm)
0	0	0
49	0	23
151	0	23
200	0	0

0	49	13
49	49	44
151	49	44
200	49	13
0	151	13
49	151	45
151	151	45
200	151	13
0	200	0
49	200	23
151	200	23
200	200	0

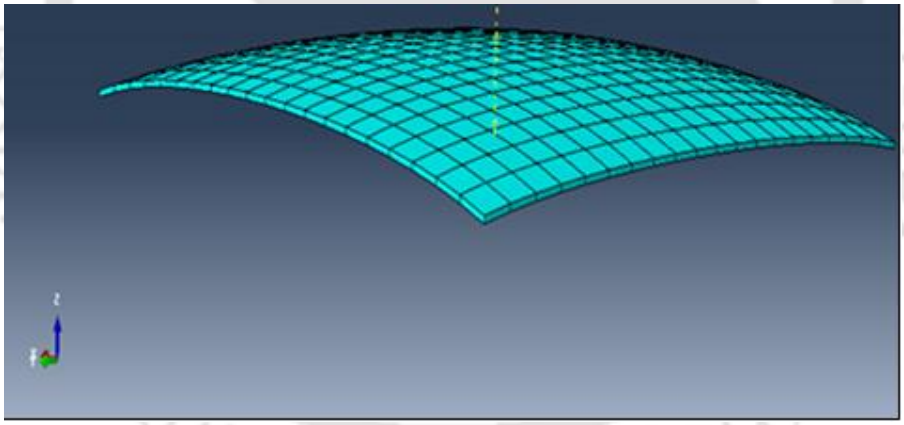

Fig.6.1 Model of Pillow shape patch

Similarly, the saddle shape was generated by using the coordinate points as shown in Table 6.2. The saddle shape was generated by FE ABAQUS software which is shown in Fig.6.2.

Table 6.2 Control points for saddle shape surface patch

X (mm)	Y(mm)	Z (mm)
0	0	19
0	66	7
0	133	-7
0	200	-19
66	0	7
66	66	3
66	133	-3
66	200	-7
133	0	-7
133	66	-3
133	133	3
133	200	7
200	0	-19
200	66	-7
200	133	7
200	200	19

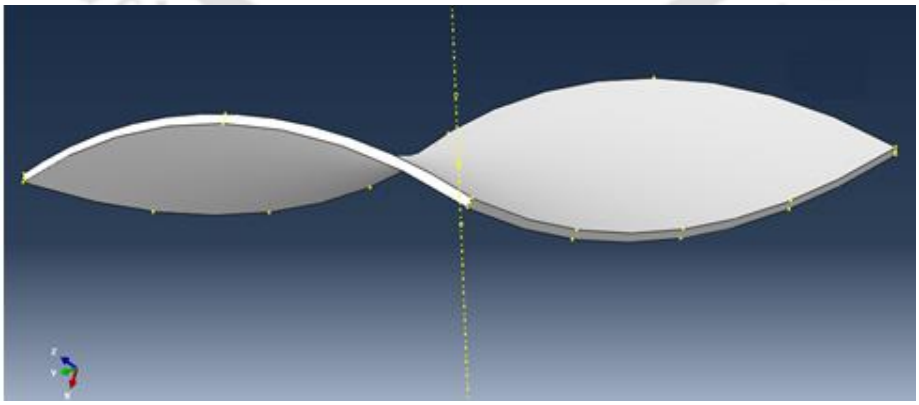

Fig.6.2 Model of saddle shape patch

6.3 FE analysis for stress-strain field distribution

The stress and strain fields of the planar shapes which are to be developed to get the desire shapes were solved by 3-D FEM model. The boundary conditions and assumptions made to flat the curved surfaces are as below:

- At first the curved surface patch which has to be flattened was attached to the punch by making coincident points. This was done for restricting the relative movement between punch and the curved surface patch.
- Large elastic deformation condition was considered.
- The die part was rigidly clamped by fixing all degrees of freedom.
- A constant velocity was applied to the top surface of the punch for loading purpose which was assigned in a step by step manner.
- The friction between the surfaces of the rigid bodies and the curved surface patch was considered to be zero.

The desired shapes were placed in between two flat rigid bodies. One body was regarded as a punch, which was used for applying compressive load and the other was used as a die. The curved shapes were then compressed with the help of these two rigid bodies and a planar shape was developed along with the generation of stress and strain field on the top and bottom surface. The top punch was given a step by step displacement towards the die until the gap between them is maintained to the sheet thickness of the desired shape. For finding out the stress and strain distribution pattern due to flattening of pillow and saddle shapes the following methodology and steps are followed.

- A die-punch model was suitably designed having a punch and die dimensions of 500 mm × 500 mm × 20 mm and 500 mm × 500 mm × 1 mm respectively.
- The curved surface patches of dimension 200 mm × 200 mm × 3 mm, which has to be flattened, was placed in between the die and the punch and load was applied in the punch in terms of uniform velocity for proper flattening of the curved patches. The flattening models for pillow and saddle shape patches are shown in Figs.6.3 and 6.4, respectively.

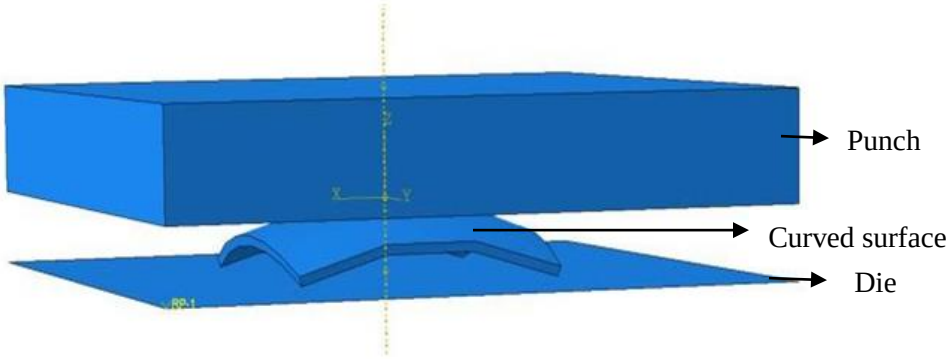

Fig 6.3 Model for flattening of Pillow shape surface patch

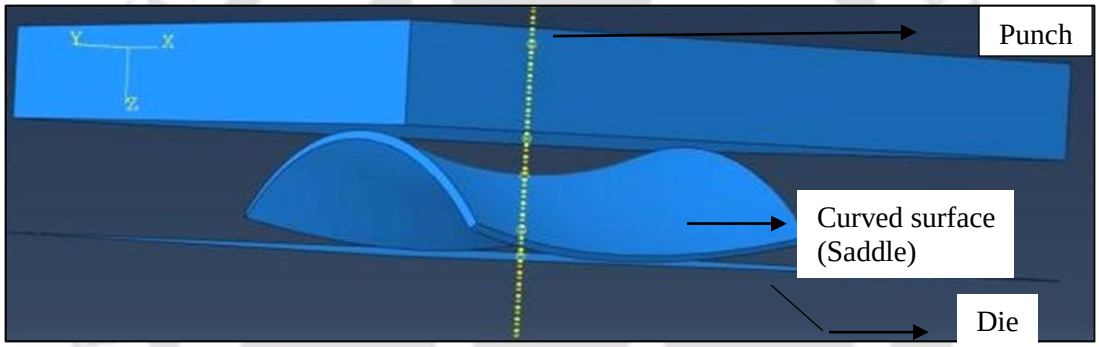

Fig 6.4 Model for flattening of Saddle shape surface patch

6.3.1 Mesh sensitivity analysis

The mesh sensitivity analysis was performed to ensure that the stresses are independent of element size. The mesh sensitivity analysis was carried for different element sizes for both pillow and saddle shapes as shown in Table 6.3 and Table 6.4, respectively.

Table 6.3 FE model details for mesh sensitivity analysis of pillow shape

Sets	**Element size**	**von Mises stress (MPa)**
1	12 mm × 12 mm × 3 mm	3.675×10^2
2	8 mm × 8 mm × 1.5 mm	2.890×10^2
3	5 mm × 5 mm × 3 mm	2.736×10^2

4	5 mm × 5 mm × 1.5 mm	2.702×10^2

In pillow shape only von Mises stresses were taken into consideration for the mesh sensitivity analysis. The mesh has to be refined globally for improving the stress prediction. Figs.6.5 & 6.6 show the variation of von-Mises stress with variation in different element size for pillow shape.

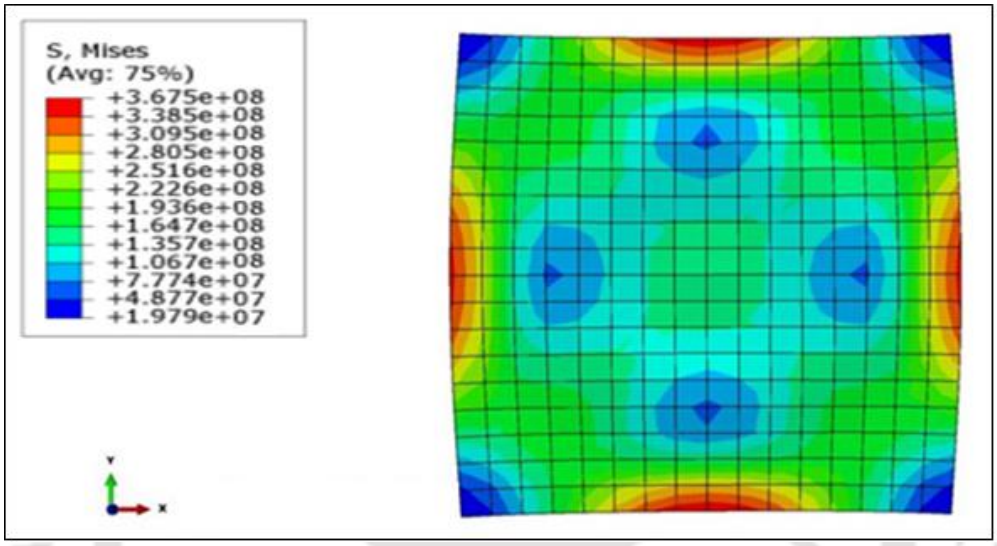

Fig.6.5 von Mises stress distribution with global mesh size of 12 mm × 12 mm × 3 mm

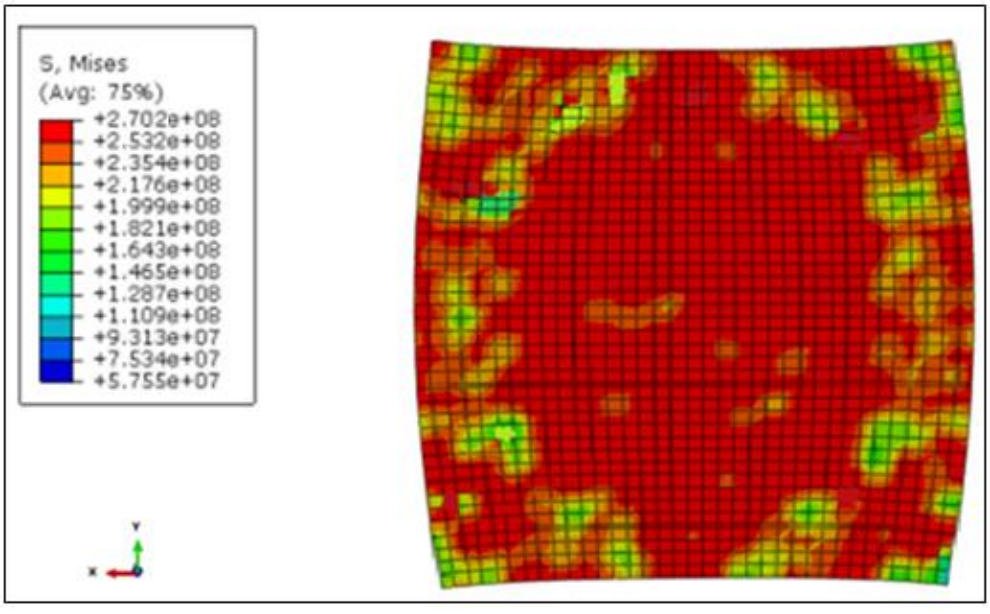

Fig.6.6 von Mises stress distribution with global mesh size of 5 mm × 5 mm × 1.5 mm

It was seen from the mesh sensitivity analysis, that the von Mises stress value beyond 5 mm × 5 mm × 1.5 mm element size does not have any significant change.

Similarly, the mesh analysis studies for different element size were also performed for saddle shape as shown in Table 6.4.

Table 6.4 FE model details for mesh sensitivity analysis of saddle shape

Sets	Element size	von-Mises stress (MPa)	Minimum principal strain
1	12 mm × 12 mm × 3 mm	3.720×10^{8}	-9.075×10^{-2}
2	8 mm × 8 mm × 3 mm	2.850×10^{8}	-8.575×10^{-2}
3	5 mm × 5 mm × 3 mm	2.730×10^{8}	-5.582×10^{-2}
4	5 mm × 5 mm × 1.5 mm	2.710×10^{8}	-5.636×10^{-2}

In saddle shape both von-Mises stress and minimum principal strain was taken into consideration for the study of mesh sensitivity analysis. Figs.6.7 - 6.8 show the variation of von-Mises stress and Fig.6.9 shows the minimum principal strain distribution for the element size for saddle shape.

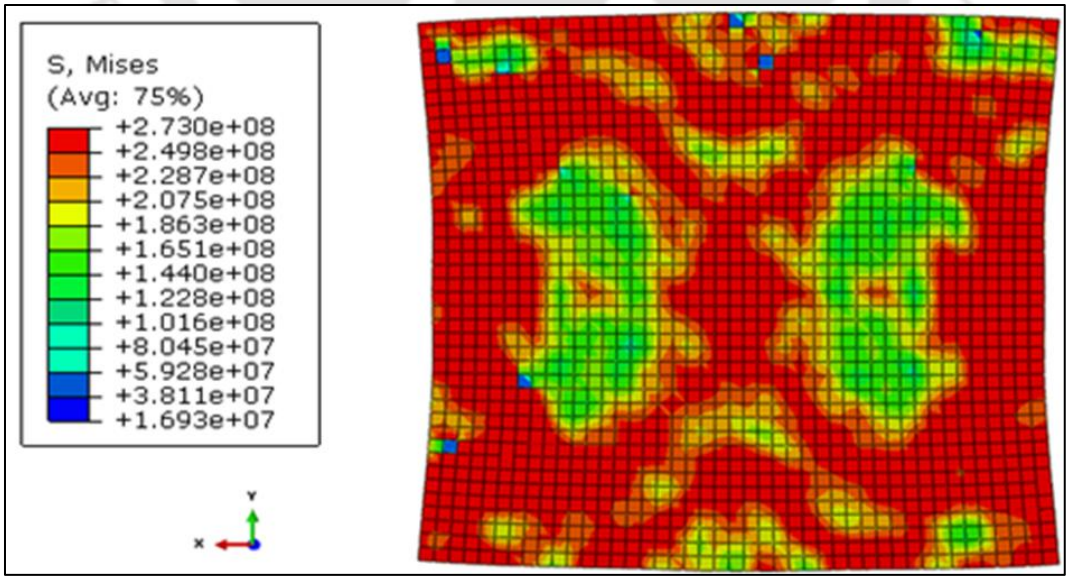

Fig.6.7 von-Mises stress distribution with global mesh size of 5 mm × 5 mm × 3 mm

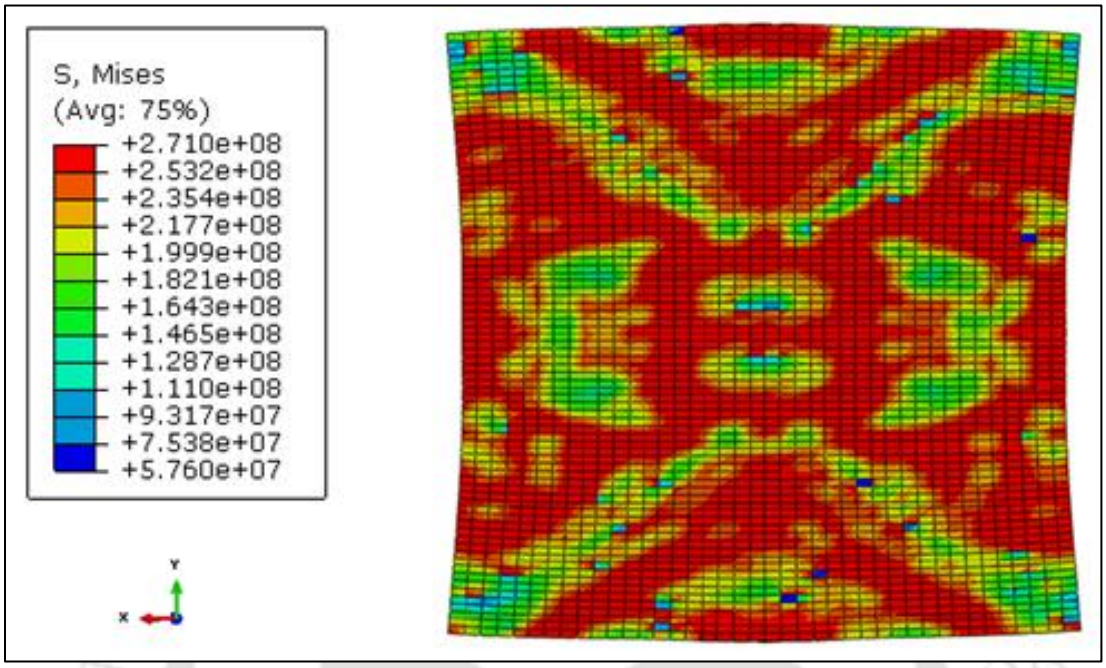

Fig.6.8 von Mises stress distribution with global mesh size of 5 mm × 5 mm × 1.5 mm

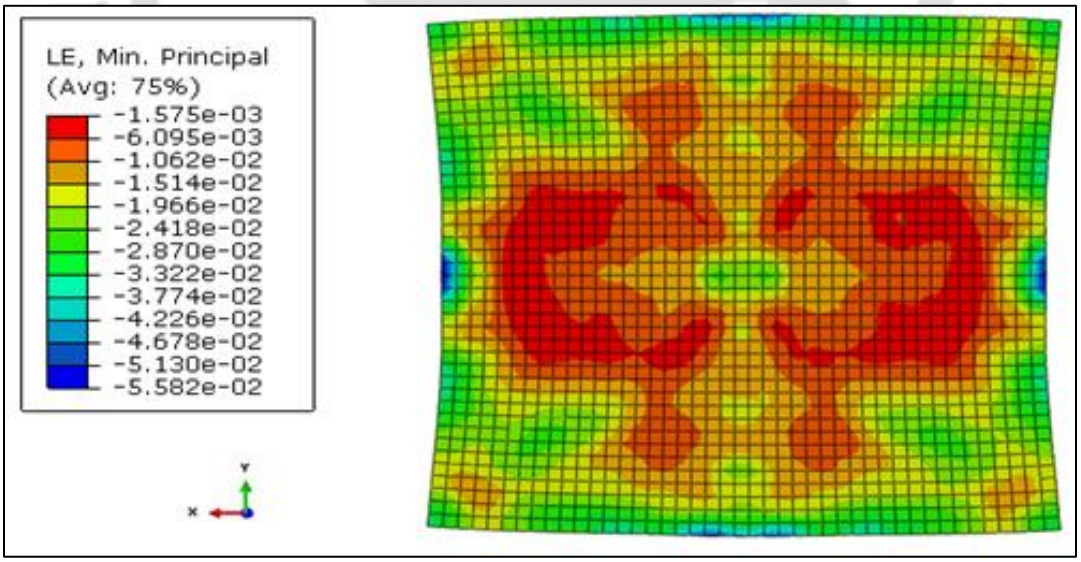

Fig.6.9 Minimum principal strain distribution with global mesh size of 5 mm × 5 mm × 3 mm

From the Figs.6.7 & 6.8, it was observed that the results of von Mises stress and minimum principal strains do not have any significant change with reduction of mesh size. So it is

confirmed from the study of mesh sensitivity analysis that the von-Mises stress and the minimum principal strains were independent of the mesh size beyond 5 mm × 5 mm × 1.5 mm. So the element size of 5 mm × 5 mm × 1.5 mm was taken into consideration for further analysis for both pillow and saddle shapes.

6.4 Prediction of heating parameters

The heating conditions to be determined include laser power P, scanning velocity V and the number of pass. It is possible to continuously vary them to generate the strain field required perpendicular to the heating line, to form the desired surface. The compound curved surfaces that has to be developed, has its own minimum principal strain distribution over the surface. The heating lines are placed perpendicular to the minimum principal strain direction. Based on the magnitude of strain required in the region, proper combination of operating parameters is required along the heating path. So, it is difficult to select the proper combination of operating parameters, for corresponding individual strains. To cater the problem and to reduce the processing time, Artificial Neural Network (ANN) was used for the process. The detailed of ANN is provided in section 6.7.1.

6.5 Results and discussion

The FE-analysis results of the pillow and saddle shapes were evaluated. Based on mesh sensitivity analysis the element size was decided for carrying out the analysis which was 5 mm × 5 mm × 1.5 mm. The FE large elastic deformation analysis was carried out for flattening the surface patches. The whole modeling and analysis were carried out using FEM based software ABAQUS.

6.5.1 Blank and principal strain field generation

The blank of the individual compound curved shape was generated after flattening the curve shape by placing the patch in between two rigid bodies. The generated blanks for pillow shape surface patch are shown in Figs.6.10 & 6.11.

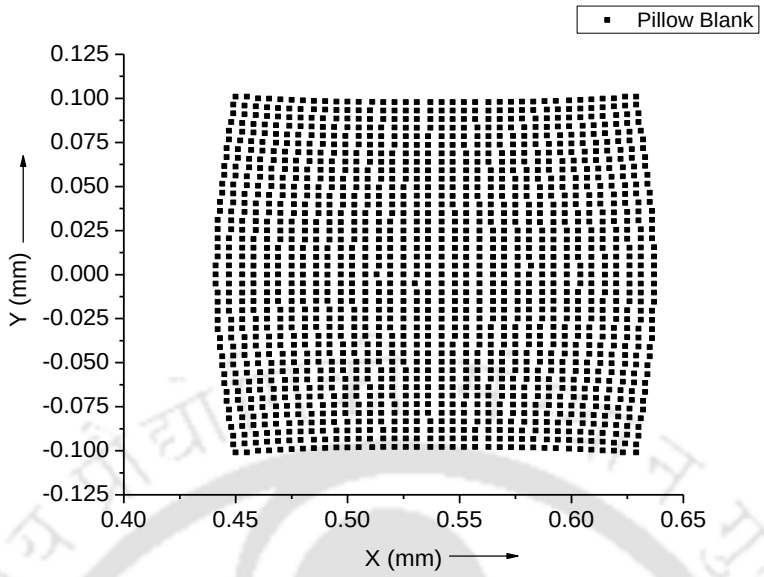

Fig. 6.10 The coordinate points of the blank of the pillow shape patch

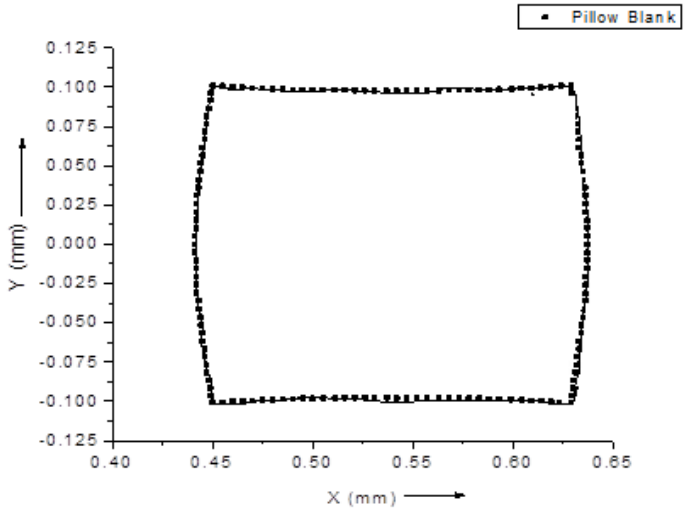

Fig. 6.11 The outline of the blank obtained for development of the pillow surface patch

For prediction of heating lines and heating parameters the minimum principal strain field distribution pattern is required. For that reason, the minimum principal strain distribution pattern was generated. The minimum principal strain field distribution for the pillow shape patch is shown in Figs.6.12 & 6.13.

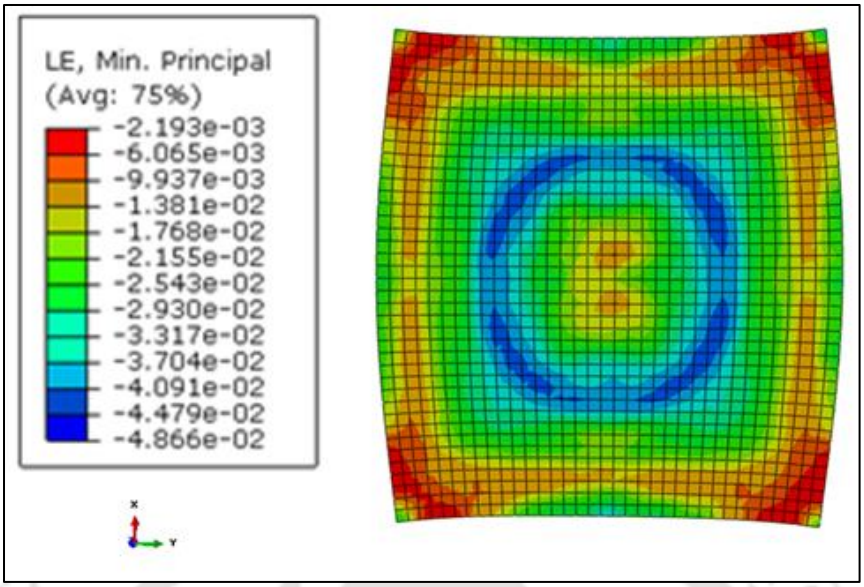

Fig.6.12 Minimum principal strain distribution for pillow surface

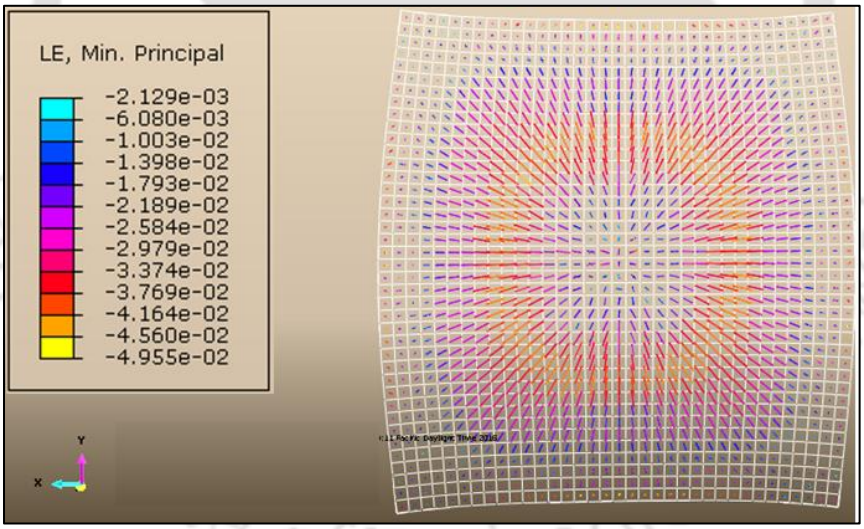

Fig.6.13 Vector plot for minimum principal strain direction of the top surface for pillow surface

Fig.6.12 shows only the magnitude of minimum principal strain field distribution after flattening the pillow shape patch. The minimum principal strain distribution along with the direction in which it is acting is shown in Fig. 6.13. The color of the individual bar in the distribution plot represents the magnitude and its orientation on the surface represents the direction on which it is

acting. The laser heating paths were to be placed perpendicular to the minimum principal strain direction. The value of the individual strains perpendicular to the laser heating path were co-related with the laser heating process parameters and the required process parameters were selected. The generated blanks for saddle shape surface patch are shown in Figs. 6.14 & 6.15 respectively.

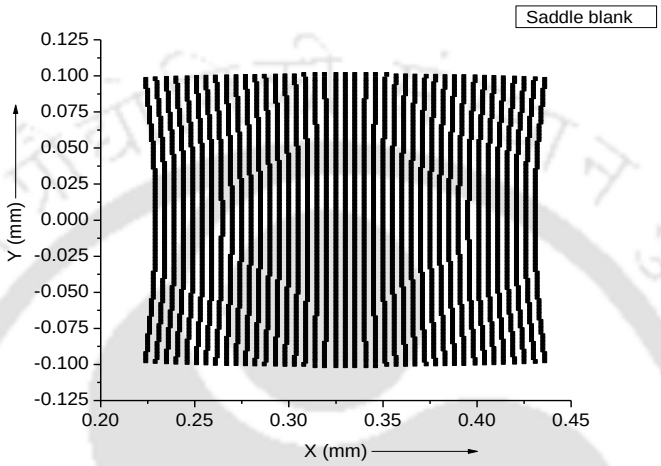

Fig.6.14 The blank of the saddle surface

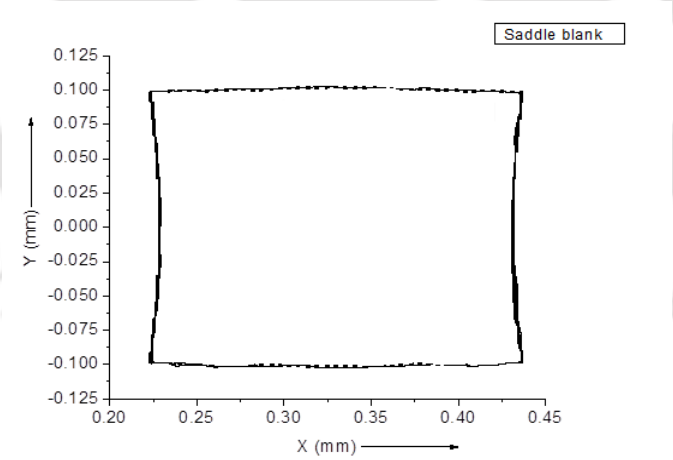

Fig.6.15 The outline of the blank obtained for development of the saddle surface patch

Similarly, in case of saddle shape for prediction of heating lines and heating parameters the minimum principal strain field distribution pattern is required. For that reason, the minimum principal strain distribution pattern was generated. The minimum principal strain field distribution for the pillow shape is shown in Figs.6.16.

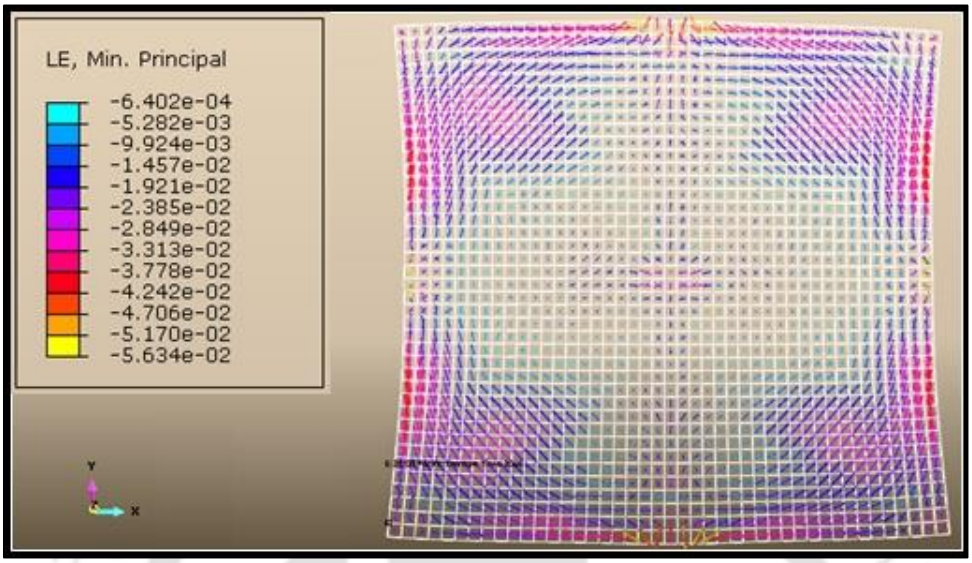

Fig.6.16 Vector plot for minimum principal strain direction for saddle surface

The minimum principal strain distribution along with the direction in which it is acting is shown in Fig. 6.16. The color of the individual bar in the distribution plot represents the magnitude and its orientation on the surface represents the direction on which it is acting. The laser heating paths were to be placed perpendicular to the minimum principal strain direction. The value of the individual strains perpendicular to the laser heating path were co-related with the laser heating process parameters and the required process parameters were selected.

6.5.2 Bending strain distribution

In the development of 3-D compound curved surface by the process of laser line heating, the side of the sheet (blank) on which the heating path is to be placed, plays a very important role. It is decided on the basis of bending strain distribution on the upper and lower surface of the curved shape which has to be developed. The bending strain can be negative or positive in nature. The meaning of negative bending strain signifies that, the surface experiences more compressive strain. In laser line heating process for straight line heating, the sheet bends towards the laser beam. This shows laser beam interaction surface experiences more compressive strains. On the

basis of bending strain into consideration, the bending strain distribution for pillow shape was generated which are shown in Figs.6.17-6.19.

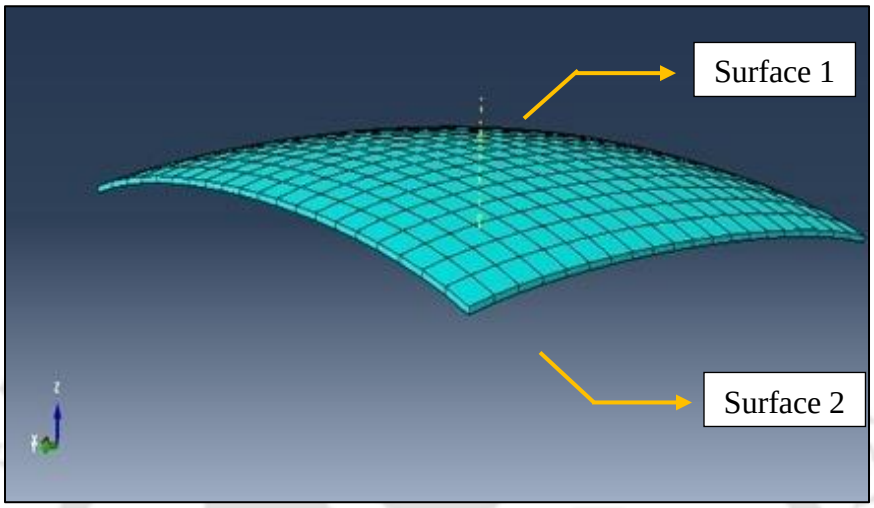

Fig.6.17 Model of Pillow shape surface patch

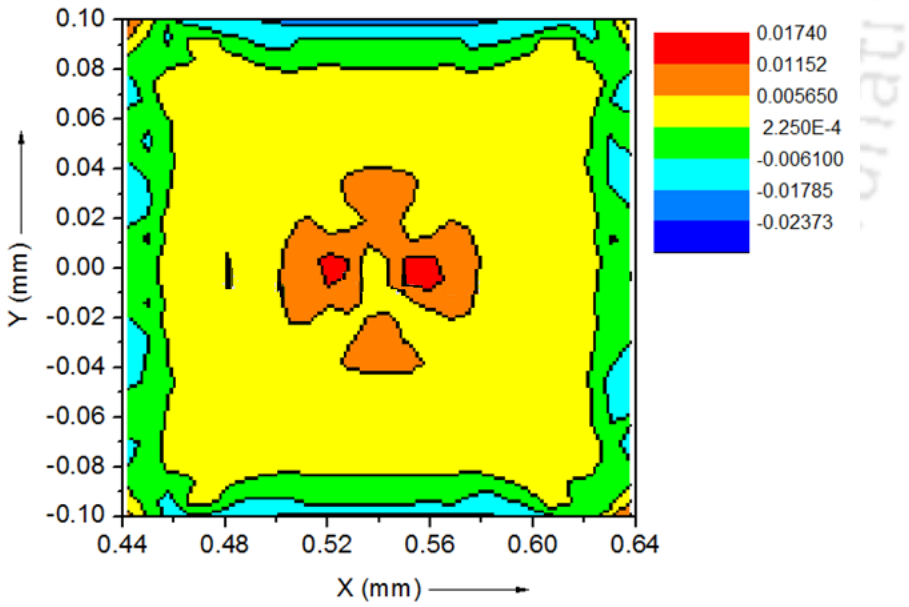

Fig.6.18 Bending strain on surface-2 of pillow shape

In reference to Fig.6.18 on flattening of the pillow patch, on surface -2 the amount of positive bending strains was found to be more as compared to the amount of negative bending strain. So, therefore the negative bending strains can be neglected for that surface. On the other hand, the

amount of positive bending strain on surface-1 was found to be less as compared to the amount of negative bending strains as shown in Fig.6.19.

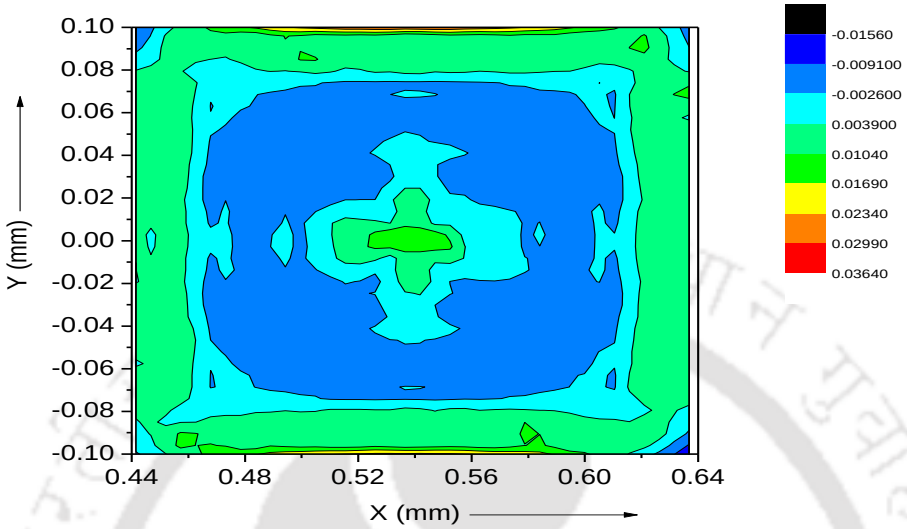

Fig.6.19 Bending strain on surface-1 of pillow shape

Now during the development of the surface, the surface which experiences more amount of positive bending strain after flattening has to be heated to develop more amount of negative bending strain. So in case of pillow shape patch as surface-2 experiences more amount of positive bending strain on flattening, the heating lines are to be placed on that side of the blank on which we want to develop surface-2. Similarly, the bending strain distribution for saddle shape was generated which are shown in Figs.6.20-6.22.

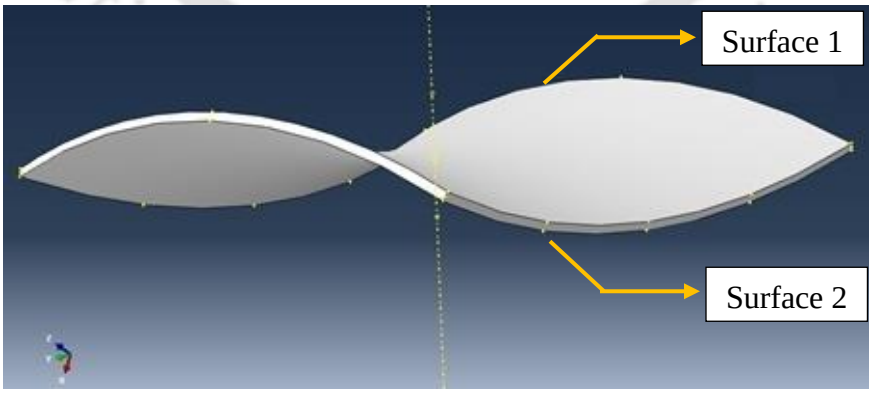

Fig.6.20 Saddle shape surface patch

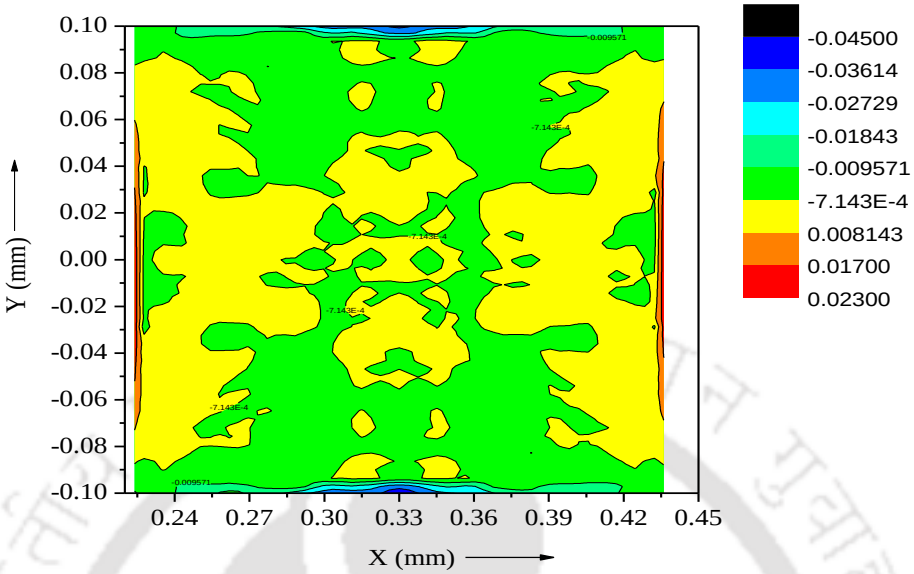

Fig.6.21 Bending strain on surface-1 of the saddle shape

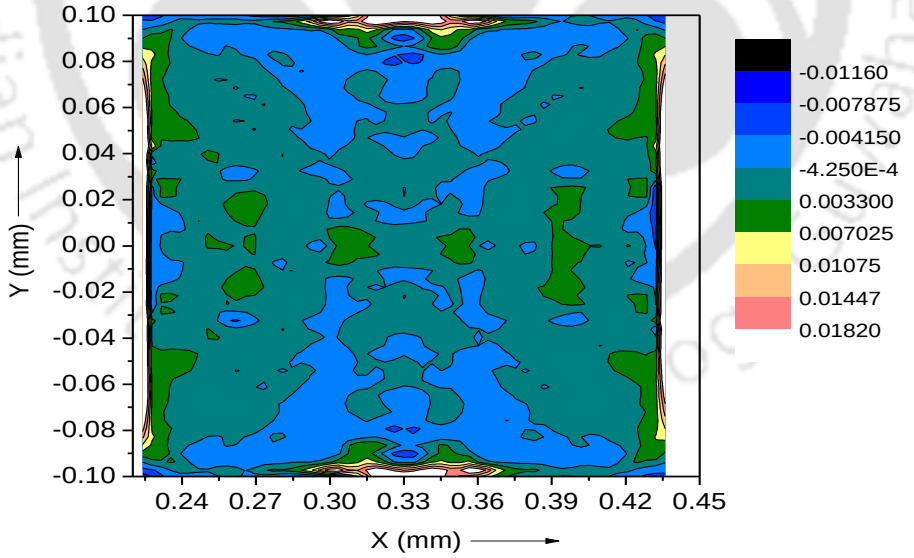

Fig.6.22 Bending strain on surface-2 of the saddle shape

Whereas in case of saddle shape it was observed that, both the surface-1 & 2 experiences sufficient amount of negative and positive bending strain after flattening. So, to develop the individual surfaces on the blank the heating lines are to be placed on both the side of the sheet (blank). The laser has to be placed on the blank in the region of the surface which experiences positive bending strain and to be placed on the opposite side of the blank in the region of the surface which experiences negative bending strain.

6.5.3 Vector plot of maximum principal strain

Figs. 6.23 & 6.24 shows the direction of maximum principal strain direction for both pillow and saddle shape surface patch. The heating paths are to be drawn perpendicular to the minimum principal strain direction. In other ways it can also be said that the heating paths are to be placed along the maximum principal strain direction. So by joining the vector direction of the maximum principal strain of the respective surfaces by a continuous line we can get the idea of heating line pattern for both pillow and saddle shape surfaces.

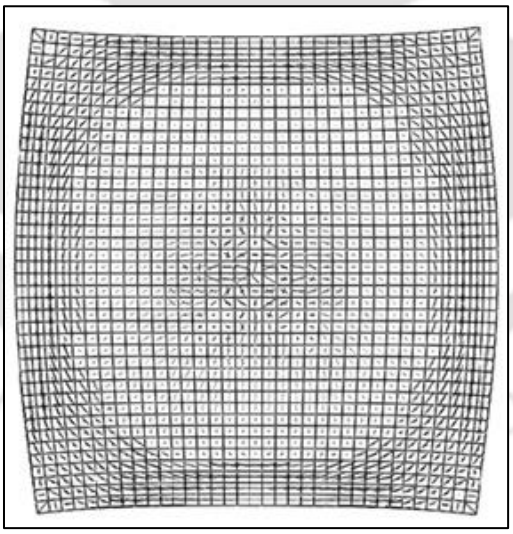

Fig.6.23 Heating path for pillow surface

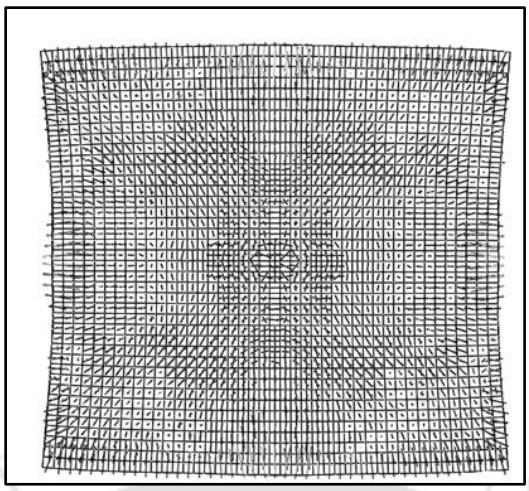

Fig.6.24 Heating path for saddle surface

6.6 Determination of heating path

The laser heating path for respective surface patches were chosen by taking the direction of minimum principal strain into consideration. The laser heating path should be placed perpendicular to the minimum principal strain direction. The side of heating of the sheet was decided on the basis of bending strain distribution. The detailed has been discussed in section 6.5.2.

The spacing between the laser heating paths should be appropriate at every region. The distance between the heating lines should be more than the laser diameter. A relation has been used for the determination of spacing between two heating path is as shown below:

$$D_{Path} = \frac{d_{laser} \times \varepsilon_{laser}}{Average\ minimum\ principal\ strain} \quad (6.1)$$

where D_{Path} represents the distance between the laser heating path, ε_{laser} represents strain generated by laser forming, d_{laser} represents the diameter of the laser beam and $Average\ minimum\ principal\ strain$ represents the average minimum principal strain between the two heating path.

6.7 Estimation of heating parameters

6.7.1 Determination of heating condition using Artificial Neural Network

The operating parameters of the line heating process have been decided based on Artificial Neural Network (ANN). In the present investigation, a neural network model was established using neural network tool box in MATLAB. Here the input layer has 3 neurons corresponding to individual laser operating parameters, which includes: laser power, traverse speed and number of pass and the desired output is the minimum principal strain (corresponds to single neuron output). The training function was selected as "TRAINLM" function and the transfer function of ANN is selected as "TANSIG" function (hyperbolic tangent sigmoid function). Here the adaptation learning function was selected as "LEARNGDM" function. The TRAINLM function is a network training function that updates the weight and bias values according to Levenberg-Marquardt optimization. The levels of the input parameters were defined based on the different combination of the laser operating parameters. Sum total outputs of 12 combinations of laser operating parameters were tested approximately three times for obtaining a total data set of 36. Table 6.5 shows the list of 36 data sets of the laser operating parameters with the results of minimum principal strains for corresponding data set as output.

Table 6.5 The datasets of laser operating parameters with subsequent values of minimum principal strain

Sl. no.	Laser Power (W)	Traverse speed (mm/min)	no. of pass	Magnitude of Minimum principal strain
1	300	300	1	-0.00138
2	350	300	1	-0.00145
3	400	300	1	-0.00175
4	450	300	1	-0.00211
5	500	300	1	-0.00271
6	550	300	1	-0.0034
7	600	300	1	-0.00409

8	300	300	2	-0.00166
9	350	200	1	-0.00191
10	350	300	1	-0.00145
11	350	400	1	-0.00136
12	350	500	1	-0.0013
13	300	300	1	-0.00138
14	350	300	1	-0.00145
15	400	300	1	-0.00175
16	450	300	1	-0.00211
17	500	300	1	-0.00271
18	550	300	1	-0.0034
19	600	300	1	-0.00409
20	300	300	2	-0.00166
21	350	200	1	-0.00191
22	350	300	1	-0.00145
23	350	400	1	-0.00136
24	350	500	1	-0.0013
25	300	300	1	-0.00138
26	350	300	1	-0.00145
27	400	300	1	-0.00175
28	450	300	1	-0.00211
29	500	300	1	-0.00271
30	550	300	1	-0.0034
31	600	300	1	-0.00409
32	300	300	2	-0.00166
33	350	200	1	-0.00191
34	350	300	1	-0.00145
35	350	400	1	-0.00136
36	350	500	1	-0.0013

Out of the total data set 20% (7 data set) of the data were selected randomly. These 7 data sets were used as a confirmation set for the obtained trained network. Table 6.6 shows the randomly selected data set for network investigation.

Table 6.6 The selected datasets for network investigation

Sl. no.	Laser Power (W)	Traverse speed (mm/min)	Number of pass
1	300	300	1
2	450	300	1
3	550	300	1
4	300	300	2
5	350	500	1
6	600	300	1
7	350	200	1

In this work, both the number of neurons and the hidden layers were varied for the selection of proper network. The network selected was based on the minimum value of the error between the predefined outputs with the predicted output for the same operating parameters. Table 6.7 shows the comparison of output data estimated by using ANN and the simulated output results. It was observed that minimum error was obtained for the neural network having 8 neurons with two hidden layers. Fig.6.25 shows the regression results of the network training obtained from the MATLAB.

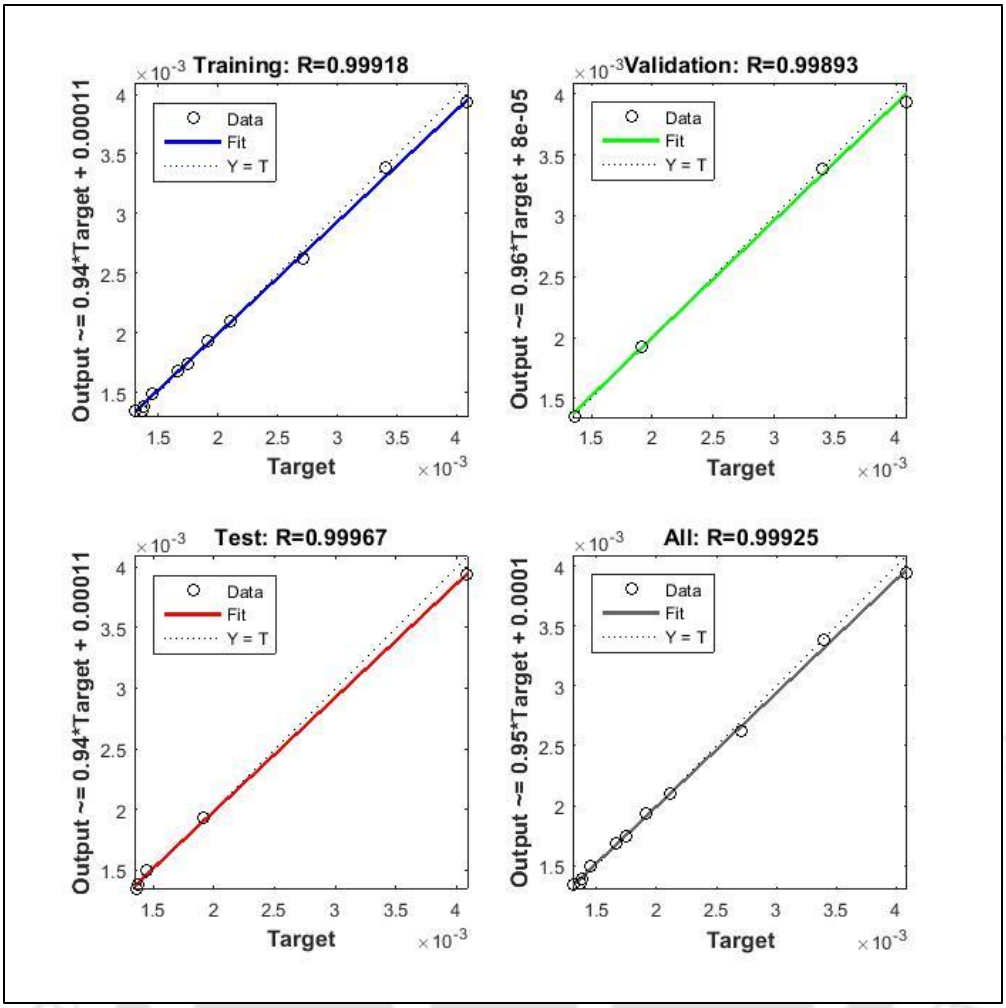

Fig.6.25 The regression results of neural network training

Table 6.7 Comparison of minimum principal strain estimated by ANN and Simulated value (for 8 neurons)

Sl.no.	Laser Power (W)	Traverse speed (mm/min)	Number of pass	Minimum Principal strain (Simulation)	Minimum Principal strain (ANN)	Percentage of error
1	300	300	1	-0.00138	-0.00139	0.72
2	450	300	1	-0.00211	-0.00209	0.94
3	550	300	1	-0.00340	-0.00338	0.58
4	300	300	2	-0.00166	-0.00168	1.20

5	350	500	1	-0.00130	-0.00135	3.84
6	600	300	1	-0.00409	-0.00394	3.66
7	350	200	1	-0.00191	-0.00193	1.05

6.8 Experimental results

Experimental development of pillow surface patch was successfully carried out by the process of laser line heating. To start with the process, the following steps were followed:

- A suitable 2-D blank with required dimension was cut from the mild steel sheet of 3 mm sheet thickness is shown in Fig.6.26. On the blank, the initial measurements were carried out at suitable locations with the help of a coordinate measuring machine.

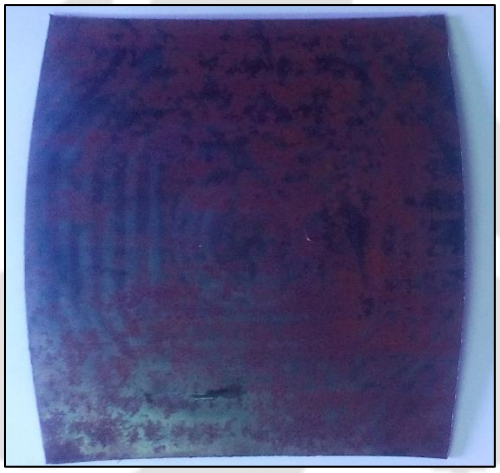

Fig.6.26 Blank for the development of pillow surface patch

- On the basis of direction of minimum principal strain that was obtained from Fig.6.13, the heating lines were drawn perpendicular to the minimum principal strain direction. The proper spacing should be maintained between the heating lines by using the relation shown in section 6.6. The heating lines were plotted with the help of design software Auto CAD 2020 as shown in Fig.6.27.

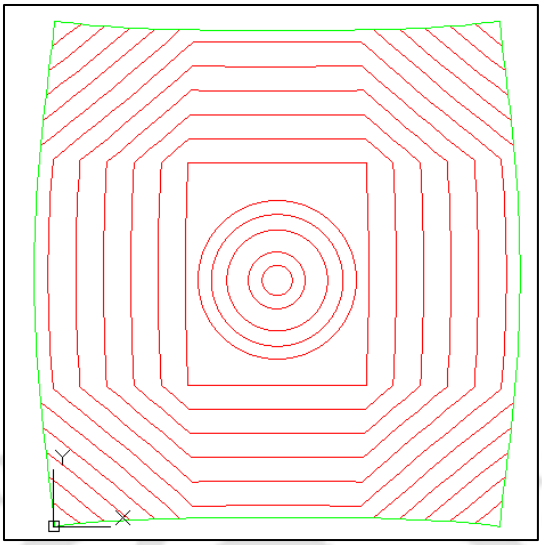

Fig.6.27 The heating line pattern developed for pillow surface patch

- The position of the heating lines was suitably programmed using CNC programming and was fed to the controller as an input to the CNC operated laser machine (Orion 3015, LVD make) as shown in Fig.6.28.
- Depending on the strain field distribution, the average strain values of the individual heating lines were selected. The operating parameters (such as laser power, traverse speed and number of pass) were suitably selected based on the results of strains obtained from thermo-mechanical analysis.

Fig.6.28 The experimental set up for development of pillow patch

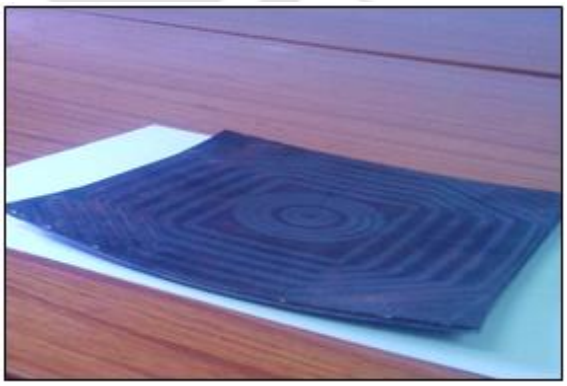

Fig.6.29 Experimentally generated pillow patch lower view

- The operating parameters of the unknown strain values were predicted by using Artificial Neural Network (ANN) and the experiment was performed for obtaining the desired pillow shape patch as shown in Figs.6.29 & 6.30.

Fig.6.30 Experimentally developed pillow patch upper view

After the sheet cooled down to the atmospheric temperature, the measurements of the sheet surface were taken at the previously mentioned locations using coordinate measuring machine. The difference between the measurements has been shown in Table 6.8.

Table 6.8 Comparison between experimental and theoretical pillow patch

X (mm)	Y(mm)	Z (mm)	Z (mm) obtained from experiment	Percentage of error
0	0	0	0	0
49	0	23	20.12	12.56
151	0	23	20.13	12.45
0	49	13	12.90	7.69
49	49	44	43.50	11.36

151	49	44	43.54	10.25
200	49	13	11.86	8.72
0	151	13	11.987	7.79
49	151	45	41.21	8.42
151	151	45	39.59	12.01
200	151	13	11.91	8.32
49	200	23	20.13	12.44
151	200	23	20.68	10.08

6.9 Summary

The brief summary of the above study is listed as below:

- The 3-D FE model methodology was successfully developed for predicting the stress-strain field distribution pattern due to flattening of 3-D compound curved patch to a 2-D blank.
- Large deformation elastic modeling criteria was considered in this analysis.
- Mesh sensitivity analysis was used to get the optimum mesh size. It was observed that mesh size has a significant effect on stresses and strains distribution pattern.
- Based on the minimum principal strain distribution, minimum principal strains direction and bending strain distribution pattern, the heating lines were successfully determined and the heating conditions were established.
- For online input data generation, an artificial neural network model (ANN) using back propagation algorithm was successfully designed for the estimation of the laser operating parameters based on the minimum principal strain.
- Heating paths were generated perpendicular to the minimum principal strain direction and depending on the bending strain distribution the heating surfaces were decided.
- It was concluded that the effect of each heating path was not affected by using the empirical relation as discussed in section 6.6. Each heating lines was not affected with transfer of heat during laser scanning of the neighbor heating line.

- Experimental study was successfully carried out to generate the compound curved surfaces. The experimentally obtained compound curved surface (i.e. pillow surface patch) matched fairly well with that of numerically obtained results with a maximum percentage of error of 12.56 %.

Chapter 7

Conclusion and Future scope

7.1 Conclusions

From the present research work the following conclusions can be drawn.

- A 3-D FE model was successfully developed for prediction of thermal history, residual deformation and stresses/strain with high accuracy. The model was validated with experimentally obtained results with maximum percentage of error of 6.63% and 3.77% for thermal history and residual deformation respectively.
- With increase in laser power there is an increase in surface peak temperature of the sheet, while increase in traverse speed and sheet thickness the surface peak temperature reduces. So, proper combination of laser power and traverse speed was identified, so that the surface temperature of the material should be maintained within the recrystallization range.
- The angular deformation increases with increase in laser power but decreases when the material surface temperature reaches close to the melting temperature. In laser line heating process the angular deformation in the sheet happens due to the temperature gradient across two surfaces of the sheet. The traverse speed inversely affects angular deformation.
- Reduction in angular deformation with an increase in traverse speed in laser line heating process is primarily due to reduction in heat input per unit length, quicker cooling rates, which results in less thermal expansion and consequently development of less angular deformation.
- The operating parameters associated with the laser line heating process was optimized using Taguchi method and ANOVA, revealing that the number of pass is found to be most influential parameter. A co-relationship was obtained among laser power, traverse speed, sheet thickness, number of pass and bend angle using multiple regression analysis.

- An artificial neural network (ANN) model was used to effectively predict the laser heating parameters required for a particular heating path. Proper heating parameters for unknown minimum principal strain values were obtained by training the model with the values of minimum principal strain derived from different laser parameters. The minimum principal strain values obtained from simulation and the values predicted by ANN validates well with a percentage error of 0.58.
- The determination of heating lines and heating conditions from magnitude of principal strain and directions enables in successful development of compound curved surfaces with experimental results closely matches with numerical predictions with maximum error of 12.56%.

7.2 Future scope of work

The study can be extended to the following future work.

- The current study basically focused on the process development of compound curved surface using mild steel. The process can be extended to other advanced materials associated with other engineering application.
- Work need to be addressed in the field of optimization of blank size and strains, so that the desired shape can be obtained from optimum number of heating lines, which leads to the reduction in processing time.
- The present study is concerned with the development of algorithm and computational procedure on development of compound curved surface. The effect of sequence of heating need to be studied further for establishment of proper line heating sequence which will enable efficient production of curved shape.

Bibliography

Adak, M. and Mandal, N.R.,2004, Thermomechanical Analysis of plates undergoing Line Heating Using Pseudolinear Equivalent Constant Rigidity System, Journal of Ship Production, 20, 2, 84-89.

Aihui, L., Wenjiao, D and Weigang, Z., 2012, Investigation of the effect of heating-lines on tensional mechanical properties of sheet metal after laser forming, Applied Mechanics and Materials,117-119,1666-1671.

Alberg, H.,2005, Simulation of welding and heat treatment modelling and validation, Ph.D. Thesis, Lulea University of Technology, Sweden.

Alberti, N., Fratini, L.andMicari, F., 1994, Numerical simulation of the laser bending process by a coupled thermal mechanical analysis, Proceedings, Laser Assisted Net Shape Engineering, Proceedings of the LANE, 1, October 12-14, Erlangen, Germany, 327-336.

Alberti, N., Fratini, L., Micari, F., Cantello, M., and Savant, G.,1997, Computer aided engineering of a laser assisted bending processes, Proceedings, Laser assisted Net Shape Engineering, Proceedings of the LANE, 2, September 23-26, Erlangen, Germany, 375-382.

Ansys, Inc., 2002, Theory reference, Southpointe, Canonsburg, .PA

Ashby,M.F. and Easterling,K.E.,1984, The transformation hardening of steel surfaces by laser beams-I, Hypo-Eutctoid steels, Acta Metall.,32,1935-1948.

Azariadis, P. and Aspragathos, N.,1997, Design of plane developments of doubly curved surfaces, Computer- Aided Design, 29, 10, 675-685.

Bae,K.Y., Yang, Y.S., Hyun, C.M. and Cho S.H., 2009, Simplified Mathematical Formulas for the Prediction of Deformations in the Plate Bending Process using an oxy-propane gas flame. Proceedings of the Institution of Mechanical Engineers, Part B, Journal of Engineering Manufacture, 223, 2, 155-161.

Bao, J.C.and Yao, Y.L., 2001, Analysis and prediction of edge effects in laser bending, Journal of Manufacturing Science and Engineering, Transactions of the ASME,123,53-61.

Bezuhov, N. L., 1968, Basics theory of elasticity, plasticity and creep, VisshayaShkola, Moscow.

Biswas, P., 2008, Thermo- Mechanical Finite Element Analysis and Manufacturing Simulation of Line Heating in Generation of Compound Curved Surfaces, Ph.D. Thesis, Indian Institute of Technology Kharagpur, India.

Biswas, P. and Mandal, N. R., 2008, Welding Distortion Simulation of Large Stiffened Plate Panels, Journal of Ship Production, 24,1, 50-56.

Biswas, P., Mandal, N.R. and Sha, O.P., 2006, Numerical and ANN prediction of thermal history of submerged arc welding, Journal of Mechanical Behavior of Materials, 17, 4, 269-286.

Biswas, P., Mandal, N.R. and Sha, O.P., 2007, Three-dimensional finite element prediction of transient thermal history and residual deformation due to line heating, Proceedings of the Institution of Mechanical Engineers, part M, Journal of Engineering for the Maritime Environment, 221,1, 17-30.

Biswas, P., Mandal, N.R. and Sha, O.P., 2009, Optimization of strain field distribution for generation of compound curve surfaces using line heating technique, Computational Materials science, 45, 1,167-175.

Biswas, P., Mandal, N.R. and Sha, O.P., 2010, Numerical and Dimensional Analysis for Prediction of Line Heating Residual deformations, Journal of Marine Science and application, 9, 1, 14-21.

Biswas, P., Mandal, N.R., Sha, O.P. and Mahapatra, M.M., 2011, Thermomechanical and Experimental Analysis of Double Pass Line Heating, Journal of Marine Science and Application, 10,190-198.

Brown, S. and Song,H., 1992, Implication of Three-Dimensional Numerical Simulation of welding of Large Structures, Welding Journal,55-62.

Casalino, G. and Ludovico, A.D., 2002, Parameter selection by an artificial neural network for a laser bending process, Proceedings of the Institution of Mechanical Engineers, Part B: Journal of Engineering Manufacture,216, 11, 1517-1520.

Chakraborty, S.S., Racherla, V. and Nath, A.K., 2012, Parametric study on bending and thickening in laser forming of a bowl shaped surface, Optics and Lasers in Engineering, 50, 1548-1558.

Chakraborty, S.S., More, H. and Nath, A.K., 2016, Laser forming of a bowl shaped surface with a stationary laser beam, Optics and Lasers in Engineering, 77, 126-136.

Chalfrant, J.S., and Maekawa, T., 1998, Design for Manufacturing using B-Spline Developable Surface, Journal of Ship research, 42, 3, 207-215.

Chandrupatala, T. R. and Belegundu, A. D., 2002, Introduction to finite element in engineering, Prentice-Hall of India Private Ltd, New Delhi.

Chen, J., Qi, Y., Shi,Y. and Bi, Z., 2010, An analytical model to predict bending angles in high frequency induction heat forming, Proceedings of the Institution of Mechanical Engineers, Part C, Journal of Mechanical Engineering Science, 224, C3, 655-660.

Chen, D, J., Wu, S.C., Xiang, Y.B. and Li, M.Q., 2002a, Simulation and Experiment of the curve-irradiated laser bending process of titanium alloy sheets, Materials science and Technology, 18, 6, 673-676.

Chen, D.J., Xiang, Y.B., Wu, S.C. and Li, M.Q., 2002b, Application of fuzzy neural network to laser bending process of sheet metal, Materials Science and Technology,18, 6, 677-680.

Cheng, P.J., and Lin, S.C., 2000a, An analytical model for the temperature field in the laser forming of sheet metal, Journal of Materials Processing Technology,101,1-3, 260-267.

Cheng, P.J. and Lin, S.C., 2000b, Using neural networks to predict bending angle of sheet metal formed by laser, International Journal of Machine Tools and Manufacture, 40, 1185-1197.

Cheng, P.J. and Lin, S.C., 2001, An analytical model to estimate angle formed by laser, Journal of Materials Processing Technology,108, 314-319.

Cheng, P., Yajun, F.Ji, Z.Yao, Y.L.Mika, D.P., Wenwu, Z.Graham, M., Marte, J. and Jones, M., 2006, Laser forming of varying thickness plate-part II: process synthesis, Transactions of the ASME, Journal of Manufacturing Science and Engineering,128, 3, 642-650.

Cheng, J. and Yao, Y.L., 2001, Cooling effects in multi scan laser forming, SME Journal of Manufacturing Processes, 3,1,60-72.

Cheng, J.G. and Yao, Y.L., 2004a, Process synthesis of laser forming by genetic algorithm, International Journal of Machine Tools and Manufacture, 44, 1619-1628.

Cheng, J.,Yao, Y.L., 2004b, Process design of laser forming for three-dimensional thin plates, Transactions of the ASME, Journal of Manufacturing Science and Engineering, 126, 2, 217-225.

Cheng, P., Yao, Y.L., Liu, C.,Pratt, D. and Fan, Y.J., 2005, Analysis and prediction of size effect on laser forming of sheet metal, Journal of Manufacturing Processes,7, 1, 28-41.

Cheng, W., 2005, On-plane shrinkage strains and their effects on welding distortion in thin-wall structures, Ph.D. Thesis, The Ohio State University, USA.

Chirillo, L.,1982, Line Heating, The National Shipbuilding Research Program, U.S. Department of Transportation and Todd Pacific Shipyard, Technical Report NSRP No.0163.

Cho, W., Patrikalakis, N.M. and Peraire, J., 1998, Approximate development of trimmed patches for surface tessellation, Computer- Aided Design, 30,14,1077-1087.

Choi, Y.h., Lee,Y.W., Choi, k., Doh, D.H. and Kim, K.J., 2012, Temperature distribution and thermal stresses in various conditions of moving heat source during line heating process, Journal of thermal science, 21, 1, 82-87.

Clausen, H.B., 2000, Plate forming by line heating, PhD thesis, Department of Naval Architecture and Offshore Engineering, Technical University of Denmark, Denmark.

Clausen, H.B., 1999, Three-Dimensional Numerical Simulation of Plate Forming by Line Heating, in Chryssostomidis, C.and Johansson, K.(editors), Proceedings of the 10th International Conference on Computer Applications in Shipbuilding, MIT Press, June 7-11, Cambridge, Massachusetts, USA, 2, 387-398.

Dan, W.J. and Zhang, W.G., 2011, Simulation Investigation the effect of Heating –lines on Tensional Mechanical Properties of Sheet Metal after Laser Scanning, Advanced Materials Research,314-316, 331-336.

Das,B. and Biswas, P., 2017, Effect of operating parameters on plate bending by laser line heating, Proc IMechE Part B: Journal of Engineering Manufacture,231,10,1812-1819.

Dearden, G. and Edwardson, S.P., 2003, Laser Assisted Forming for Ship Building,Proceedings, SAIL, June 2-4 Williamsburg V.A.

Edwardson, S.P., Watkins, K.G. and Magee, J., 2001, 3D Laser Forming of Saddle Shapes, Proceedings, 3rd International Conference on Laser Assisted Net Shaping (LANE 2001), August 28-31 Erlangen, Germany, 559-568.

Edwardson, S.P., 2004, A study into the 2D and 3D Laser Forming of Metallic Components, Ph.D.Thesis, Department of Engineering, The University of Liverpool, U.K.

Fanous, F.Z.Ihab., Younan, Maher,Y.A. and Wifi,S.Abdalla, 2003, 3-D Finite element modelling of the welding processusing element birth and element movement techniques, Tran. ASME, Journal of Pressure vessel Technology,125,144-150.

Fausett, L., 1994, Fundamentals of neural networks, Prentice-Hall, New York.

Fay, R.H., 1967, Heat Transfer from Fuel Gas Flames, Welding Research Supplement.

Geiger, M., Holzer, S. and Vollertsen, F., 1994,Laserstrahlbiegen-simulation eines 3-dimensionalen, thermomechanischenProzesses, Metal forming Process Simulation in Industry, 335-352.

Griffiths, J., 2012, Modeling of Laser Forming at Macro and Micro Scales, Ph.D. Thesis, School of Engineering, The University of Liverpool, U.K.

Ha, Y.S., and Jang, C.D., 2007, An improved inherent strain analysis for plate bending by line heating considering phase transformation of steel, Journal of offshore and Polar Engineering, 17,2,139-144.

Haykin, S., 1994, Neural networks. A Comprehensive foundation, Prentice-Hall, Englewood, NJ.

Hemmati, S.J. and Shin, J.G., 2007, Estimation of flame parameters for flame bending process, Journal of Machine Tools and Manufacturing, 47,799-804.

Hennige, T., 2000, Development of irradiation strategies for 3D-laser forming, Journal of Materials Processing Technology, 103,102-108.

Hinds, B.K.,McCartney, J. and Woods, G., 1991, Pattern development for 3D Surfaces, Computer-Aided Design,23, 8,583-592.

Holzer,H. , Arnet, M. and Geoger, M., 1994, Physical and numerical modelling of the buckling mechanism, Proceedings, Laser assisted Net Shape Engineering(LANE 1994), October 12-14, 1,Erlangen,Germany,379-386.

Hsiao, Y.C., Shimizu, H., Firth, L., Maher, W. and Masabuchi, K., 1997, Finite element modelling of laser forming, in: Proceedings, International Congress on Applications of Lasers and Electro-optics (ICALEO'97), Section A, November 17-20, SanDiego, Orlando, F L, 31-40.

Hsieh, H. and Lin, J., 2004, Thermal-mechanical analysis on the transient deformation during pulsed laser forming, International Journal of Machine Tools and Manufacture, 44, 191-199.

Hu, Z., Kovacevic, R.andLabudovic, M., 2002, Experimental and numerical modelling of buckling instability of laser sheet forming, International Journal of Machine Tools and Manufacture, 42,1427-1439.

Hu, Z., Labudovic, M., Wang, H. and Kovacevic, R., 2001, Computer simulation and experimental investigation of sheet metal bending using laser beam scanning, International Journal of Machine Tools and Manufacture, 41,589-607.

Hu, J., Xu, H. and Dang, D., 2013, Modeling and reducing edge effects in laser bending, Journal of Materials Processing Technology,213, 1989 -1996.

Ishiyama,M., Tango,Y. and shiri, M., 1999, An Automatic System for Line Heat Bending , Processing Method Utilizing FEM Application, Proceedings,10th International Conference on Computer Applications in Ship building(ICCAS'99), June 7-11, MIT Press, Cambridge, Massachusetts, USA.,2,419-435,

Iwamoto,K., Kizuka, Y. and Tsujino, Y., 2010, Plate bending by line heating with interactive support through monocular video see-through head mounted display, Proceedings, IEEE International Conference on Systems, Man and Cybernatics (SMC 2010), October 10-13,Istanbul,Turkey, 185-190.

Iwamura, y. and Rybicki, E.F., 1973, A transient elastic- plastic thermal stress analysis of flame bending, Journal of Engineering for Industry, 95, 1,163-171.

Jang, C.D., Kim, T.H., Ko,D.E., Lamb, T. and Ha, Y.S., 2005, Prediction of steel plate deformation due to triangle heating using the inherent strain method, Journal of Marine Science and Technology,10, 211-216.

Jang, C.D. and Moon, S.C., 1998, An Algorithm to Determine Heating Lines for Plate Forming by Line Heating Method, Journal of Ship production,14,4,238-245.

Jang, C.D., Seo, S.I. and Ko, D.E., 1997, A sltudy of the Prediction of deformations of plates due to line heating using a simplified thermal elasto-plastic analysis, Journal of Ship Production,13,1,22-27.

Jeng, J.Y., Mau, T. and Leu, S.M., 2000, Prediction of laser butt joint welding parameters using back propagation and learning vector quantization networks, Journal of Materials Processing Technology, 99,207-212.

Ji, Z. and Wu, S., 1998, FEM simulation of temperature field during the laser forming of sheet metal, Journal of Material Processing Technology,74, 89-95.

Kalyon, M. and Yilbas, B.S., 2001, Analytical solution for thermal stresses during the laser pulse heating process, Proceedings of the Institution of Mechanical Engineers (IMechE), Part C, Journal of Mechanical Engineering Science, 215,1429-1445.

Karlik, B. and Olgac, A.V., 2011, Performance analysis of various activation functions in generalized MLP architecture of neural networks, International Journal of Artificial Intelligence and Expert Systems (IJAE),1,111-122.

Khan, O.U. and Yilbas, B.S., 2004, Laser heating of sheet metal and thermal stress development, Journal of Materials Processing Technology,155-156, 2045-2050.

Kim, Y.Park, J., Shin, J., Hyun, C.andKo, K., 2009, The determination of heating shapes and locations for triangle heating, Journal of Manufacturing Science and Engineering,131, 2,021007(1-12).

Kitamura, N., Sakai, Y. and Murayama, H., 1996, 3-Dimensional Line Heating System for Curved Shell Plate for Ship building, Technical report, NKK Tsu Laboratories, 1 Kokan-choKumozu, Tsu, 514-03 Japan.

Kolahan, F., Manoochehri, M. and Hosseini A., 2011, Application of Taguchi method and ANOVA analysisfor simultaneous optimization of machining parametersand tool geometry in turning, World Academy of Science, Engineering and Technology, 74, 82-85.

Kraus, J., 1997, Basic Processes in laser bending of extrusions using the upsetting mechanism, Proceedings, Laser Assisted Net Shape Engineering 2 (LANE 1997), 2, September 23-26, Erlangen,Germany,431-438.

Kyrsanidi, A.K., Kermanidis, T.B. and Pantelakis, S.G., 2000, An analytical model for the prediction of distortions caused by the laser forming process, Journal of Materials Processing Technology,104, 94-102.

Lamb, T., 1995, Shell Development Computer Aided Lofting-Is there a Problem or Not? Journal of Ship Production,11,1,34-46.

Lambiase, F., Ilio, A.D. and Paoletti, A., 2015, Optimization of Multi-Pass Laser Bending by means of Soft Computing Techniques, Procedia CIRP, 33, 502-507.

Lee, J.H., 1999, Relations between input parameters and residual deformations in line heating process using finite element method and multi-variate analysis, Ph.D. Thesis, College of Engineering, Seoul National University.

Lee, J.S., 1996, Development of automatic marking generation system for plate forming by line heating, Journal of Ship production, 12, 4, 247-253.

Lee, J. and Um, K., 2000, A Comparison in back- bead prediction of gas metal arc welding using multiple regression analysis and artificial neural network, Optics and Laser in Engineering, 34, 149-158.

Letcher, Jr. J. S., 1993, Lofting and Fabrication of Compound-curved Plates, Journal of Ship Production, 37, 2,166-175.

Li, W. and Lawrence, Y., 2001, Numerical and experimental investigation of convex laser forming process, Journal of Manufacturing processes, 3, 2, 73-81.

Liang, W., Itoh, S., Vega, A. and Murakawa, H., 2006, Numerical Study of Inherent Deformation Produced in Thick Plate through Bending by Line Heating, Trans JWRI (Join Weld Res. Inst. Osaka Univ.),35, 1, 77-82.

Liu, Y., Guo, P., Ji, Z. and Deng, Y., 2006, Investigations of technique parameter prediction method of line heating based on genetic algorithm, Journal of Dalian University of Technology,46, 2, 235-240.

Liu, C. and Yao, Y.L., 2005, FEM based process design for 3D laser forming, Journal of Manufacturing Processes, 7, 2,109-121.

Liu,C., Yao,Y.L., and Srinivasan,V., 2004, Optimal process planning for laser forming of doubly curved shapes, Journal of Manufacturing Science and Engineering, 126, 1, 1-9.

Magee, J., Watkins, K.G., Steen, W.M., Calder, N., Sidhu, J. and Kirby, J., 1997, Edge effects in laser forming, Proceedings, Laser Assisted Net Shape Engineering (LANE 1997), September 23-26, Erlangen, Germany, 2, 399-408.

Majumdar, J.D. and Manna, I., 2003, Laser processing of materials, Sadhana, Indian Academy of Science,28, 3 & 4, 495-562.

Manca, O., Morrone, B. and Naso, V., 1995, Quasi –steady-state three-dimensional temperature distribution induced by a moving circular Gaussian heat source in a finite depth solid, Journal of Heat and Mass Transfer, 38, 7, 1305-1315.

Mandal, N. R., 2004, Welding and distortion control, Narosa Publishing House, New Delhi.

Manning, J.R., 1980, Computerized pattern cutting methods based on an isometric tree, Computer-Aided Design, 12,1,43-47.

Marya, M. and Edwards, G.R., 2002, An analytical model for the optimization of the laser bending of titanium Ti-6Al-2Sn-4Zr-2Mo, Journal of Materials Processing Technology,124, 3, 337-344.

Michaleris, P. and De Biccari, A., 1997, Prediction of welding distortion, Welding Journal, 76, 4, 172s-180s.

Morinobu, I. and Yoshihiko, T., 1999, Advanced line heating system applying FEM computer simulation, Ishikawajima-Harima Engineering Review, 39, 2, 60-64.

Moshaiov, A. and Latorre, R., 1985, Temperature distribution during plate bending by torch flame heating, Journal of Ship Research,29,1,1-11.

Moshaiov, A. and Shin J.G., 1991, Modified Strip Model for Analyzing the Line Heating Method – Part 2: Thermo-elastic –plastic plates, Journal of Ship Research, 35, 3, 266-275.

Moshaiv, A. and Vorus, W.S., 1987, The Mechanics of the Flame Bending Process: Theory and applications, Journal of Ship Research, 31, 4, 269-281.

Mucha, Z., 2007, Deformations and stresses induced in materials by moving beam of CO_2laser, Proceedings, SPIE, August 27, San Diego, CA, 65980M.1 – 65980M.9.

Mucha, Z., Hoffman, J., Kalita, W. and Mucha, S., 1997, Laser forming of thick free plates, Proceedings, Laser Assisted Net Shape Engineering (LANE),2, September 23-26, Erlangen,Germany, 383-392.

Mucha, Z., Widlaszewski, J., Cabaj, M. and Gradon, R., 2003, Surface temperature in laser forming, Archives of thermodynamics, 24, 2, 89-105.

Mulay, S.M., Ramesh Babu, N., 2017, Numerical modelling of laser forming of curved surfaces, Proceedings, 10th International Conference on Precision, Meso, Micro and Nano Engineering (COPEN 10), December 7-9, Indian Institute of Technology Madras, Chennai,43-46.

Nguyen, T-T. and Yang, Y., 2009, Using neural network for predicting induction-heating paths in ship yard, Proceedings, 2009 International Conference on Computer Technology and Development (ICCTD 2009), November 13-15, Kota Kinabalu, Malaysia,134-138.

Nguyen, T.T, Yang, Y. and Bae, K., 2009b, The development of an artificial neural network model to predict heating-line positions for plate forming in induction heating process, Mechanics Based Design of Structures and Machines, 37, 2, 201-227.

Nguyen, T.T., Yang, Y.S. and Kang, Y.B., 2009a, Analysis of bending deformation in triangle heating of steel plates with induction heating process using laminated plate theory, Journal of Mechanics Based design of structures and Machines, 37, 2, 228-246.

Nutbourne, A.W., McLellan, P.M. and Kensit, R.M.L., 1972, Curvature profiles for plane curves, Computer Aided Design, 4,176-184.

Ogawa, J., Kamichika, R. and Isao, N., 1994, A Simulation on the Thermo-elastic-plastic Deformation of Induction Heated Steel Plate, Proceedings, 8th International Conference on Computer Applications in Ship building (ICCAS'94), Brodda, J. and Johansson, K.(editors), September 5-9, Bremen, Germany, 1, 3.29-3.44.

Okuda, K., Shimoyama, S. and Nunobiki, M., 2004, Plastic bending of the magnesium alloy plate by a laser forming process, Key Engineering Materials, 257-258,541-546.

Osawa, N., Hashimoto, K., Sawamura, J., Kikuchi,J., Deguchi,Y. and Yamaura, T., 2007, Development of heat input estimation technique for simulation of shell forming by line heating, Computer Modelling in Engineering and Sciences, 20,1,43-53.

Parker, D. B., 1985, Learning logic, Technical Report TR-47, MIT Center for Computational Economics and Statistics, Cambridge.

Patrikalakis, N.M. and Maekawa, T., 2002, Shape Interrogation for Computer Aided Design and Manufacturing, 1st ed., Heidelberg, Germany, Springer- Verlag.

Patterson, D.W., 1995,Artificial neural networks: theory and applications, Prentice-Hall, Englewood, NJ.

Rafiq, M.Y., Bugmann, G. and Easterbrook, D.J., 2001,Neural network design for engineering applications, Computers and Structures, 79, 17, 1541-1552.

Rajasekaran, S. and Pai, G.A.V., 2003, Neural networks fuzzy logic and genetic algorithm synthesis and applications, New Delhi, Prentice Hall of India Ltd.

Rao, P.N., 1998, Manufacturing Technology, Tata McGraw-Hill Pub. Co. Ltd., New Delhi.

Reddy, J.N., 2003, An Introduction to the Finite Element Methods, 2nded,, Tata McGraw-Hill Pub. Co. ltd., New Delhi.

Rogers, D.F. and Adams, J.A., 2003, Mathematical elements for computer graphics, 2nd ed., Tata McGraw- Hill Publication, New Delhi.

Rosenthal, D., 1946,The theory of moving sources of heat and its application to metal treatment, Transactions of the ASME, 849-866.

Roy, R., 1990, A Primer on the Taguchi method, Society of Manufacturing Engineers, Michigan,USA

Rykalin, N.N., 1960, Calculation of heat processes in welding, Mashinostroenije, Moscow.

Safari, M. and Farzin M., 2015, Experimental investigation of laser forming of a saddle shape with spiral irradiating scheme, Optics and Laser Technology, 66,146-150.

Safari, M. and Mostaan, H., 2016, Experimental and numerical investigation of laser forming of cylindrical surfaces with arbitrary radius of curvature, Alexandria Engineering Journal, 55,1941-1949.

Scully, K., 1987, Laser line heating, Journal of Ship Production,3,4,237-246.

Shahabad, S. I., Naeini, H.M., Roohi, A.H., Tavakoli, A. and Nasrollahzade, M., 2017, Experimental investigation of laser forming process to produce dome-shaped products, International Journal of Advance Manufacturing Technology, 90, 1051-1057.

Shen, H., Shi, Y.J. and Yao, Z. Q., 2006b, Numerical simulation of the laser forming of plates using two simultaneous scans, Computational Materials Science,37,3,239-245.

Shen, H., Shi, Y.J and Yao, Z.Q., 2006c, Laser forming of plates using two sequent scans of different intervals, Proceedings of the Institution of Mechanical Engineers, Part C: Journal of Mechanical Engineering Science,220,4, 507-511.

Shen, h., Shi, Y., Yao, Z. and Hu, J., 2005, Analysis of varying velocity on edge effects in laser bending, Transactions of the Non-ferrous Metals Society of China,15, 255-259.

Shen, H., Shi, Y.J., Yao, Z.Q. and Hu, Z., 2006d, An analytical model for estimating deformation in laser forming, Journal of Computational Materials Science,37,4,593-598.

Shen, H., Shi, Y.J., Yao, Z.Q. and Hu, J., 2006e, Fuzzy logic model for bending angle in laser forming, Materials Science and Technology,22, 8,981-986.

Shen, H. and Yao, Z.Q., 2008, Analysis of varying velocity scanning schemes on bending angle in laser forming, Proceedings, International Workshop on Thermal Forming and welding Distortion, April 22-23, Bremen, Germany, 215-217.

Shen,H., Yao, Z.Q., Shi, Y.J. and Hu, J., 2006a, An analytical formula for estimating the bending angle by laser forming, Proceedings of the Institution of Mechanical Engineers, Part c,: Journal of Mechanical engineering Science,220, 2 ,243-247.

Shen, H., Yao, Z.Q., Shi, Y.J. and Hu, J., 2007a, The simulation of temperature field in the laser forming of steel plates, International Journal of Modelling, Identification and Control, 2,3, 241-249.

Shen, H., Zhou, J. and Yao, Z.Q., 2007b, Study on overlapping of two sequential scans in laser forming, Proceedings of the Institution of Mechanical Engineers, Part C: Journal of Mechanical Engineering Science, 221,9, 993-997.

Shen, H., Zhou, J., Shi, Y.J., Yao,Z.Q. and Hu,J., 2007c, Varying velocity scan in laser forming of plates, Journal of Material Science and Technology,23,4,483-486.

Shen, H., Hu, J. and Yao, Z., 2010, Analysis and control of edge effects in laser bending, Optics and Laser Technology, 48, 305- 315.

Shi,Y.J., Liu,Y.C.,Yao, Z.Q. and Shen, H., 2008, A study on bending direction of sheet metal in laser forming, Journal of Applied Physics,103, 053101,doi:10.1063/1.2887995.

Shi, Y., Liu, Y., Yi, P. and Hu, J., 2012, Effect of different heating methods on deformation of metal plate under upsetting mechanism in laser forming, Optics and Laser Technology,44, 486-491.

Shi, Y., Lu, x., Yi, P. and Liu, Z., 2013, Effect of heating paths on strain distribution of plate in laser forming, International Journal of Advanced Manufacturing Technology, 66,515-521.

Shi, Y.,Shen, H., Yao, Z. and Hu, J., 2007, Temperature gradient mechanism in laser forming of thin plates, Optics and Laser Technology, 39, 4,858-863.

Shin, J.G. and Kim, W.D., 1997, Kinematic analysis of the process planning for compounding ship hull plates, Journal of Ship Production, 13, 1, 28-35.

Shin, J.G., Kim, W.D. and Lee, J.H., 1996, Numerical Modelling for Systemization of line heating process, Journal of Hydrospace Technology,2, 1, 41-54.

Shin, J.G., Lee, J.H. and Park, S.K., 1999, A numerical thermo plastic analysis of line heating processes for saddle type shells with the application of an artificial neural network, Journal of Ship Production,15,1, 10-20.

Shin, J., Kim, W. and Lee, J., 1995, Numerical modeling for systematization of line heating process, Department of Naval Architecture and Ocean Engineering, Seoul National University, Seoul, Korea ,151-742.

Sistaninia, M. and Moeanodini, H., 2009, Laser forming of plates using rotating and dithering beams, Journal of Computational Materials Science, 45,2, 480-488.

Son, K.J., Yun, J.O., Kim, Y.W. and Yang, Y.S., 2007, Analysis of angular distortion in line-heating, International Journal of Mechanical Sciences, 49,10, 1122-1129.

Tangyunyong,P., 2003, Thermal modelling of localized laser heating in multi-level interconnects, Journal of Microelectronics Reliability,43, 2,297-305.

Tetsuya,A., Hironori, A.B.E., 2011, Effect of heating direction on saddle laser forming based on geodesic in-plane strain method, Quarterly Journal of the Japan Welding Society, 29,3, 210-217.

Tomita, Y., Hashimoto, K., Osawa, N. and Shinkai, N., 2001, Study on heat transfer between gas flame and plate during line heating process, in: Y.S.Wu,W.C.Cui and G.J. Zhou (ed) Practical design of ships and other floating structures, Elsevier,1,389-396.

Tsoukalas, L.H. and Robert, A.V., 1996, Fuzzy and neural approaches in engineering, John Wiley and Sons Inc., New York, NY.

Ueda, Y., Murakawa, H., Rashwan, A.M., Neki, I., Kamachika, R.Ishiyama, M. and Ogawa, J., 1994a, Development of computer-aided process planning system for plate bending by line heating (Report-1), Relation between final form of plate and inherent strain, Journal of Ship Production,10,1,59-67.

Ueda, Y., Murakawa, H., Rashwan, A.M., Neki, I., Kamachika, R., Ishiyama, M. and Ogawa, J., 1994c, Development of computer-aided process planning system for plate bending by line heating (Report 3)-Relation between heating condition and deformation, Journal of Ship Production, 10, 4,248-257.

Vega, A., Osawa, N., Rashed, S. and Murakawa, H., 2010, Analysis and prediction of edge effect on inherent deformation of thick plates formed by line heating, Journal of Computer Modelling in Engineering and Sciences, 69,3, 261-279.

Vega, A., Rashed, S., Tango, Y., Ishiyama, M. and Murakawa, H., 2008, Analysis and prediction of multi-heating lines effect on plate forming by line heating, Computer Modelling in Engineering and Science,28,1, 1-14.

Venkadeshwaran, K., Das, S. and Misra, D., 2010, Finite element simulation of 3D laser forming by discrete section circle line heating, International Journal of Engineering Science and Technology,2, 4, 163-175.

Vollertsen, F., 1994,An analytical model for laser bending, Lasers in Engineering 2,261-276.

Vollertsen, F., Komel, I. and Kals, R., 1995,The laser bending of steel foils for micro parts by the buckling mechanism: A model, Modelling and Simulation in Materials Science and Engineering, 3,107-119.

Vollertsen, F., Geiger, M. and Li, W.M., 1993, FDM and FEM simulation of laser forming: A comparative study, Advanced Technology of Plasticity, Proceedings, Fourth International Conference on Technology of Plasticity, September 5-9, Beijing, China,1793-1798.

Walczyk, D.F. and Vittal, S., 2000, Bending of titanium sheet using laser forming, Journal of Manufacturing Processes,2,4, 258-269.

Wang, J., Wang, J., Zhao, Y., Yang,Z. and Hao,H., 2002, Design of Intelligent robot controller for steel plate by line heating and cooling, Proceedings of the 4th World Congress

on Intelligent Control and Automation.(Cat. No. 02EX527), June 10-14, 2, Shanghai, China,1215-1218.

Wang, J., Liu, Y., Ji,Z.Deng, Y.,Guo,P.,Jin,S. and Zhang, J., 2006a, A comprehensive Line Heating Process for Automatic Formation of Double Curved Plates. Selected Papers of China Soc., Naval Archiect, Marine Engineering, Ship building, China, 17,180-189.

Wang, J., Liu, Y., Ji, Z.Deng, Y., Guo, P. and Zhou, B., 2006c, Study on the automatic process of line heating for pillow shape plate, Journal of Marine Science and Application, 5,1,31-38.

Wang, J., Liu, Y., Ji, Z., Deng,Y., 2006b, Investigations on parameters of heat input model in numerical simulation of line heating, Journal of Dalian University of Technology, 46,3,367-371.

Watanabe,M. and Satoh, K., 1961, Effect of welding conditions on the shrinkage and distortion in welded structures, Welding Journal,40,8,377s-384s.

Xiufeng, W., Xiaodong, L., Shiguang, H. and Guangnan, C., 2003, Simulation and verification of the temperature field in laser bending sheet metal, Journal of Beijing University of Aeronautics and Astronautics,29,5, 377-381.

Xuebiao, Z., Zhuoshang,J. and Yujun, L., 2005, Curvature Analysis Method for Ship Hull Plate Forming, Journal of Ship Production,21, 2, 65-72.

Yau, C.L., Chan, K.C. and Lee, W.B., 1997, A new analytical model for laser bending, Proceedings, Laser Assisted Net Shape Engineering, Proceedings of the LANE, September 23-26, Erlangen,Germany, 2, 357-366.

Yilbas, B.S. and Al-Aqeeli, N., 2003, Formulation of Laser-induced thermal stresses: Stress boundary at the surface, Proceedings of the Institution of Mechanical Engineers, Part C: Journal of Mechanical Engineering Science, 217,423-434.

Yilbas, B.S. and Akhtar, S.S., 2014, Laser bending of metal sheet and thermal stress analysis, Optics and Laser Technology, 61, 34-44.

Yu, G., Anderson, R.J., Maekawa, T. and Patrakalakis, N.M., 2001a, Efficient simulation of shell forming by line heating, International Journal of Mechanical Sciences,43,2349-2370.

Yu, G. Masubuchi, K. and Maekawa, T., 1999, A Finite Element Model for Metal Forming by Laser Line Heating, in Chryssostomidis, C. and Johansson, K. (editors), Proceedings,10th International Conference on Computer Application in ship Building(ICCAS'99), MIT Press, Cambridge, Massachusetts, USA, 2, 409-418.

Yu, G., Masubachi, K., Maekawa, T. and Patrikalakis, N.M., 2001b, FEM simulation of laser forming of metal plates, Journal of Manufacturing Science and Engineering, 123, 405-410.

Zhang, x., Ji, z., Liu, Y. and Deng, Y., 2006, The effect of line heating factors on angular deformation generated by line heating, Journal of Shanghai Jiatong University,40, 6, 1010-1014.

Zhang, L. and Michaleris, P., 2004, Investigation of Lagrangian and Eulerian finite element methods for modelling the laser forming process, Finite Elements in Analysis and Design, 40,383-405.

Zhang, L., Reutzel, E.W. and Michaleris, P., 2004, Finite element modelling discretization requirements for the laser forming process, International Journal of Mechanical Sciences, 46, 623-637.

Zhang,X., Yang, Y. and Liu, Y., 2011, Feasibility research on application of a high frequency induction heat to line heating technology, Journal of Marine Science and Application, 10, 4, 456-464.

Zhihui, Y., Liang, G., Mi, X. and Lei, Y., 2011, DOE-based numerical investigation on factors affecting temperature field during line heating, Journal of Advanced Materials Research, 314-316, Pt.1, 620-625.

Zhou, J. and Shen, H., 2011, Bending angle estimated based on inherent strain theory during laser forming, Materials Science Forum, 663-665,947-951.

Zhu. H and Yang.X, 2012, Heating path generation and simulation for ship plate steel, Advanced Materials Research, 421, 250-253.

Zienkiewicz, O.C., 2001,The Finite Element Method, Third Edition, Tata McGraw- Hill Pub. Co. Ltd., New Delhi.

Zhang, P., Guo, B., Shan, D.B., Ji,Z., 2007, FE Simulation of laser curve bending of sheet metals, Journal of Materials Processing Technology,184,157-162.

Publications

International Journals

- Biplab Das and Pankaj Biswas (2017) “Effect of Operating Parameters on Plate bending by Laser Line Heating”, Part B: Journal of Engineering Manufacture Processes, Vol.231 (10),1812-1819.
- Biplab Das and Pankaj Biswas (2018) “A Review of Plate Forming by Laser Line Heating”, Journal of Ship Production and Design, Vol.34(2), pp.155-167.
- Biplab Das and Pankaj Biswas “Experimental and Numerical Investigation of Single Pass Laser Line Heating” Journal of Materials Processing. (under preparation).
- Biplab Das and Pankaj Biswas “Thermo-mechanical Analysis of Plate forming by Laser Line Heating” (under preparation).
- Biplab Das and Pankaj Biswas “Development of Compound curved surface by Laser Line heating” (under preparation).

Book Chapter

- Biplab Das and Pankaj Biswas (2015), “Mathematical Formulation for Development of Compound Curve Surface by Laser Line Heating”, in S.N.Joshi and U.S.Dixit (eds.), Laser Based Manufacturing, Topics in Mining, Metallurgy and Materials Engineering, DOI 10.1007/978-81-322-2352-8_6, Springer India.,pp.93-105.

Conferences

- Biplab Das, KishorGajrani and Pankaj Biswas (2012) “Prediction of thermal history in laser line heating”, 21st International Symposium on Processing and Fabrication of Advanced Materials PFAMXXI, Guwahati, India, Vol-2, December 2012.

- Biplab Das and Pankaj Biswas (2014) “Mathematical formulation for the development of Compound curve surface by Laser Line Heating”, 5th International and 26th All India Manufacturing Technology, Design and Research Conference, AIMTDR 2014.
- Biplab Das and Pankaj Biswas (2016) “Prediction of Heating Lines for Plate Forming by Laser Line Heating”, 6th International and 27th All India Manufacturing Technology, Design and Research Conference, AIMTDR 2016.